

**POSSIBILITIES OF POWER GENERATION IN PAKISTAN FROM  
GEOHERMAL ENERGY RESOURCES**

A Dissertation  
Presented to  
The Academic Faculty  
By

**Engineer Syed Ahsan Mustaqeem  
NUST-PNEC-MS PhD- Mech(N)-14**

Advisor  
**Professor Dr. Waqar A Khan**

in Partial Fulfillment  
of the Requirements for the Degree of

**Master of Science**  
In Mechanical Engineering  
(With Specialization in Thermal Power)



National University of Sciences and Technology  
2014

**Dedicated To  
Those Martyred Guarding the Ideological  
Frontiers of Pakistan.**

## **ACKNOWLEDGEMENT**

All praise to *ALLAH* (Exalted Be He) who granted me strength, knowledge and opportunity to complete this research on time.

I take immense pleasure in thanking *Prof. Dr. Shafiq Ur Rahman Qureshi* Head of Postgraduate Program for having permitted me to carry out this research work.

I wish to express my deep sense of gratitude to my Advisor, Professor Dr. Waqar Ahmed Khan, Guidance and Evaluation Committee Members; Professor Dr. Shafiq Ur Rahman Qureshi, Professor Dr. Ghulam Murshed Arshad and Dr. Muhammad Nauman Qureshi for their able guidance, useful suggestions and beneficial cooperation which enabled me in completing the research work.

Finally, yet importantly, I would like to express my heartfelt thanks to my beloved parents for their blessings, my siblings, friends and relatives for their help and wishes for the successful completion of this project.

<b>TABLE OF CONTENTS</b>		
<b>Sr. No</b>	<b>Contents</b>	<b>Page No.</b>
---	List of figures	--
---	List of tables	--
---	Abstract	--
<b>Chapter I</b>	<b><u>INTRODUCTION</u></b>	<b>1-9</b>
1.1	World Energy Outlook	1
1.2	World Renewable Energy Outlook	3
1.3	Pakistan Energy Outlook	5
1.4	Geothermal Energy	7
1.5	Scope and Purpose	9
1.6	Thesis Outline	9
<b>Chapter II</b>	<b><u>GEOTHERMAL ENERGY</u></b>	<b>10-22</b>
2.1	World Geothermal Energy Outlook:	10
2.2	Classification of Geothermal sources	11
2.3	Geothermal Power Generation	12
2.4	Classification of Geothermal Power Generation systems	13
2.4.1	Dry Steam Geothermal Power Plants:	15
2.4.2	Flash Geothermal Power Plants	16
2.4.3	Binary Geothermal Power Plants	17
2.4.4	Hybrid Geothermal Power Plants	18
2.4.4.1	Direct Steam Binary or Back Pressure Geothermal Power Plants	18
2.4.4.2	Single Flash Binary Geothermal Power Plants	19
2.4.4.3	Integrated Single and Double Flash Binary Geothermal Power Plants	20
2.4.4.4	Hybrid Fossil Geothermal Power Plants	21
<b>Chapter III</b>	<b><u>GEOTHERMAL ENERGY RESOURCES IN PAKISTAN</u></b>	<b>22-28</b>
3.1	Geothermal Energy Potential in Pakistan	22
3.2	Geothermal Energy Resources in Pakistan	25
3.2.1	Geo Pressurized Sources	26
3.2.2	Seismo Tectonic and Suture Related Systems	27
3.2.3	Geo Thermal System Related to Neo-gene Quaternary Volcanism	28

<b>CHAPTER - IV</b>	<b><u>LITERATURE REVIEW</u></b>	29-33
4.1	Literature Survey:	29
4.2	Optimum Cycle and Working Fluid Selection and Performance Evaluation	30
4.3	Summary and Conclusion	33
<b>CHAPTER - V</b>	<b><u>MATHEMATICAL MODELLING</u></b>	35-50
5.1	Energy and Exergy Analysis	35
5.2	Performance Analysis	36
5.3	Optimum Power Plant Configuration Selection:	37
5.3.1	Basic ORC:	38
5.3.2	ORC with IHE	39
5.3.3	Regenerative ORC	42
5.3.4	Regenerative ORC with IHE	44
5.4	Selection of Optimal Working Fluid	46
5.5	Methodology	48
5.6	Assumptions	48
5.7	Reference Conditions	50
5.8	Mathematical Model Validation:	50
<b>CHAPTER -VI</b>	<b><u>ANALYSIS</u></b>	
6.1	Performance Analysis of Organic Binary Fluids	58
6.2	Performance Analysis of ORC configurations	80
<b>CHAPTER -VII</b>	<b><u>CONCLUSION</u></b>	96-97
	<b>REFERENCES</b>	104 - 112

## LIST OF FIGURES

<u>Fig No.</u>	<u>Description</u>	<u>Page No</u>
FIG 1.1	Total Global Primary Energy Supply 1971-2011	1
FIG 1.2	Global Electricity Consumption 1985-2011	2
FIG 1.3	Sector wise Global Electricity Consumption in 2011	2
FIG 1.4	Energy Related Global Carbon Dioxide Emissions 1965-2011	3
FIG 1.5	Renewable Power generation projections 2020-2035	4
FIG 1.6	Gross Electricity Generation in Pakistan 2006-2012	5
FIG 1.7	Electricity Generation in Pakistan 2011-12	6
FIG 1.8	Global Technical Geothermal Energy Potential	8
FIG 2.1	Global Geothermal Power Generation Capacity in 2010	10
FIG 2.2	Global Geothermal Power Generation Projections for 2015	11
FIG 2.3	Minimum Geothermal Energy Production Depth	12
FIG 2.4	Application Ranges of Geothermal Power Plants	14
FIG 2.5	Geothermal Power Generation Installed Capacity	14
FIG 2.6	Geothermal Power Generation Units in Operation	15
FIG 2.7	Dry-steam Geothermal Power Plant	16
FIG 2.8	Flash Geothermal Power Plant	17
FIG 2.9	Binary Geothermal Power Plant	18
FIG 2.10	Dry Steam Binary Geothermal Power Plant	19
FIG 2.11	Single Flash Binary Geothermal Power Plant	20
FIG 3.1	Theoretical Potential of geothermal resources in Pakistan	22
FIG 3.2	Technical Potential of geothermal resources in Pakistan	23
FIG 3.3	Minimum Production Depth of geothermal resources in Pakistan	24
FIG 3.4	Maximum Production Temperature of geothermal resources in Pakistan	25
FIG 3.5	Performance Indicator of geothermal resources in Pakistan	26
FIG 3.6	Occurrences of geothermal sources in Pakistan	27
FIG 3.7	hot spring occurrences on Karakorum–Himalayan thrust zone	28
FIG 5.1	Basic Organic Rankine Cycle	38
FIG 5.2	T-S Diagram of Basic Organic Rankine Cycle	38
FIG 5.3	Organic Rankine Cycle with IHE	40
FIG 5.4	T-S Diagram of Organic Rankine Cycle with IHE	40
FIG 5.5	Regenerative Organic Rankine Cycle	42
FIG 5.6	T-S Diagram of Regenerative Organic Rankine Cycle	42
FIG 5.7	Regenerative Organic Rankine Cycle with IHE	44
FIG 5.8	T-S Diagram of Regenerative Organic Rankine Cycle with IHE	45
FIG 6.1	Net Work output per Kg of geo fluid at the temperature of 100°C for Basic Organic Rankine Cycle	58

FIG 6.2	Net Work output per Kg of geo fluid at the temperature of 100 °C for Organic Rankine Cycle with IHE	59
FIG 6.3	Net Work output per Kg of geo fluid at the temperature of 100 °C for Regenerative Rankine Cycle	59
FIG 6.4	Net Work output per Kg of geo fluid at the temperature of 100 °C for Regenerative Rankine Cycle with IHE	60
FIG 6.5	Net Work output per Kg of geo fluid at the temperature of 150 °C for Basic Organic Rankine Cycle	60
FIG 6.6	Net Work output per Kg of geo fluid at the temperature of 150 °C for Organic Rankine Cycle with IHE	61
FIG 6.7	Net Work output per Kg of geo fluid at the temperature of 150 °C for Regenerative Rankine Cycle	62
FIG 6.8	Net Work output per Kg of geo fluid at the temperature of 150 °C for Regenerative Rankine Cycle with IHE	62
FIG 6.9	Cycle thermal efficiency for geo fluid at the temperature of 150 °C for Basic Organic Rankine Cycle	63
FIG 6.10	Cycle thermal efficiency for geo fluid at the temperature of 150 °C for Organic Rankine Cycle with IHE	63
FIG 6.11	11 Cycle thermal efficiency for geo fluid at the temperature of 150 °C for Regenerative Organic Rankine Cycle	64
FIG 6.12	Cycle thermal efficiency for geo fluid at the temperature of 150 °C for Regenerative Organic Rankine Cycle with IHE	64
FIG 6.13	13 First Law Efficiency (based on geo fluid inlet state conditions) for geo fluid at the temperature of 150 °C for Basic Organic Rankine Cycle	65
FIG 6.14	First Law Efficiency (based on geo fluid inlet state conditions) for geo fluid at the temperature of 150 °C for Organic Rankine Cycle with IHE	66
FIG 6.15	First Law Efficiency (based on geo fluid inlet state conditions) for geo fluid at the temperature of 150 °C for Regenerative Organic Rankine Cycle	66
FIG 6.16	First Law Efficiency (based on geo fluid inlet state conditions) for geo fluid at the temperature of 150 °C for Regenerative Organic Rankine Cycle with IHE	67
FIG 6.17	Second Law Efficiency (based on geo fluid inlet state) for geo fluid at the temperature of 150 °C for Basic Organic Rankine Cycle	68
FIG 6.18	Second Law Efficiency (based on geo fluid inlet state)for geo fluid at the temperature of 150 °C for Organic Rankine Cycle with IHE	68
FIG 6.19	Second Law Efficiency (based on geo fluid inlet state)for geo fluid at the temperature of 150 °C for Regenerative Organic Rankine Cycle	69
FIG 6.20	Second Law Efficiency (based on geo fluid inlet state) for geo fluid at the temperature of 150 °C for Regenerative Organic Rankine Cycle with IHE	69

FIG 6.21	Second Law Efficiency (based on energy input)for geo fluid at the temperature of 150 °C for Basic Organic Rankine Cycle	70
FIG 6.22	Second Law Efficiency (based on energy input) for geo fluid at the temperature of 150 °C for Organic Rankine Cycle with IHE	71
FIG 6.23	Second Law Efficiency (based on energy input) for geo fluid at the temperature of 150 °C for Regenerative Organic Rankine Cycle	71
FIG 6.24	Second Law Efficiency (based on energy input)for geo fluid at the temperature of 150 °C for Regenerative Organic Rankine Cycle with IHE	72
FIG 6.25	Cycle Effectiveness for geo fluid at the temperature of 150 °C for Basic Organic Rankine Cycle	73
FIG 6.26	Cycle Effectiveness for geo fluid at the temperature of 150 °C for Organic Rankine Cycle with IHE	73
FIG 6.27	Cycle Effectiveness for geo fluid at the temperature of 150 °C for Regenerative Organic Rankine Cycle	74
FIG 6.28	Cycle Effectiveness for geo fluid at the temperature of 150 °C for Regenerative Organic Rankine Cycle with IHE	74
FIG 6.29	Mass flow rate of binary fluid per kg/s of geo fluid at the temperature of 150 °C for Basic Organic Rankine Cycle	75
FIG 6.30	Mass flow rate of binary fluid per kg/s of geo fluid at the temperature of 150 °C for Basic Organic Rankine Cycle with IHE	76
FIG 6.31	Mass flow rate of binary fluid per kg/s of geo fluid at the temperature of 150 °C for Regenerative Organic Rankine Cycle	76
FIG 6.32	Mass flow rate of binary fluid per kg/s of geo fluid at the temperature of 150 °C for Regenerative Organic Rankine Cycle with IHE	77
FIG 6.33	Overall Plant Irreversibility at the geo fluid temperature of 150 °C for Basic Organic Rankine Cycle	78
FIG 6.34	Overall Plant Irreversibility at the geo fluid temperature of 150 °C for Basic Organic Rankine Cycle with IHE	78
FIG 6.35	Overall Plant Irreversibility at the geo fluid temperature of 150 °C for Regenerative Organic Rankine Cycle	79
FIG 6.36	Overall Plant Irreversibility at the geo fluid temperature of 150°C for Regenerative Organic Rankine Cycle with IHE	79
FIG 6.37	Comparison of net work output of different Organic Rankine Cycle Configurations	80
FIG 6.38	Comparison of Thermal Efficiency of different Organic Rankine Cycle Configurations.	81
FIG 6.39	Comparison of First Law Efficiency of different Organic Rankine Cycle Configurations.	82



FIG 6.40	Comparison of Second Law Efficiency (based on geo fluid inlet state) of different Organic Rankine Cycle Configurations	83
FIG 6.41	Comparison of Second Law Efficiency (based on exergy input) of different Organic Rankine Cycle Configurations.	84
FIG 6.42	Comparison of Cycle Effectiveness of different Organic Rankine Cycle Configurations.	85
FIG 6.43	Comparison of Overall Plant Irreversibility of different Organic Rankine Cycle Configurations.	86
FIG 6.44	Comparison of Fuel Depletion Ratio of different Organic Rankine Cycle Configurations at turbine inlet temperature of 100°C	87
FIG 6.45	Comparison of Fuel Depletion Ratio of different Organic Rankine Cycle Configurations at turbine inlet temperature of 110°C	88
FIG 6.46	Comparison of Fuel Depletion Ratio of different Organic Rankine Cycle Configurations at turbine inlet temperature of 120°C	88
FIG 6.47	Comparison of Relative Irreversibility of different Organic Rankine Cycle Configurations at turbine inlet temperature of 100°C	90
FIG 6.48	Comparison of Relative Irreversibility of different Organic Rankine Cycle Configurations at turbine inlet temperature of 110°C	90
FIG 6.49	Comparison of Relative Irreversibility of different Organic Rankine Cycle Configurations at turbine inlet temperature of 120°C	91
FIG 6.50	Comparison of Productivity lack of different Organic Rankine Cycle Configurations at turbine inlet temperature of 100°C	92
FIG 6.51	Comparison of Productivity lack of different Organic Rankine Cycle Configurations at turbine inlet temperature of 110°C	91
FIG 6.52	Comparison of Productivity lack of different Organic Rankine Cycle Configurations at turbine inlet temperature of 120°C	922
FIG 6.53	Comparison of Net Work Output at different geo fluid temperatures	93
FIG 6.54	Comparison of Net Work Output at different Condenser temperatures	94
FIG 6.55	Comparison of Net Work Output at different Pinch Point temperatures	95

## LIST OF TABLES

<b><u>Table</u></b> <b><u>No.</u></b>	<b><u>Description</u></b>	<b><u>Page</u></b> <b><u>No</u></b>
TAB 2.1	Classification of Geothermal Energy Sources	12
TAB 5.1	Properties of selected Refrigerants	47
TAB 5.2	Model Validation for Basic ORC using R123	51
TAB 5.3	Model Validation for Basic ORC using n-Pentane	51
TAB 5.4	Model Validation for Basic ORC using R113	52
TAB 5.5	Model Validation for ORC with IHE using R123	52
TAB 5.6	Model Validation for ORC with IHE using n-Pentane	53
TAB 5.7	Model Validation for ORC with IHE using R113	53
TAB 5.8	Model Validation for regenerative ORC using R123	54
TAB 5.9	Model Validation for regenerative ORC using n-Pentane	54
TAB 5.10	Model Validation for regenerative ORC using R113	55
TAB 5.11	Model Validation for regenerative ORC with IHE using R123	55
TAB 5.12	Model Validation for regenerative ORC with IHE using n-Pentane	56
TAB 5.13	Model Validation for regenerative ORC with IHE using R113	56

## **ABSTRACT**

World is presently facing an unprecedented energy challenge. This situation is even graver in developing and under developed countries like Pakistan. Future solution of this challenge lies in harnessing renewable and other sustainable energy resources. Geothermal energy is one of such options. This thesis presents an analysis of possibilities of exploiting this resource in Pakistan. Geological research underlines presence of several geothermal resources in country. Most of the geothermal resources of the world lie near the seismic belts and Pakistan too is situated in the western rifted margin of Indo-Pakistan sub continental plate. The presence of geothermal resources is strengthened by the development of alteration zones and fumaroles in different regions of the country, presence of hot springs and indication of quaternary volcanism. There exist several medium and low temperature geothermal sources up to temperatures of 200°C in different areas of Pakistan. The present work addresses the idea of power generation from geothermal energy sources in Pakistan. The work encompasses the review of geothermal resources in Pakistan and the application of engineering principles for the exploitation of these resources. The work includes a comparative Energetic and Exergetic study of different geothermal power plant concepts, based on the source temperature. Cycles incorporated in this study are basic Organic Rankine Cycle (ORC), Organic Rankine Cycle with an Internal Heat Exchanger, Regenerative Organic Rankine Cycle & Regenerative Organic Rankine Cycle with an Internal Heat Exchanger. A thermodynamic model is developed for ORC and validated using available data from literature. Numerical and analytical analysis is carried out for finding the optimum working conditions and working fluid. The performance of each configuration of cycle has been analyzed in terms of energetic & Exergetic efficiency, exergy destruction rate, fuel depletion ratio, relative

irreversibility and productivity lack. It is observed that the increase in geothermal source temperature results in an exponential increase in maximum cycle output and a linear increase in turbine inlet temperature. It is also proposed to use internal heat exchanger and regeneration to increase the effectiveness of cycle.

# CHAPTER - I

## INTRODUCTION

### 1.1 World Energy Outlook:

The world is facing an unprecedented energy challenge, rapid industrialization; urbanization and exponential growth in population are the key drivers behind the ever increasing demand for energy. The Global Primary Energy supply had been 13113 MTOE in 2011 and the demand is projected to increase by more than one third to 17440 MTOE in 2035. [1]

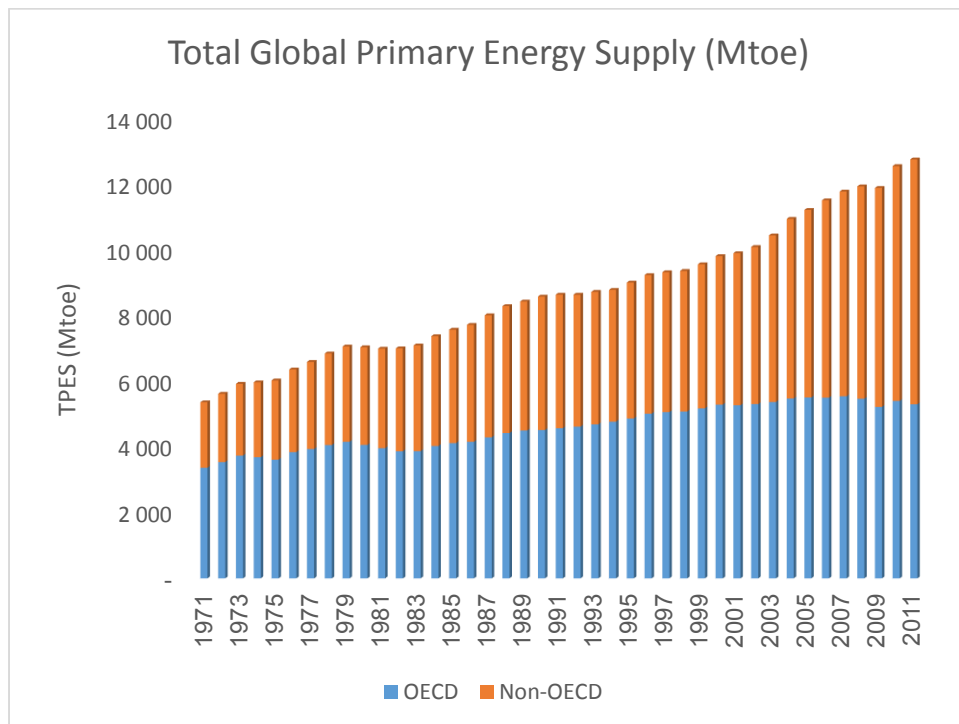


FIG 1.1 – Total Global Primary Energy Supply 1971-2011 [1]

The global Electricity consumption has been 20407 TWh in 2011 of which residential, commercial and agricultural sector consumed 55.8%, Transportation sector consumed 1.6% and Industrial Sector consumed 42.6% electricity. [1]

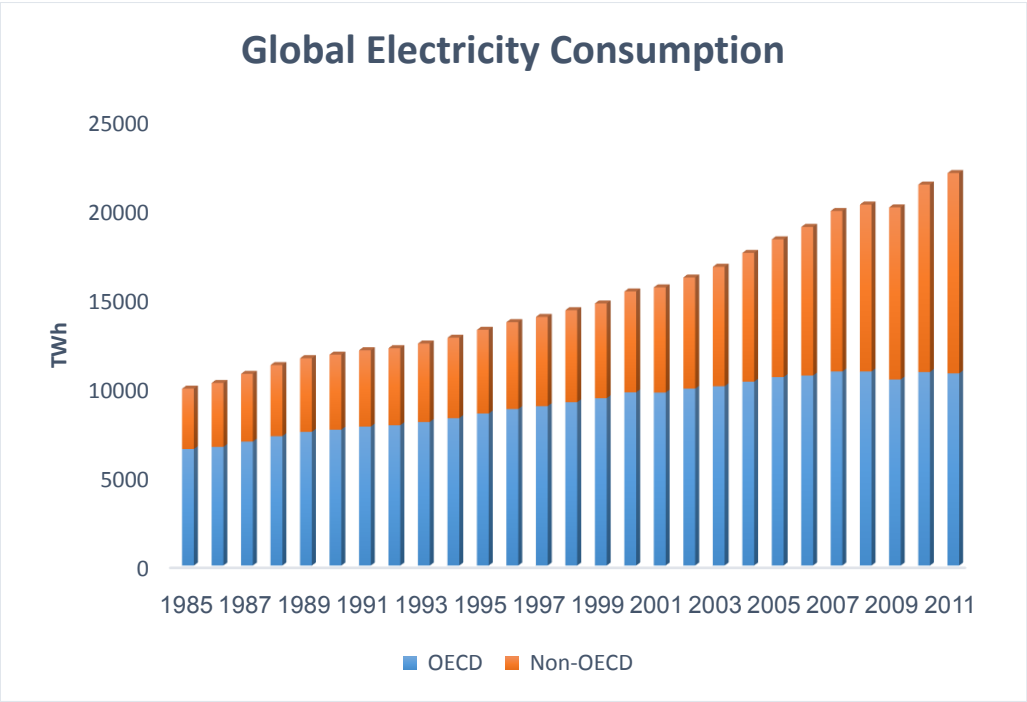


FIG 1.2 – Global Electricity Consumption 1985-2011 [1]

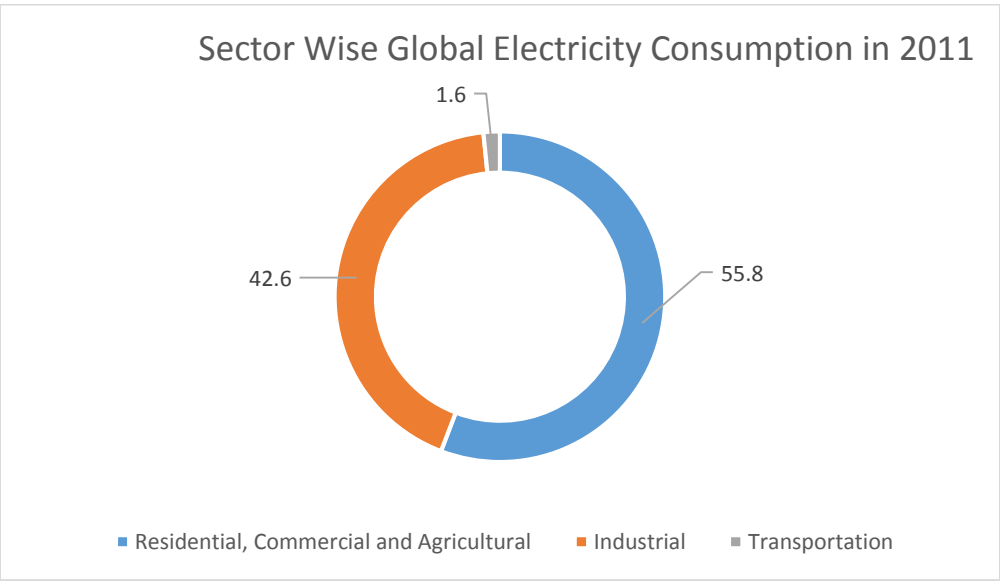
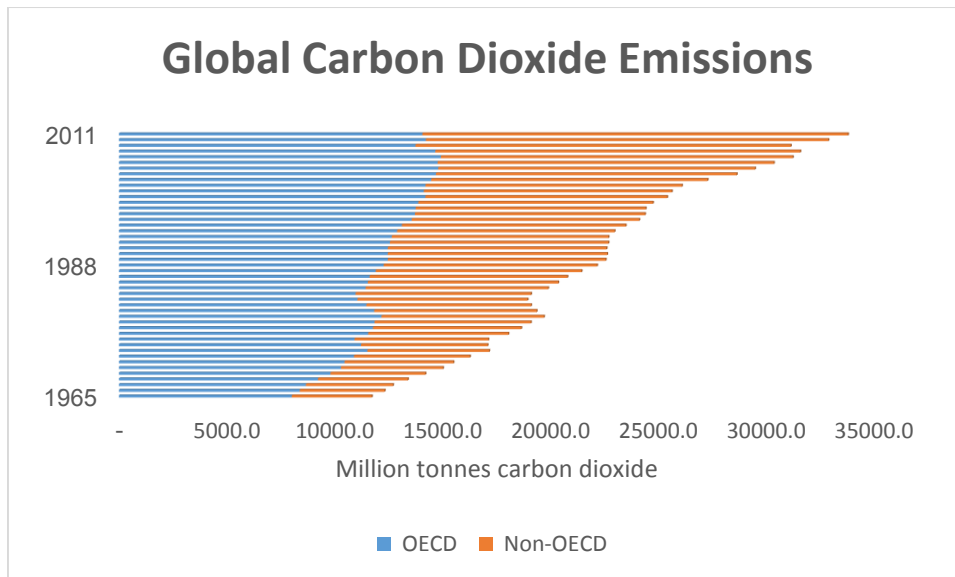


FIG 1.3 – Sector wise Global Electricity Consumption in 2011 [1]

Still in 2011 Fossil fuels have been the major source of generation of electricity with Coal, Natural gas and Oil producing 41.3%, 21.9% and 4.8% of electricity respectively, while the remaining electricity is generated by Hydro 15.8%, Nuclear 11.7% and Renewable Sources 4.5%. The carbon emissions from fossil fuels pose a serious threat to eco system and are culpable for global warming crisis [1].



*FIG 1.4 – Energy Related Global Carbon Dioxide Emissions 1965-2011*  
[2]

It is projected that, by 2035 the energy related Carbon Emissions alone will rise to 37.2Gt from 32.34 Gt in 2011 consequently resulting in a long term global temperature increase of 3.6°C which is far above the international allowable limit of 2°C. This increase in Carbon Emissions which is contributed majorly by the excessive use of fossil fuels can be quelled by the use of alternate energy resources [2].

## **1.2 World Renewable Energy Outlook:**

In 2011, Renewable Energy resources met 13% of the global primary energy demands. The primary Renewable Energy Demand is forecasted to increase to 18% in 2035 [3]. This projected increase in primary Renewable Energy Demand is induced by the advancement in Renewable Energy technologies, achievement of Economics of scale, enforcement of Carbon Pricing, Depletion of fossil fuels resources and increase in prices of fossil fuels.

Very steadily, Renewable Energy resources are becoming a part of global power generation mix and are projected to grow strongly. The global primary Renewable Energy power generation is projected to increase by over 7000 TWh between 2011 and 2035 from 4482 TWh to 11612 TWh [3]. The share of

renewable energy resources in global power generation stands at 20% in 2011 and is projected to rise to 26% in 2020 and 31% by 2035 [3]. Rapid increase in utilization of wind and solar photovoltaic technologies is projected complemented by a steady increase in hydropower, geothermal and bio-energy resources in the energy mix.

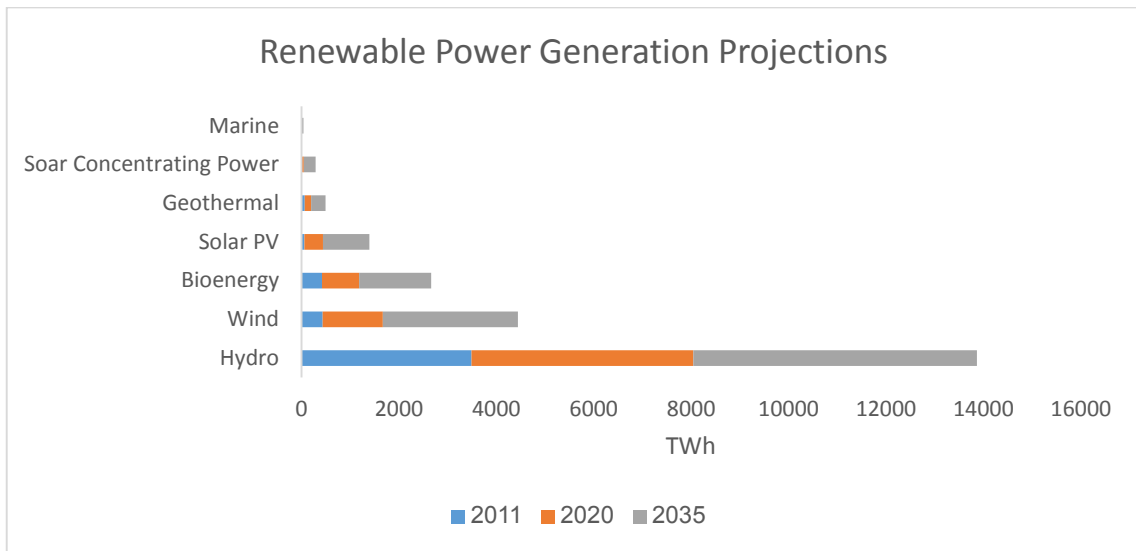


*FIG 1.5 – Renewable Power generation projections 2020-2035 [3]*

It is also projected that the rapid penetration of renewable in the power generation sector shall draw 62% of all investments in the power generation sector. Renewable energy is projected to emerge as the second largest power generation sources by 2015 and is forecasted to approach coal as the largest power generation source by the end of 2035 [3]. There is major shift from fossil fuels towards renewable fuels in Non OCED countries with 53% share of global renewable power generation in 2011 to 62% in 2035 [3].

### **1.3 Pakistan Energy Outlook:**

The burgeoning energy crisis that the beleaguered country is battling with has been one of the major hurdles in the economic growth during the current fiscal year. The energy crisis has aptly complemented the prevalent structural problems like escalating security issues, ever rising inflation, precipitously declining investments, and low tax revenues, thus declining the GDP growth. The



hefty amount of subsidy government has to bear on power and losses in the state run enterprises have further exacerbated the economic situation. The energy crisis that seems to have engulfed the whole country, is neither an aberration nor an unexpected phenomenon, rather it is an outcome of years of neglect and lack of proper planning, which is likely to intensify in the years to come. During the FY2012-13 the average system computed Electricity demand had been approx. 14800MW and the peak hour shortfall had been 3400 MW on average [4].

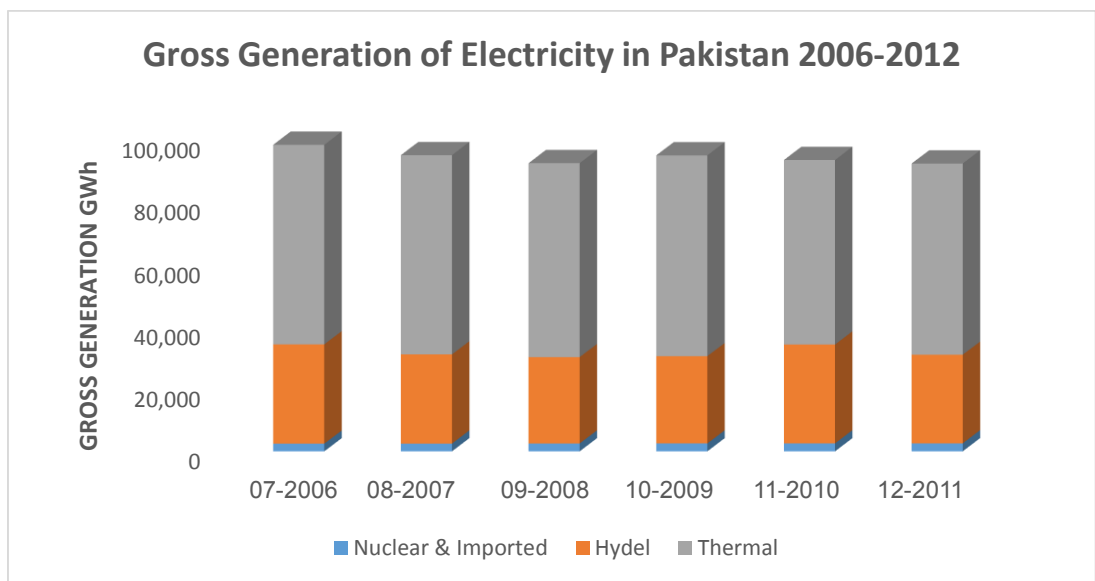


FIG 1.6 – Gross Electricity Generation in Pakistan 2006-2012 [4]

The energy policy of Pakistan is characterized by overreliance on fossil fuel. Out of 95,365 GWh produced in FY 2011-12 35.2%, 29.03%, 0.1%, 29.9%, 5.8% of the electricity has been produced from Oil, Gas, Coal, Hydel and Nuclear resources respectively. 4720 MW of WAPDA, 2381 MW of KESC and 8353 MW of 27 IPPs' installed capacities are fossil fuel based. The status of supply of fossil fuel is yet another alarming situation. During the FY2012-13, the daily demand of Furnace Oil ranged from 37450 Metric Tons to 28000 Metric Tons which was partially met by the supplies and the shortfall of 14900 to 4000 Metric Tons marred the power generation in Thermal Power Plants. Power Plants operating on natural gas suffered more adversely by the acute shortage of natural gas, the supply of which was short by 800 to 140 MMCFD against the demands ranging from 1705 to 222 MMCFD. This sorry state of affairs speak volume of the lack of planning on the part of government that despite the forecast of tight supply

of fossil fuel, emphasis had been on thermal power generation and 1214 MW of IPPs and 560 MW of KESC were added to the Installed National Thermal Power generation capacity in 2011 thus increasing the share of thermal power generation from 57.2% in 2010 to 62.9% in 2011. Though the installation of thermal power plants initially helped in ameliorating the energy situation on short term basis, it resulted in substantial increase in power tariff and aggravating the fossil fuel shortage for transportation and industrial sectors. The tariff of IPPs range from Rs. 5.5/kWh to as high as Rs. 18/kWh for flexi fuel power plants running on High Speed Diesel in case of unavailability of Natural gas. [4]

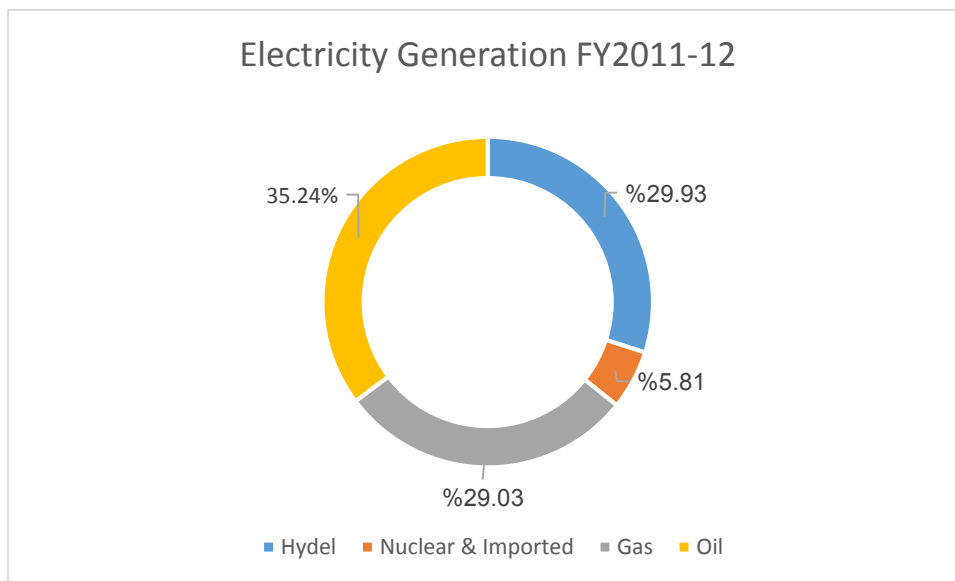


FIG 1.7 – Electricity Generation in Pakistan 2011-12 [4]

By virtue of its geographical location, Pakistan has been blessed with abundant water resources but due to the insufficient storage capacity only 13 % of the annual flow could be stored. The current storage capacity of Pakistan is around 16 Million Acres Feet out of the total annual flow of 136 MAF. The current storage capacity is also fast depleting due to excessive inflow of the sediments with the river water. It has been projected that by the year 2025, the current storage capacity will reduce by 6.27 MAF. Out of the economically viable 52980 MW of Hydro Power potential, the installed capacity lies at 4900 MW. The power generation of installed Hydro Electric Power Stations ranged between 4200 & 4700 MW. The cost hydroelectric power had been as low as Rs. 1.5-2/kWh. [4].

Pakistan is also blessed with tremendous coal reserves. It has been estimated that the coal reserves of Pakistan are more than 185 billion Tons, which are the fourth largest reserves in the world. Out of 185 billion Tons, 175 Billion Tons of coal lies in Tharparker, Sindh alone. However, in contrast to 40% share of coal in power generation in the world, only 7% of the power is derived from coal in Pakistan. Although the coal available in Pakistan is of mediocre quality, low calorific value (12.68 MJ/Kg), high moisture content and high stripping ratio (6 cu.m/ton) [4], the unavailability of basic infrastructure also adds to the cost of Power generation through coal, still coal is one of the most economically viable options. PPIB has issued LOI for establishing one 1200 MW Coal Fired Power Plant in Thar and a 405 MW Plant at Sonda Jherruk. PPIB is also working on a 1200 MW Imported Coal Fired Power plant at Karachi and a 300 MW imported Coal based power plant in Jamshoro.

Nuclear Power accounts for 3% of the Power produced in Pakistan. The commissioning of Chasnup-II in March 2011 was a major highlight for the year 2011 and the plants adds 300MW to the National Grid. [4]. However, Kanupp at Karachi with a power generation capacity of 137 MW has completed its design life and is destined for decommissioning in 2015. PAEC is also working on a 1200 MW Kanupp-II Power plant at Karachi.

Pakistan produces 0.05% of its total energy by Renewable Energy means. However 10,000MW of Solar Energy and 20,000MW of Wind energy has been found economically viable by PCRET. Three Projects of 50 MW each are in progress at Jhampir and Gharo for the generation of Wind Power by ZulroEnergi, FFECL and Foundation Wind Energy Ltd. On May 29, 2012 a 356kW Solar PV plant has been inaugurated at Islamabad which has marked Pakistan's entry in to generation of commercial Solar Energy. [4]

## 1.4 Geothermal Energy:

Geothermal energy is the internal energy stored inside the Earth surface, flowing towards the surface of the Earth at the rate of 44.2 TW [4], this internal energy was stored inside the Earth surface during the formation of Earth and it replenishes naturally by the radioactive decay of minerals, tectonic, seismic and volcanic activities and solar heat absorption in the Earth surface. [5]



*FIG 1.8 – Global Technical Geothermal Energy Potential [7]*

The theoretical Global Geothermal Energy potential is estimated to be  $42 \times 10^6$  EJ, with the current global energy consumption at 500EJ/year, geothermal energy has the potential to fulfill the global energy requirements for next 100,000 years. [6] However, due to technological impediments, it is impossible to extract all the geothermal energy.

Geothermal energy is available at each and every place in the Earth but since it is not economically and technically feasible to extract the energy at all places, generally a place with a thermal gradient of  $3.1^{\circ}\text{C}/100\text{m}$  can qualify to be a potential geothermal energy extraction source. [8]

Mankind has been using geothermal energy since ages for medicinal purposes especially for bathing since geothermal fluid is rich in minerals which was later expanded to spas, swimming pools, fish farms and green houses.

Technological advancements in early twentieth century enabled geothermal energy to be used as a source for electricity generation. The first geothermal power plant was commissioned on July 4, 1914 at Larderello, Italy to generate 250 KW of electricity to run pumps to extract boric acid from volcanic mud [9]

### **1.5 Scope and Purpose:**

The purpose of the present study is to carry out the analysis of available geothermal resources to check the possibilities of geothermal power generation in Pakistan.

Different cycle configuration are analyzed keeping in view the resource potential in country. Exergy and energy analysis is carried out for optimization of working fluid and working conditions. The performance of each configuration of cycle has been analyzed in terms of energetic & exergetic efficiency, exergy destruction rate, fuel depletion ratio, relative irreversibility and productivity lack.

### **1.6 Thesis Outline:**

Chapter 1 of the Thesis comprises of thesis objective, motivation and introduction to the concept of geothermal generation. Chapter 2 elaborates the geothermal power generation and power generation cycles, Chapter 3 analyses the geothermal resources of Pakistan. Chapter 4 reviews the literature on geothermal power generation. Chapter 5 elucidates the Mathematical Modelling Process and Chapter 6 analyses the results obtained from Mathematical Modelling. Chapter 7 concludes the thesis with the recommendations.

## CHAPTER - II

### GEOTHERMAL ENERGY

#### 2.1 World Geothermal Energy Outlook:

Currently geothermal Energy is being used directly (district heating, spas, swimming pools, desalination, fish farming, green houses and several agriculture and industrial application) as well as indirectly (for power generation).

The theoretical potential for direct utilization is 61.4 EJ/Year out of which 10.092 EJ/Year can be exploited for direct consumption economically [10], the current installed capacity for direct utilization of geothermal energy stands at 50583 MW. [11]

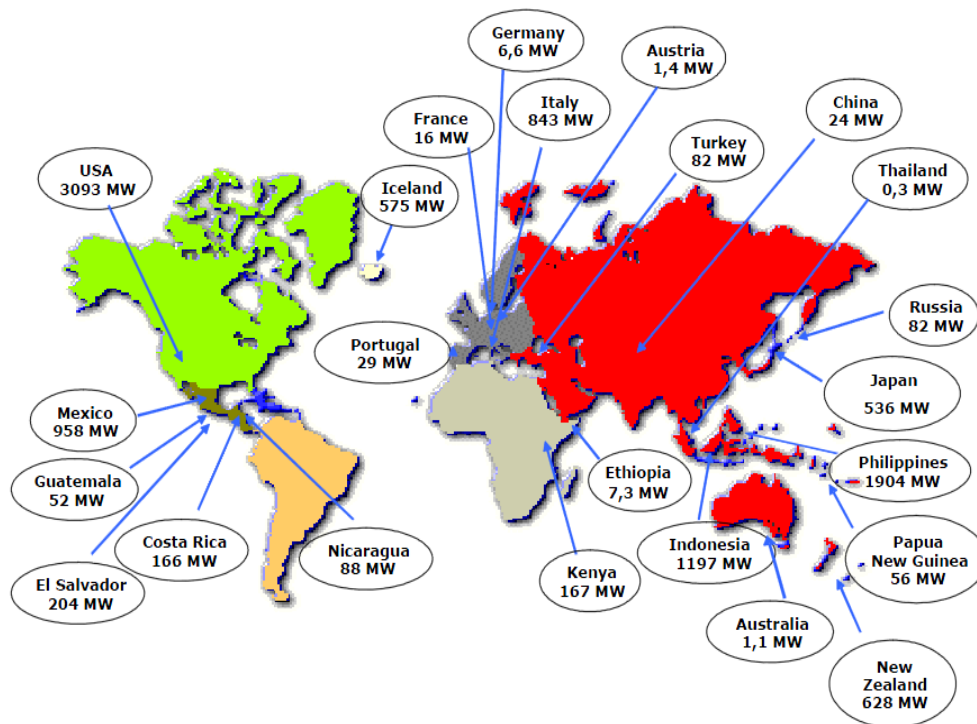


FIG 2.1 – Global Geothermal Power Generation Capacity in 2010[10]

The current installed capacity of geothermal power generation stands at 10,715MW as of 2010 producing 67TWh of electrical power. It is projected that the installed capacity will reach 18500MW by the end of 2015 producing 116TWh of electricity. This rapid increase power generation capacity is due to development of Binary ORC based power plants which have enabled to exploit

the medium and low temperature geothermal energy resources for economic electric power generation. [10]

It is projected that if the current Enhanced Geothermal System (EGS) pilot projects are successful, the geothermal power generation capacity will reach 140GW corresponding to generation of 66EJ/year by 2050. By 2050 geothermal energy will be fulfilling 8.3% of global power requirements, serving 17% of the global population and reducing CO<sub>2</sub> Emissions by 1000 Million Tons per year. [10]

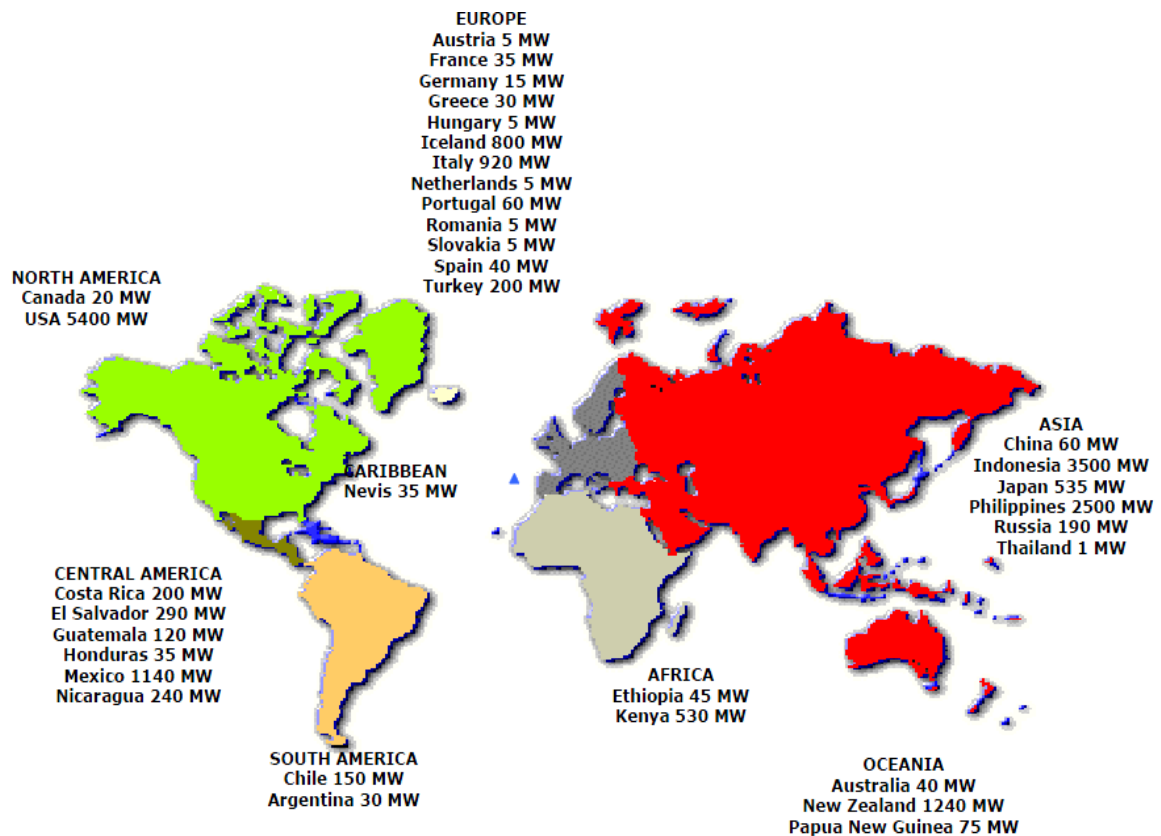


FIG 2.2 – Global Geothermal Power Generation Projections for 2015 [10]

## 2.2 Classification of Geothermal sources:

Geothermal sources are classified on the basis of geo fluid temperature, during literature survey it is elicited that several authors have used different temperature ranges for classification, a summary of which is provided in the table:

Source	Muffer and Cataldi [12]	Hochstein [13]	Benderitter and Cormy [14]	Haenal et al. [15]
Low	<90°C	<125°C	<100°C	<150°C
Medium	90°C-150°C	125°C-225°C	100°C-200°C	-
High	>150°C	>225°C	>200°C	>150°C

TABLE 2.1 – Classification of Geothermal Energy Sources [12, 13, 14, 15]

### 2.3 Geothermal Power Generation:

Before the advancement of geologic exploration, deep drilling and power generation technologies the exploitation of geothermal power was limited to areas of hydro geothermal manifestations, where sub terrain reservoir of hot geo fluid or steam are present [16] and can be extracted at highest temperature from the aquifer at the edges of tectonic plates, sedimentary hot rocks, magmatic or volcanic sites and hot fractured granite [5]

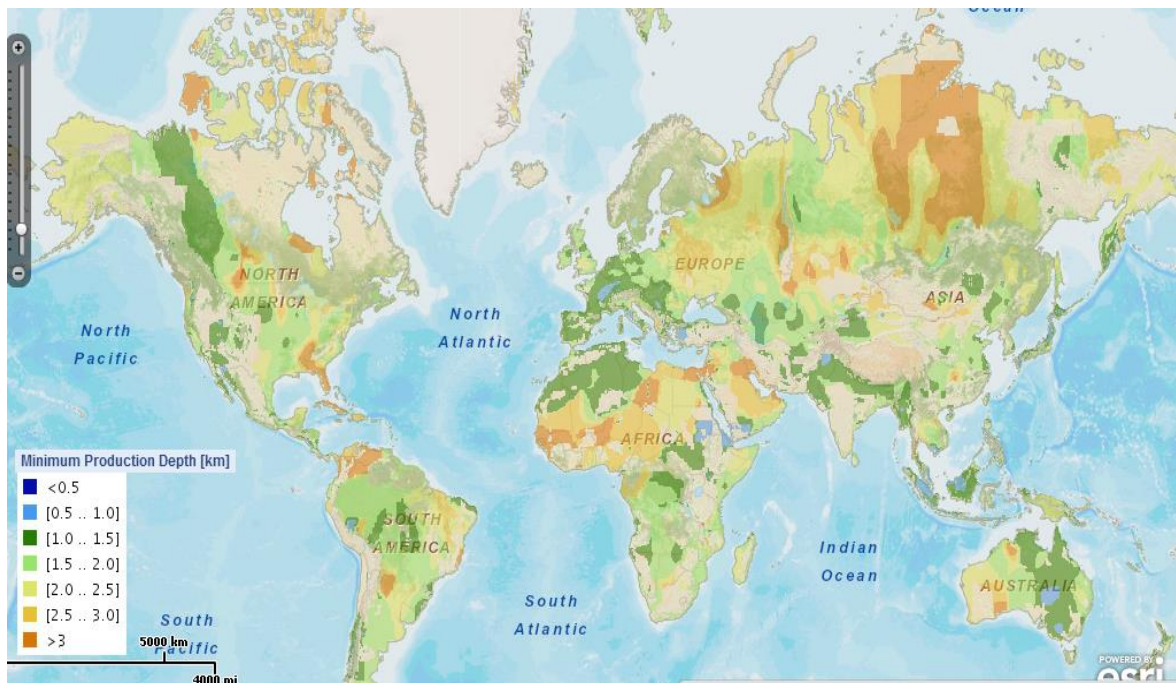


FIG 2.3 – Minimum Geothermal Energy Production Depth (where the temperature is at least 40°C above the surface temperature)

[7]



However, with the advent of technology, new power cycles and deep drilling techniques have enabled the geothermal energy to be extracted wherever the thermal gradient lies in the favorable range [5]. Now the geothermal energy can be extracted by drilling a hole at the surface around 200m to deep underground at 2Km below the surface depending upon the thermal conductivity, heat storage capacity, porosity and degree of saturation of hot rocks and sediments and vicinity of magma energy chambers or reservoirs of hot geo fluid. [17]

A new technology in the field of geothermal power generation called enhanced Geothermal Systems has enabled exploitation of petro thermal or deep crust geothermal energy reservoirs by pumping of pressurized water to drilled hole which after heat transfer is pumped back to the surface at very high temperature and pressure. [10]

#### **2.4 Classification of Geothermal Power Generation systems:**

The mechanical power required to generate electricity is derived from steam which runs the turbine. The steam extracted from geothermal sources can either be dry or wet or it can be generated by flashing the high temperature and high pressure geo fluid. From low and medium, water dominated resources, steam is generated by using the hot geo fluid to evaporate a low boiling point binary working fluid.

So the geo thermal power plants can be categorized on the basis of their mode of operation in to three broad categories, a) Dry Steam Power Plants b) Flash Power Plants and c) Binary Power Plants. This classification is based upon geothermal fluid temperature and quality. Clauser C. 2006 [18] has classified the types of geothermal power plants according to unit power and geothermal fluid temperatures.

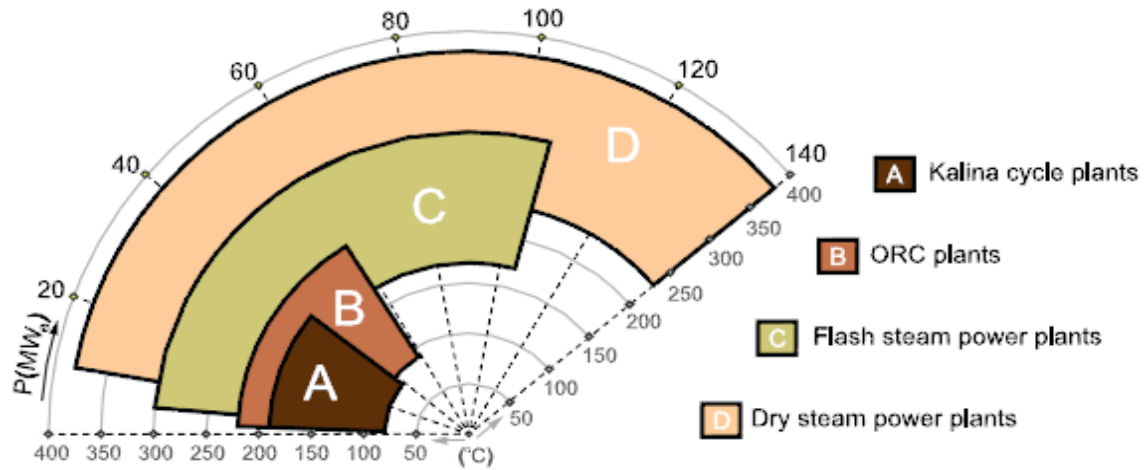


FIG 2.4 – Application Ranges of Geothermal Power Plants [18]

Out of 526 Geothermal Power Plants in operation in 2010, producing 10715 MW of electricity, the highest number of power plants i.e.; 236 units are binary power plants but since the average capacity per unit is very low at 5 MW/unit for binary power plants the total installed capacity of binary power plants in 1178 MW. 145 back pressure power plants with an average capacity of 6MW/unit produce 145 MW. Dry Steam Power plants have the highest average capacity of 46 MW with 62 units in operation producing 2878 MW. 141 Single flash Power Plants with average capacity of 31MW produce 4421 MW and 61 Double Flash Power Plants with average capacity of 34MW/unit produce 2092MW of electricity. [10]

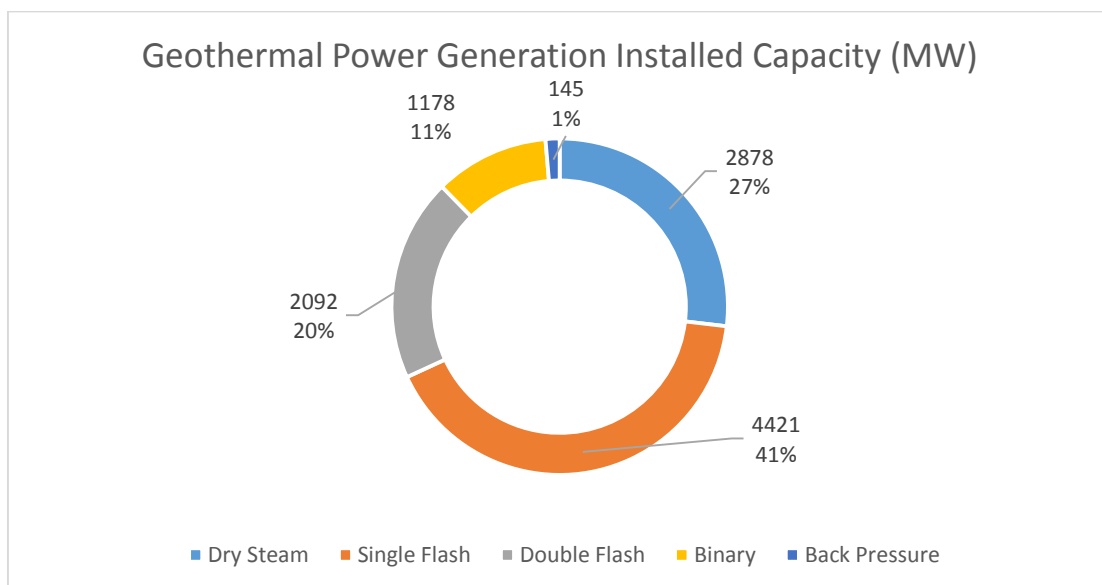


FIG 2.5 – Geothermal Power Generation Installed Capacity [10]

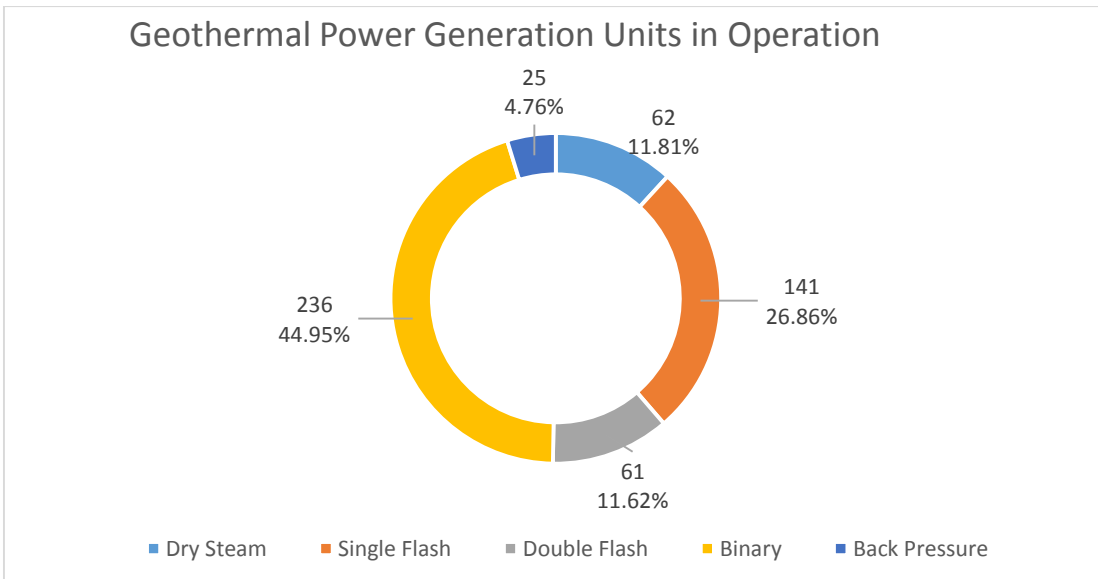


FIG 2.6 –Geothermal Power Generation Units in Operation [10]

**2.4.1 Dry Steam Geothermal Power Plants:**

Reservoirs with geo fluid temperature above 170°C [5] consist of dry steam with a minimal amount of hot water. The steam is used to drive the steam turbine to generate electricity. Once expanded the steam is condensed in the condenser and the condensate is pumped back to the geothermal reservoir for replenishment. [19]

Dry Steam geothermal power plants are single cycle power plants and resemble the conventional thermal power plants in operation. Dry Steam geothermal power plants have the highest per unit generation capacity amongst all the geothermal power plants. Various units of Dry Steam geothermal power plants are in operation like 120 MW Plant at The Geysers, California USA, 57 MW Plant at 110 MW Plant at Darajat, Indonesia, 60 MW plant at Nuova Serrazzano and 57 MW Plant at Sonoma, USA to name a few. [10]

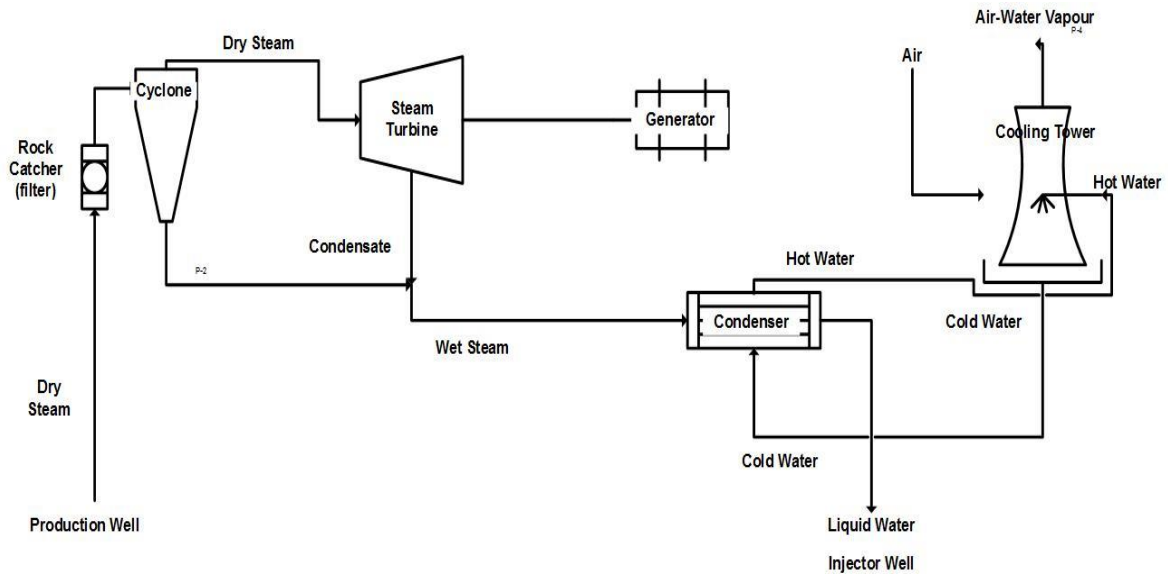


FIG 2.7 – Dry-steam Geothermal Power Plant [19]

#### 2.4.2 Flash Geothermal Power Plants:

Geothermal resources producing high pressure liquid geo fluid at temperatures above 150°C [5] can be exploited by using the flash power plants. Flash Power plants are single cycle systems in which high pressure high temperature geo fluid is evaporated in to vapor state in of pressure tanks. Upon expansion followed by condensation in the condenser, the condensate is pumped back into the geothermal well. [19]

For double flash power plant configuration, the high pressure geo fluid is flashed in two different pressurized tanks to yield steam at two different pressures for high and low pressure turbines respectively. [5]

Several Flash Power plants are in operation, 117 MW Single Flash Plant at Wayang Windu Indonesia, 78 MW Single Flash Plant Malitbog Philippines, 55MW Single Flash Plant at Guanacaste, Costa Rica, 100 MW Double Flash Plant at Kawerau, New Zealand, 110 MW Double Flash Plant at Cerro Prieto III, Mexico and 63 MW Double Flash Plant at Mak-Ban, Philippines are some examples. [10]

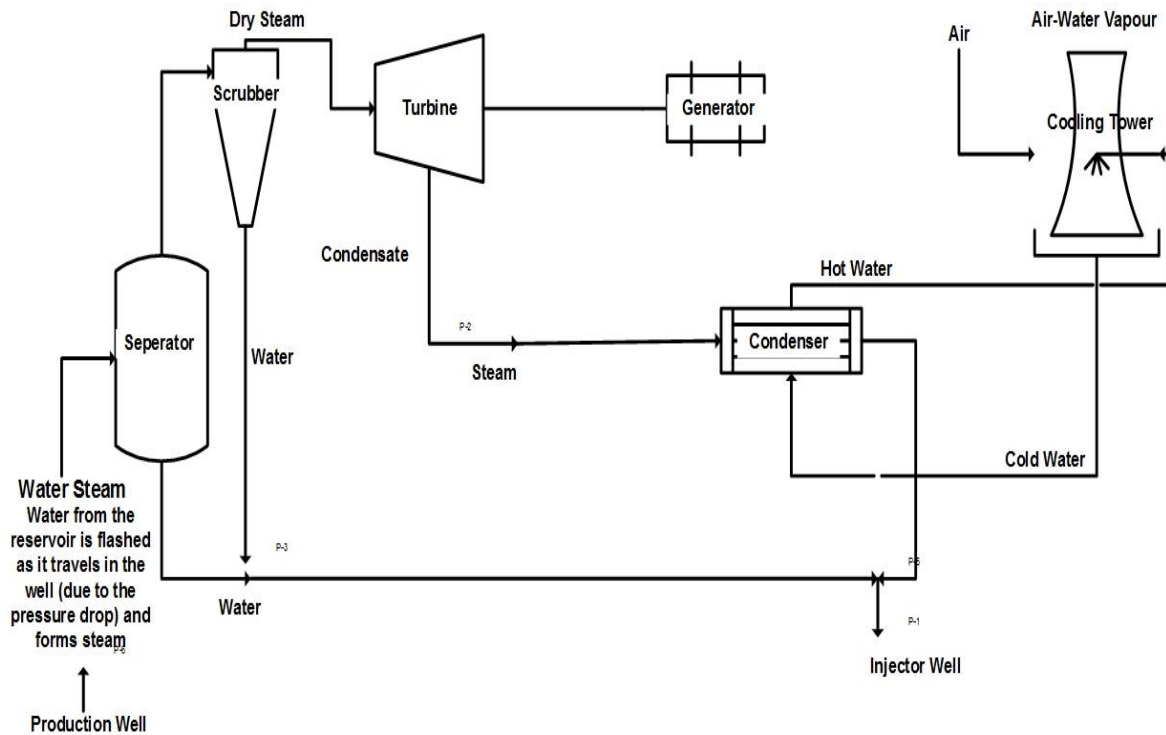


FIG 2.8 – Flash Geothermal Power Plant [19]

### 2.4.3 Binary Geothermal Power Plants:

The dual cycle binary geothermal power plants utilize the heat from the moderate pressure geo fluid at temperatures below 150°C [5] to evaporate a low boiling point and high vapor pressure binary fluid in a closed pipe heat exchanger. The evaporated binary fluid is then used to drive the turbine and the geo fluid after condensation is pumped back to the geothermal well for replenishment and maintaining the source pressure. A wide variety of geo fluids can be used with the binary geothermal power plants, Kalina Cycle based Binary power plants operates on mixture of water and ammonia as working fluid, whereas a host of working fluids can be used for an Organic Rankine Cycle based binary geothermal power plants like, Hydro Carbons (HC), Hydro Fluoro Carbons (HFC), Hydro ChloroFloro Carbons (HCFC), ChloroFloro Carbon (CFC), Fluoro Carbons (PFC), Siloxanes, Alcohols, Aldehydes, Ethers, Hydrofluoro Ethers (HFE), Amines, Zeotropic and Azeotropic Mixtures And Organic Fluids. [20].

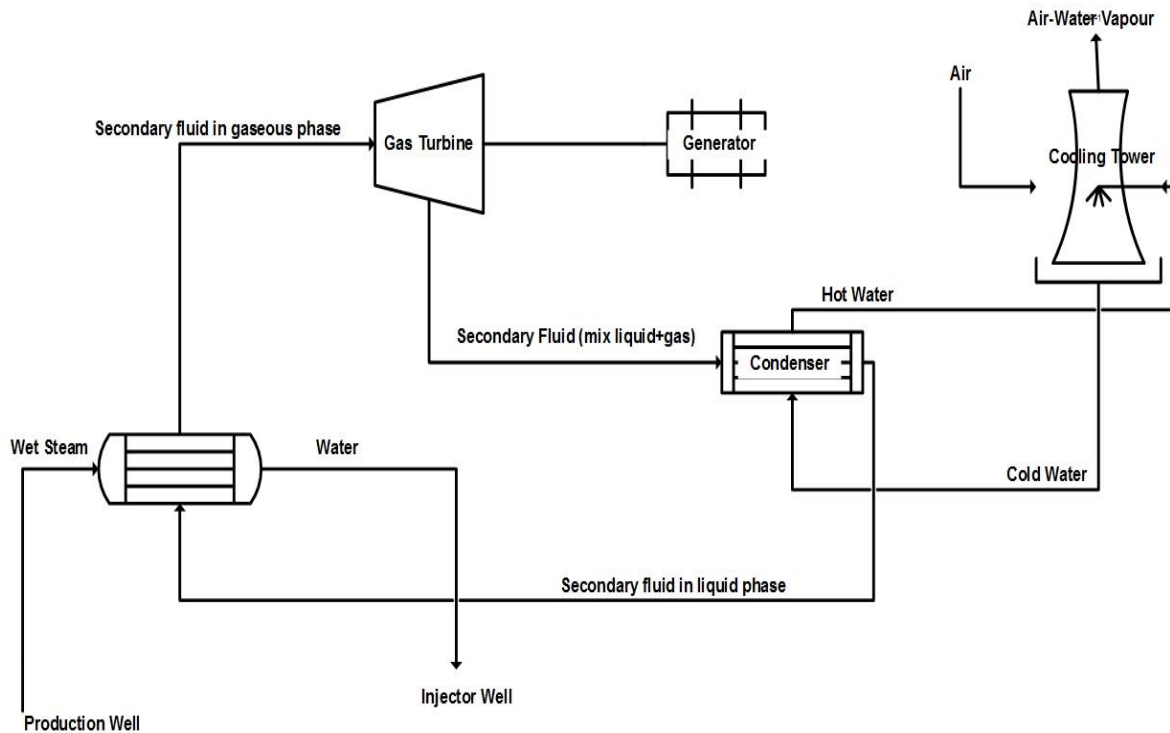


FIG 2.9 – Binary Geothermal Power Plant [19]

Currently 236 binary geothermal power plants are in operation, the most prominent among them are 65 MW binary geothermal power plant at Heber, California, USA, 49 MW binary geothermal power plant at North Brawley, USA, 13 MW binary geothermal power plant at Raft River USA and 24 MW binary geothermal power plant at Amatitlán, Guatemala. [10]

#### 2.4.4 Hybrid Geothermal Power Plants:

A hybrid geothermal power plant utilizes both steam and hot liquid extracted from the geothermal source to generate electricity by combining two or more geothermal power generation technologies [5]

##### 2.4.4.1 Direct Steam Binary or Back Pressure Geothermal Power Plants:

Direct Steam Binary or Back Pressure Geothermal Power Plant utilizes the steam from a geothermal source to run a dry steam turbine, the back pressure exhaust of that dry steam turbine is used to evaporate a binary fluid which is used to run a binary fluid turbine. [21]

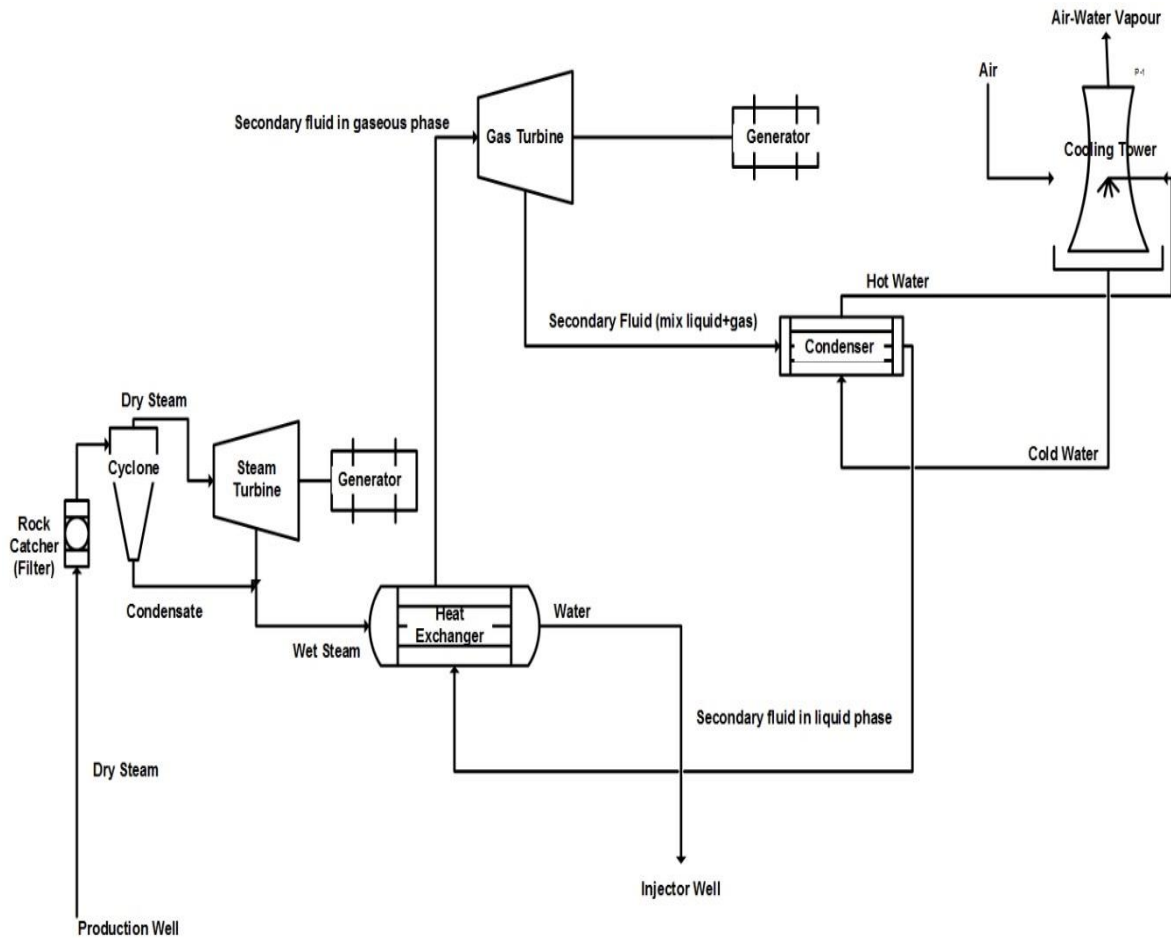


FIG 2.10 –Dry Steam Binary Geothermal Power Plant [19]

Examples of dry steam binary hybrid plants are 10.8 MW at Millard and Beaver, Utah, USA, 5 MW dry steam binary hybrid plant at Los Humeros, Mexico and 10 MW dry steam binary hybrid plant at San Jacinto-Tizate, Nicaragua. [21]

#### 2.4.4.2 Single Flash Binary Geothermal Power Plants:

Single Flash Binary Power plant utilizes a combination of single flash and binary power plant configurations. The hot water from the flash tank after flashing is used to evaporate a binary fluid that is used to drive a binary turbine. [21]

A 25 MW Single Flash Binary Power plant is operational at Puna, Hawaii [21]

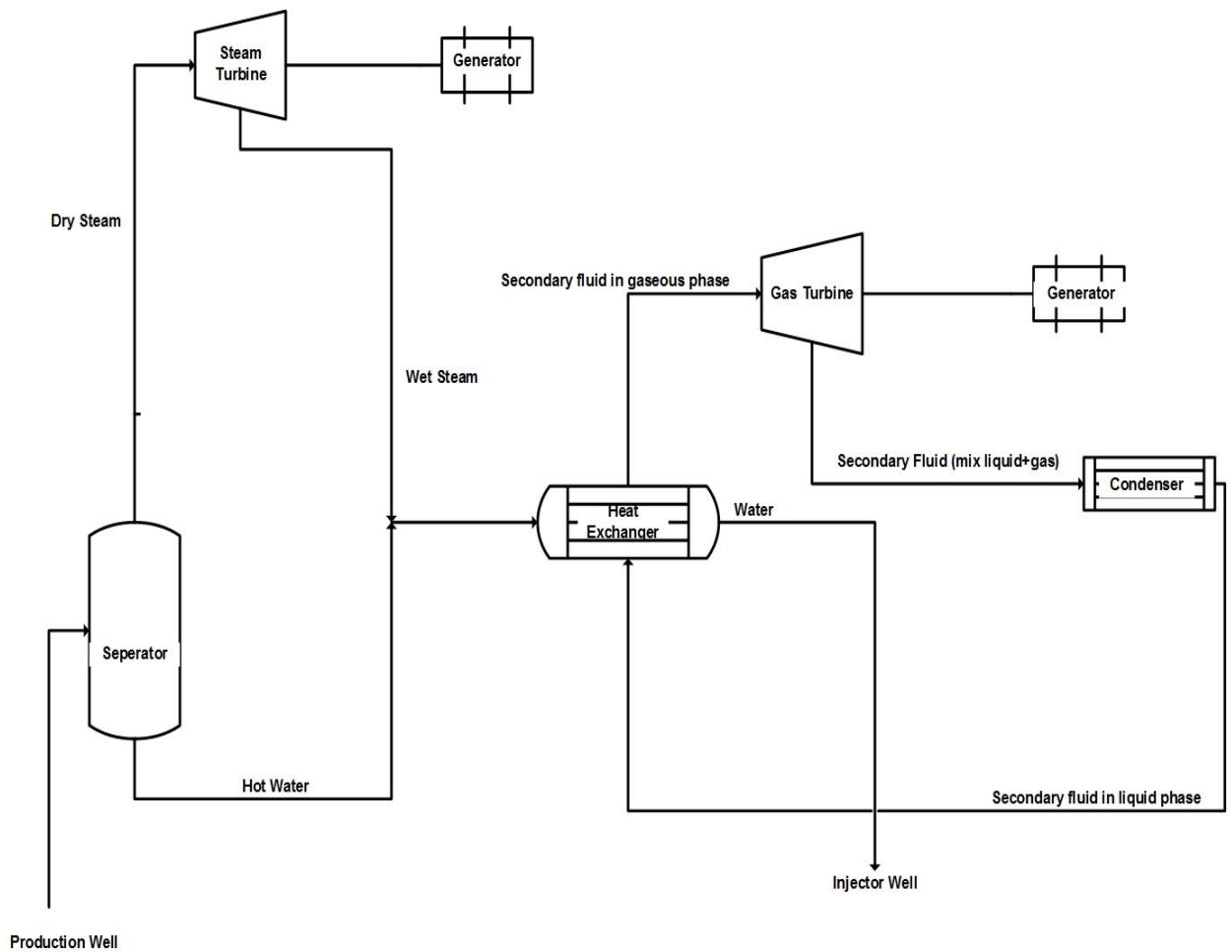


FIG 2.11 – Single Flash Binary Geothermal Power Plant [19]

#### **2.4.4.3 Integrated Single and Double Flash Binary Geothermal Power Plants:**

In this configuration the waste hot geo fluid from the evaporator tank of the single flash system is flashed again to a lower pressure tank by an orifice plate or control valve into a low pressure vapor or steam. This steam is expanded in a low pressure turbine or a dual pressure dual admission turbine of double flash power plant. [21]

Examples are 180 MW Integrated Single and Double Flash Binary Geothermal Power Plant at Cerro Prieto Mexico and 95 MW Integrated Single and Double Flash Binary Geothermal Power Plant at Ahuachapán, El Salvador [21]



#### **2.4.4.4 Hybrid Fossil Geothermal Power Plants:**

A hybrid fossil geothermal power generation system utilizes the heat from the geothermal fluid to pre heat the feed water of the conventional fossil fuel power plant. Alternatively, the hot exhaust from a conventional fossil fuel power plant can effectively be used to superheat the geo fluid for use in a dry steam or flash type geothermal power plant.

A 30 MW hybrid waste wood and geothermal power plant is operational in Honey Lake, California, USA. [21]

## CHAPTER III

### GEOTHERMAL ENERGY RESOURCES IN PAKISTAN

#### 1.1 Geothermal Energy Potential in Pakistan:

The theoretical potential of Geothermal energy in Pakistan is quite high with more than one third of the total area lying in the potential geothermal energy zone, Karakorum–Himalayan thrust zone and Nanga Perbat Haramosh Massif constitute the area with the highest theoretical potential in the range of 450-500 PJ/Km<sup>2</sup> and the Indus basin area with moderate theoretical potential of 300-350 PJ/Km<sup>2</sup> and the Indus basin area with moderate theoretical potential of 300-350 PJ/Km<sup>2</sup> [7]

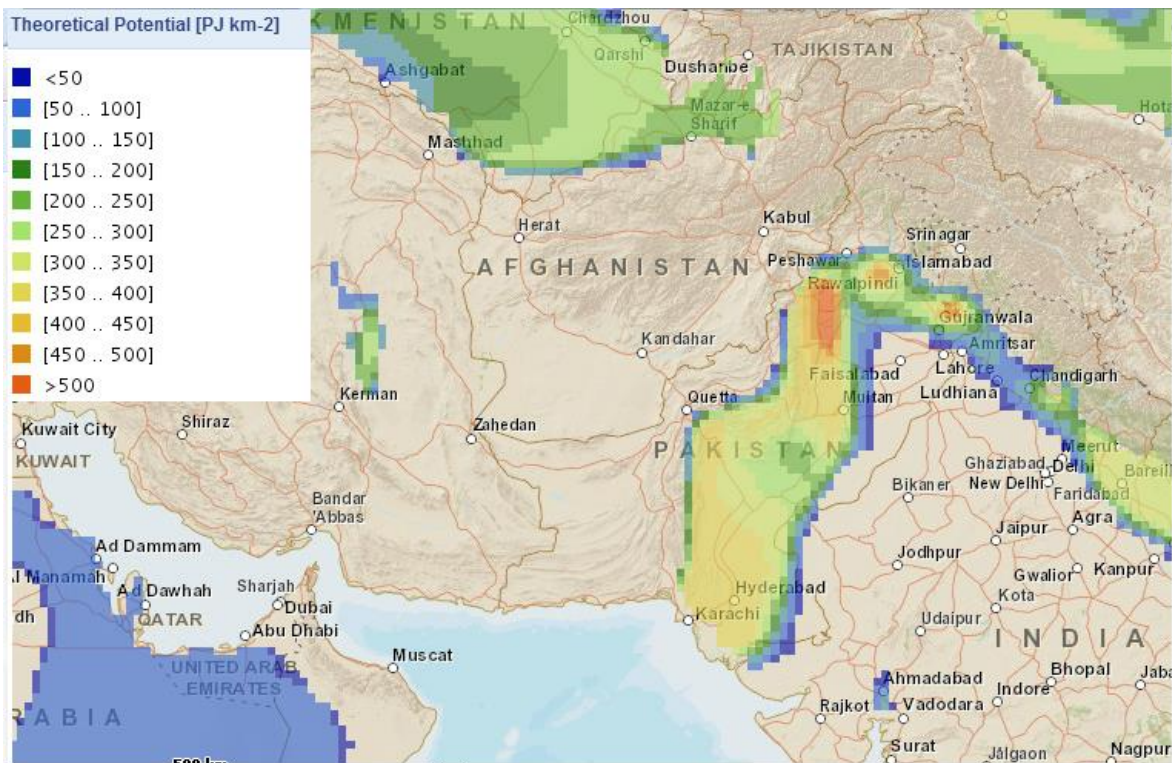


*Fig 3.1 Theoretical Potential of geothermal resources in Pakistan [7]*

The technical potential of exploitable geothermal resources in Pakistan is rather high, due to the availability of geothermal resources at lesser depths. In the range of 1 to 1.5 km, where the resources in the Karakorum–Himalayan thrust zone and Nanga Perbat Haramosh Massif zone can be exploited at the depth of

0.5 to 1km which is also evident from the several hydro geothermal manifestations in the area. [7]

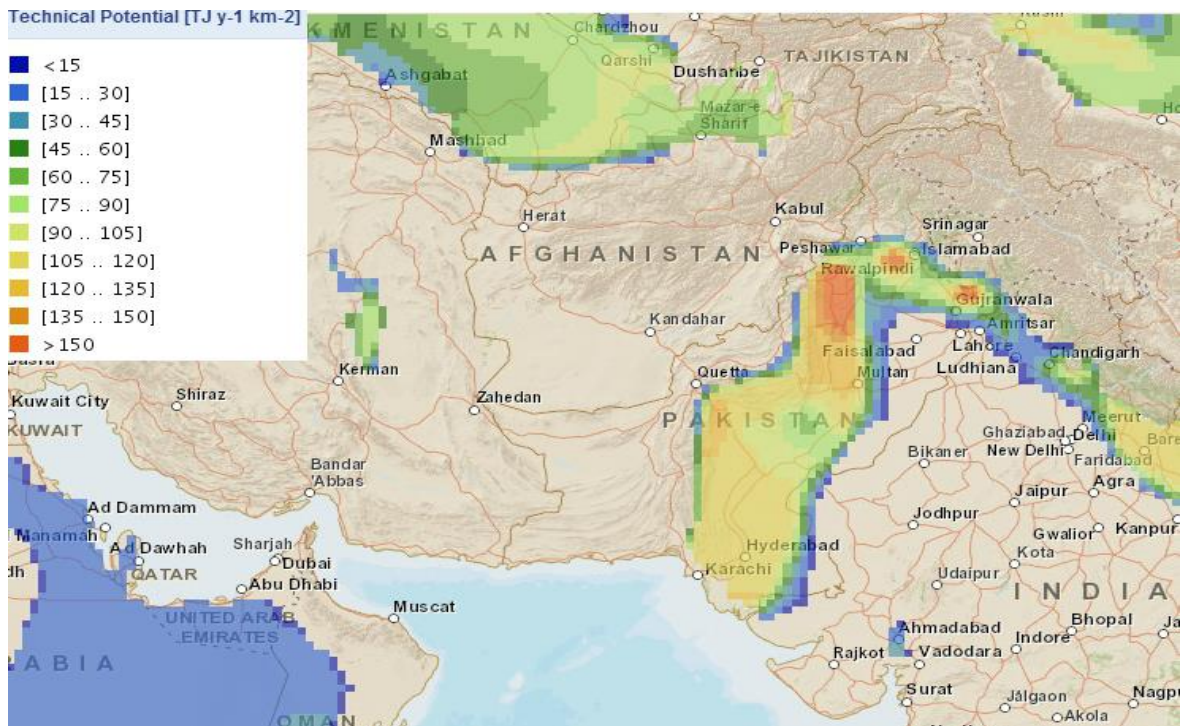


Fig 3.2 Technical Potential of geothermal resources in Pakistan [7]

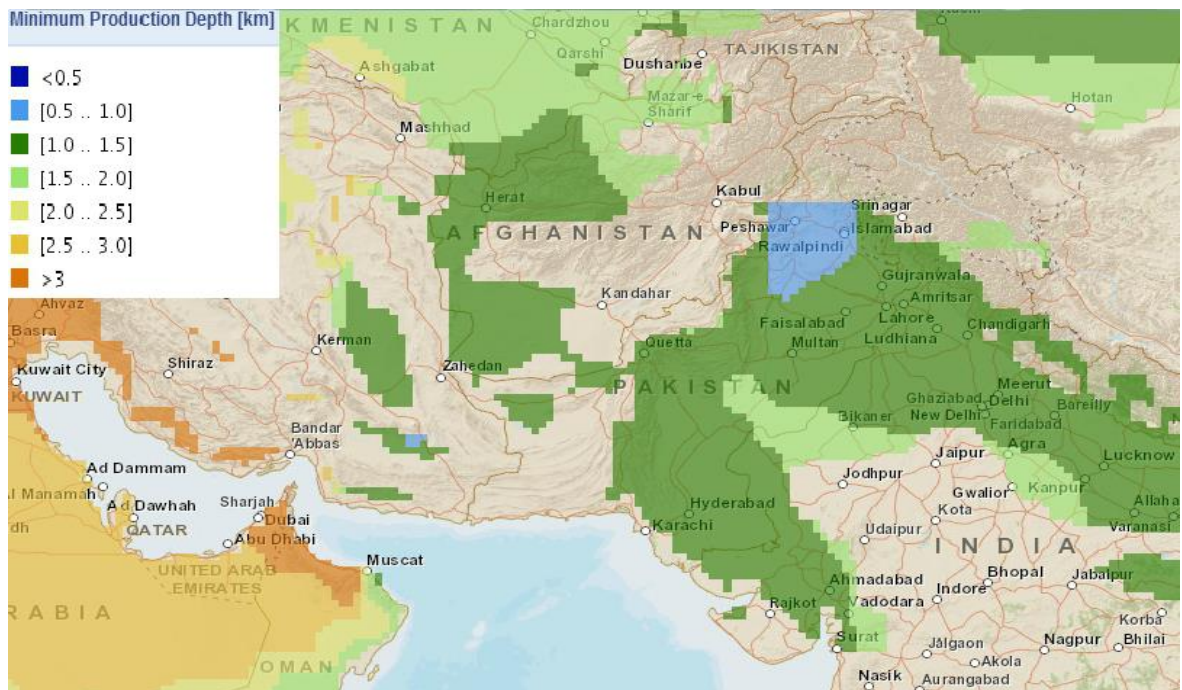


Fig 3.3 Minimum Production Depth of geothermal resources in Pakistan [7]

The maximum production temperature of geothermal areas in Pakistan lie in the range of 105°C to 150°C for low potential areas mainly in the Indus River Basin and 150°C to 180°C in the high potential areas in the mountainous thrust regions. Which according to the geothermal resource classification lie in the Low and Medium Temperature Resources domain [12, 13, and 14]. The performance Index of geothermal resources in Pakistan ranges from good to very good in the Karakorum–Himalayan thrust zone and Nanga Perbat Haramosh Massif zone [7]

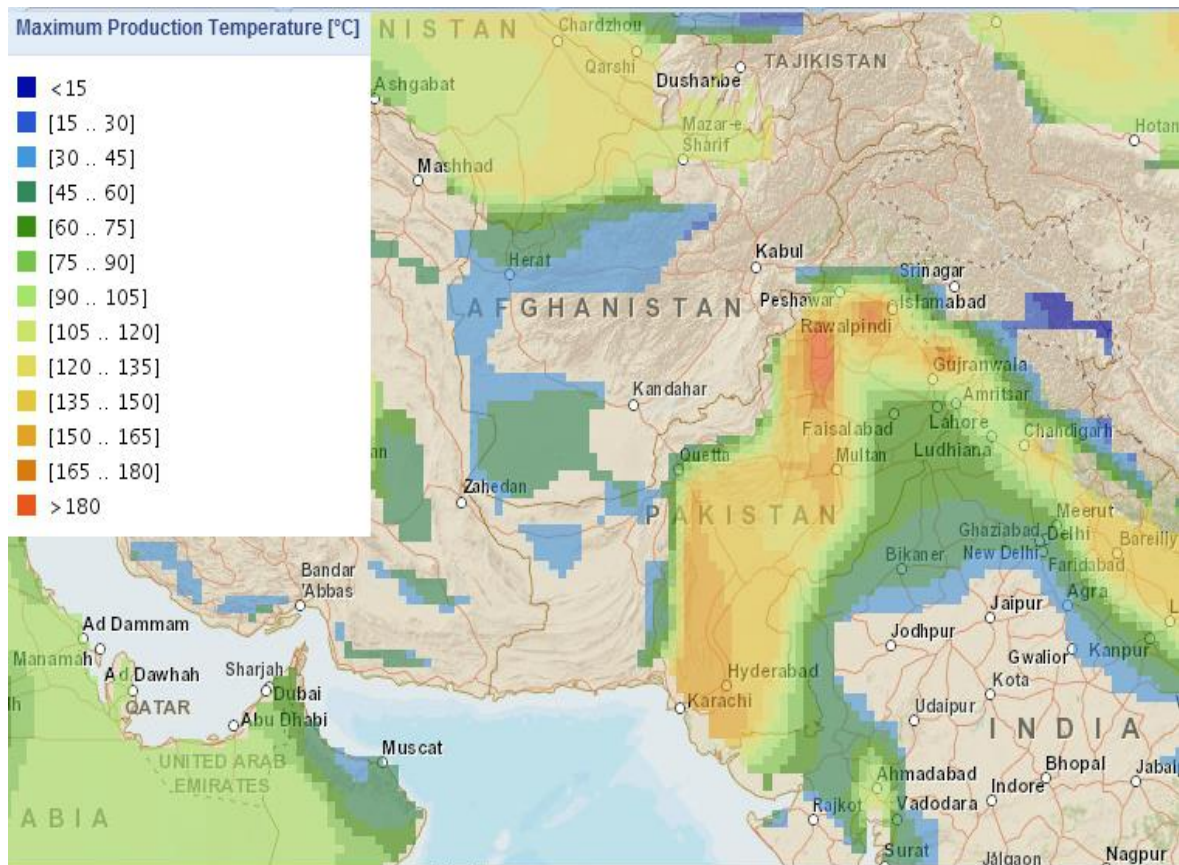


Fig 3.4 Maximum Production Temperature of geothermal resources in Pakistan

[7]



*Fig 3.5 Performance Indicator of geothermal resources in Pakistan [7]*

### **3.2 Geothermal Energy Resources in Pakistan:**

In Pakistan geological research, underlines presence of several geothermal resources. The energy mix of the country can be enhanced by exploiting these geothermal resources. Most of the geothermal resources of the world lie near the seismic belts and Pakistan too is situated in the western rifted margin of Indo-Pakistan sub continental plate.

The presence of geothermal resources in Pakistan is strengthened by the development of alteration zones and fumaroles, presence of hot springs and indication of quaternary volcanism in different regions of the country. [41-46]

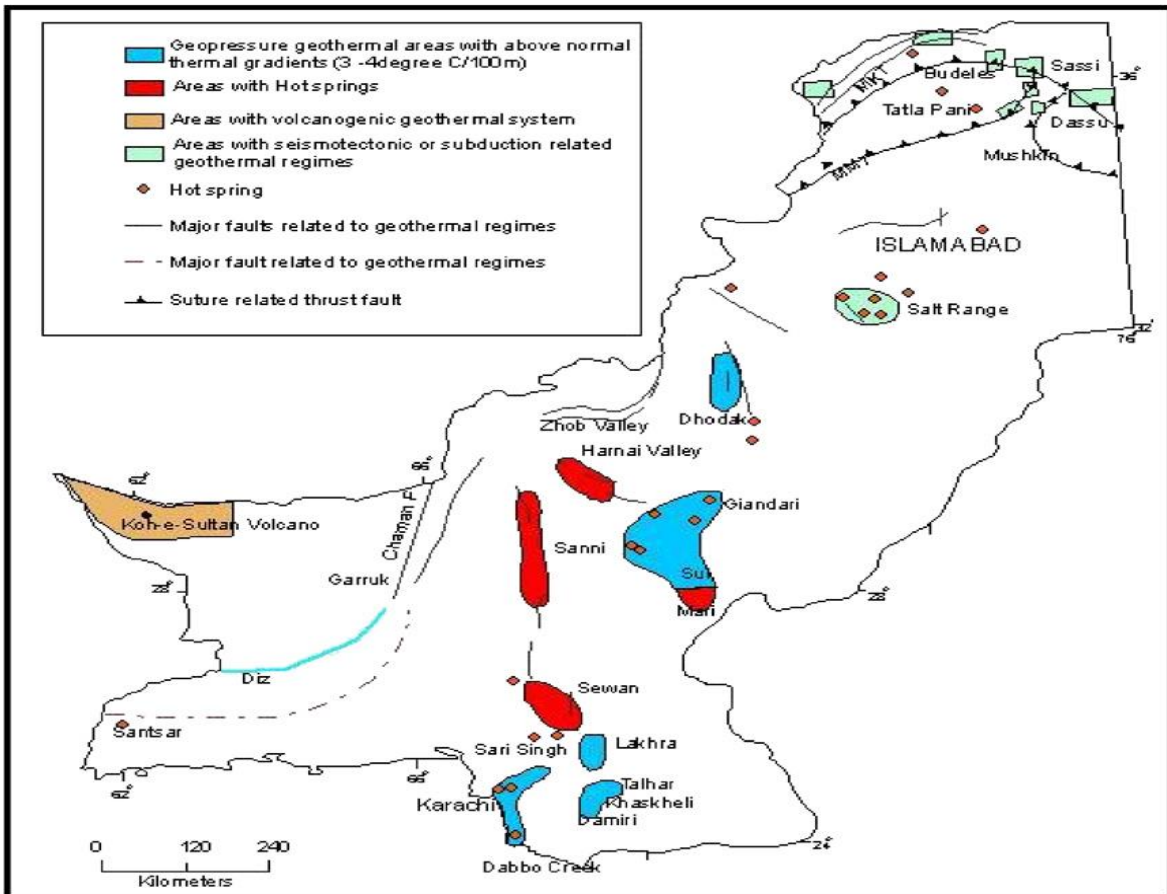


Fig 3.6 Occurrences of geothermal sources in Pakistan [47]

### 3.2.1 Geo Pressurized Sources:

Geo pressurized systems are characterized by entrapment of heat flow by insulating impermeable beds, that result in a high temperature and high pressure hot connate water leakage with a temperature ranging from 19 °C to 150 °C. [48]

In Pakistan such geo pressure frames are present within the Indus River Basin which constitute south Suleiman, South Kirthar and Lower Indus geological structures [49]

The Southeastern part of Sulaiman Fore deep exhibits the existence of geothermal resources which is evident by the frequent earthquakes of magnitude 3 – 7 on Richter scale in the region. [50] and prevalence of leakage of geo fluid particularly in the Giandri, Uch, Garam Aab, ZindaPir, Taunsa and Bakhar Regions [51, 52]

The geothermal resources in the South Kirthar Zone are characterized by frequent shallow earth quakes of magnitude 3 to 5 on Richter scale, the high thermal gradient of 3.3°C/100m at Oil and Gas wells drilled at Larkana and existence of hot springs like the ones in the Manghopir and Karsaz Regions of Karachi. [53]

The geological developments in the lower Indus geological structures strongly hint at presence of geothermal resources in region. The gradients of 4 °C/100m [54] at Damiri-1 Oil and Gas well, 3.0°C– 3.5°C/100m at Talher and Kashkeli Walls and 3.7 °C/100m at off shore well at Dabbo Creek [55] clearly exhibit the existence of geothermal resources in the region.

### 3.2.2 Seismo Tectonic and Suture Related Systems:

The northern part of the Pakistan is comprised of Karakorum, Hindu Kush and Himalaya thrust mountainous belts which exhibit strong seismic activities particularly in the form of hot water springs in Chitral, Murtazabad, Budelas, Sassi, Dassu, Tatta Pani and Mush Khin.

In Chitral region, hot springs are present in Garam Chashma Valley, [56], near Pechas Glacier and in Rawat village. [52]

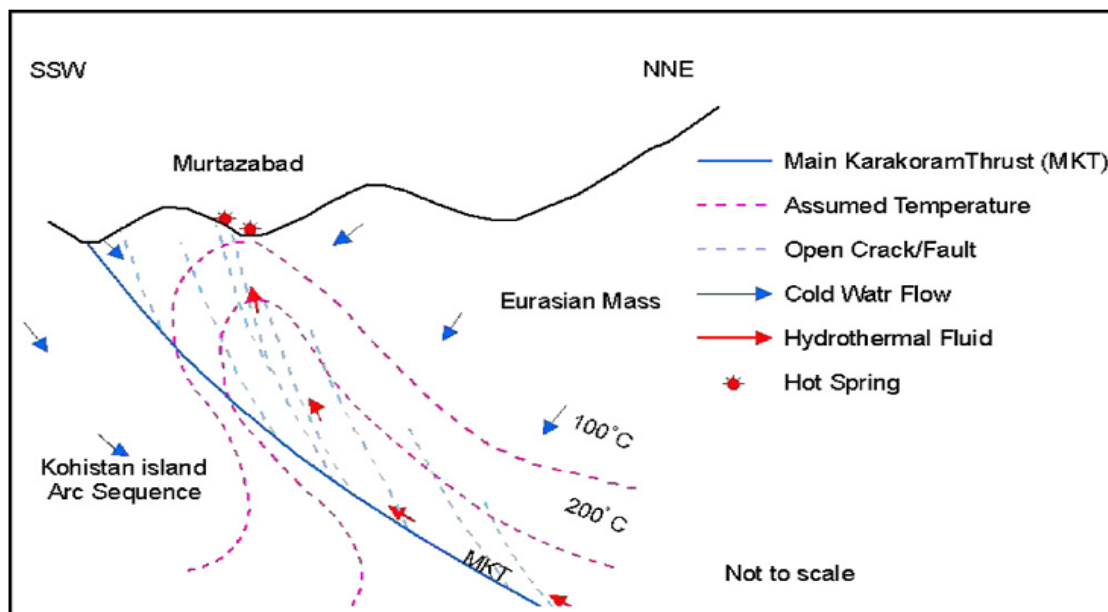


Fig 3.7 hot spring occurrences on Karakorum–Himalayan thrust zone [59]

In the Hunza valley the geo thermal springs are present in Murtazabad Village, the geo fluid temperature ranges from 26°C to 91°C [57], whereas the reservoir temperature has been noted to be in the range of 198 °C to 212 °C. In Skardu District several springs are reported in Dassu Area with geo fluid temperature of 71 °C.

The geo thermal systems in Nanga Parbat Haramosh Massif forms hot springs near Mushkin with the geo fluid temperature of 57 °C and the reservoir temperature ranges from 86 °C to 90 °C [58].

Several geo thermal hot springs are present in the Tatta Pani Area spread over an area of 8 KM. Hot springs also emanate from the Rani Kot fault zone at Sassi with a geo fluid temperature of 54 °C and the reservoir temperature in the range from 40 °C to 68 °C [59]

In other parts of Indus and Baluchistan sedimentary basins, geothermal manifestation are scattered in the form of hot springs. Three hot springs are located near Sanni along the Mach and Kirthar faults [54].

In the Harnai Valley several springs are located along the Harnai and Tatra faults where earthquake of magnitudes 6 to 7 on Richter scales are frequent. [50, 52, 60].

Furthermore two hot springs in the high seismic activity area north of Zohb valley are located.

### **3.2.3 Geo Thermal System Related to Neo-gene Quaternary Volcanism:**

Geo thermal systems associated with Chagai magmatic arc are manifested by thermal springs in the vicinity of Miri carter volcano region. The geo fluid temperature of these springs ranges from 25.6 °C to 32 °C [45].

The Koh-e-Sultan region has the highest geothermal potential in the country which lies in the south western part of Koh-e-Sultan volcanic are region. The reservoir temperature in the region is estimated to be in the range of 150 °C to 175 °C [57].



## CHAPTER - IV

### LITERATURE REVIEW

#### 4.1 Literature Survey:

The work potential of an energy system at a specified state is the maximum work that can be obtained from the system. The system will deliver the maximum work as it goes from its initial state to a thermodynamic state that is in equilibrium with its surroundings. This maximum useful work potential at a specified state represents the available energy i.e.; exergy. Second Law of Thermodynamics analysis by the virtue of employment of exergy principle provides the basis for design, analysis, and performance analysis and optimization of energy systems. Exergy analysis has been the most effective tool for reduction in irreversibility of the system, minimization of entropy generation and increasing the second law efficiency of system components to maximize the cycle output and efficiency.

From literature survey it is evident that Exergy analysis has extensively been used to analyze quantitatively and alleviate the causes of thermodynamic imperfections of the energy systems. Hepbasli [22] has reviewed the application of exergy analysis for a variety of renewable energy systems including solar, biomass, wind, geothermal and hybrid renewable energy systems. For the particular case of geothermal energy systems, literature survey suggests that the exergy analysis is performed for selection of optimum geothermal resource temperature, power plant configuration and working fluid.

The purpose of the literature survey is twofold; first to determine the extent of previous work that has dealt with the exploitation of medium and low temperature geothermal resources similar to the resources available in Pakistan, the basis selection of power plant configuration, working fluid and optimum working conditions. Second to review the existing results those have been obtained to validate the mathematical model and compare it with our study.

The main focus of geothermal research had been on the energetic and Exergetic analysis and performance evaluation based on second law analysis. Subbiah, S and Natarajan R [23], have performed the analysis of Binary ORC for geothermal power generation. It was concluded that second law analysis provides the required basis for identifying the optimal working conditions for maximizing the work output.

Ronald DiPippo [24], has carried out the performance comparison of Kalina Cycle and ORC configurations for generation from geothermal sources and has concluded that Second Law of Thermodynamics i.e.; the employment of exergy concept provides the most appropriate and consistent basis for comparison of different power plant configurations and working fluids.

#### **4.2 Optimum Cycle and Working Fluid Selection and Performance Evaluation:**

Mortaza Yari [25] has analyzed the possibilities of power generation from geothermal energy resources in Iran. Several geothermal energy resources have been discovered in the northern and north western areas of Iran, where the maximum geothermal temperature is predicted to be 240°C. Seven configurations of geo thermal power plants were analyzed for exploiting the available high temperature geothermal energy sources. The configurations analyzed were Single Flash, Double Flash, Combined Flash, Basic ORC, ORC with Internal Heat Exchanger, regenerative ORC and regenerative ORC with Internal Heat Exchanger. Each cycle was analyzed for first and second law efficiency and exergy destruction. It was found that ORC with IHE with R123 as the working fluid offers the highest efficiency.

There exist several medium temperature geothermal energy resources in Republic of Croatia in the range of 90°C to 140°C. Zvonimir Guzovic´et al [26] has compared the performance of Kalina Cycle with ORC for power generation from these sources. It was concluded that ORC provides better efficiency (13.5% Vs 12.8%) and higher net power (2225.5 KW Vs 2101.4 KW ) as compared to Kalina Cycle, this phenomenon is explained by the relatively higher temperature

of cooling air at 15°C at the inlet of condenser, which exerts an unfavorable effect on the condenser pressure in Kalina Cycle

Turkey has the second largest geothermal energy potential in Europe but exploitation is rather low. Ramzan Kose [27] has analyzed the geothermal resources in the Kutahya Simav region of Turkey and has concluded that a binary ORC with R134a as working fluid is the most efficient configuration with an efficiency of 12.93%.

Chao Luo et al [28] have analyzed the geothermal resources with geo fluid temperatures below 130°C and have concluded that for this temperature range Binary ORC configuration provides the optimum efficiency.

Daniel Walraven et al. [29], has compared different configurations of Kalina cycle with ORC for power generation from medium temperature sources in the range of 100°C to 150°C. The power plant configurations analyzed are Basic ORC, ORC with recuperation, ORC with turbine bleeding, Triple Pressure ORC and Kalina Cycle. For the low and medium temperature sources, Trans critical and multi pressure sub critical systems with a lower condenser temperature and small temperature difference in the heat exchanger were found to be efficient.

Carlos Eymel et al. [30] have conducted Exergetic and economic analysis of Kalina Cycle and ORC for power generation from low temperature geothermal sources in Brazil. Upon comparison it was found that for low temperature resources below 100°C R290 provides the highest efficiency and a levelised electricity cost of 0.22€/KWh can be achieved.

Florian Heberle and Dieter Bruggemann [31] have performed an analysis for selection of optimal binary fluid for the ORC based geothermal power plant. It was found that the efficiency of combined heat and power generation systems is relatively higher than that of standalone power generation systems. Working fluids such as iso pentane, iso butane, R245fa and R227ea were analyzed. It was concluded that for combined heat and power generation systems working

fluids with higher critical temperature such as iso pentane are preferred where as standalone power generation systems working fluids with lower critical temperature such as iso butane and R227ea were found to be more efficient.

Fu Zhen Zhang and Pei Xue Jiang [32] have carried out thermodynamic analysis of an ORC for the selection of optimum binary fluid on the basis of geo fluid temperature. Four working fluids i.e.; R134a, iso butane, iso pentane and R245fa for four geo fluid temperatures below 200°C were analyzed and it was concluded that the working fluid with critical temperature near the geo fluid temperature provides optimum efficiency.

T. Guo et al. [33], has analyzed 27 working fluids for a novel co-generation plant driven by a low temperature geo thermal sources. It was concluded that R236ea provides the highest net power output per unit mass flow rate of geo fluid.

Al Essadro Franco 2011 has analyzed the exploitation of low temperature water dominated geothermal energy resources in the range of 100°C to 130°C by means of regenerative ORC system. The working fluids considered are R134a, iso butane, iso pentane, n pentane and R245fa. It was found that by application of recuperation although the performance increase is minimal but it results in decrease in the heat exchanger area up to 20% [34]

Since the low temperature geothermal resources have a very large potential as a viable renewable energy resource [35] as the amount of available energy is large but the conversion efficiency is rather low due to low temperature of the source, various authors have proposed innovative methods for increasing the efficiency of geothermal power generation from low and medium temperature sources.

Mehmet Kongolu and Ali Bolatturk [36], carried out performance and parametric Exergetic analysis of an existing 12.4 MW dual-level binary geothermal power plant in Turkey to find the components with highest rate of exergy destructions. It was found that the substantial rate of exergy is destroyed in the brine reinjection, heat exchanger and condenser.

Ronald DiPippo [8] has concluded that the efficiency of Kalina Cycle can substantially be increased by using a recovery heat exchanger with a cascade of evaporators with both high- and low-pressure turbines.

Gnutek and Bryszewska-Mazurek [37] have concluded that a multi cycle with different thermodynamic properties will be most efficient, whereas Desai and Bandyopadhyay [38] have recommended use of ORC with Turbine Bleeding and Regeneration for increasing the efficiency.

H.D. Madhawa et al.[39] has analyzed that the ratio of total heat exchanger area to the net power output can be used as the optimum design criterion for the design of ORC geothermal power generation plant.

Allessandro Franco and Marco Villani [40] have analyzed brine specific consumption as the design criteria for the power generation from low temperature water dominated geothermal resources in the range of 100°C to 150°C. It was found that brine specific consumption of 20Kg/s to 120 Kg/s can be achieved with second law efficiency in the range of 20% to 45%.

#### **4.3 Summary and Conclusion:**

For summarizing the literature survey, it is concluded that Second Law analysis (Exergy Analysis) provides the basis of design, analysis, performance evaluation and optimization of geothermal power plants. Low and Medium temperature geothermal resources in the temperature ranges that are available in Pakistan are found in various countries and literature survey suggests that an ORC is the optimum cycle configuration for power generation from these sources economically. Different researchers have carried out the study on modification of ORC by the incorporation of Regeneration, recuperation, turbine bleeding, multi pressure systems and regenerative heat exchangers and the effects on first and second law efficiency and exergy destruction. A host of working fluids are analyzed by researchers in pursuit of finding the optimum working fluid and it was found that for power generation systems binary fluids having low critical

temperature in the range of geothermal source temperature provide the optimum output.

During the literature survey, it is revealed that no work has yet been carried out aimed at the exploitation of geothermal resources in Pakistan, several geological investigators have however, highlighted presence of geothermal energy resources at various locations in Pakistan. This work which is first of its kind in Pakistan, therefore, aims at the selection of optimum geothermal power plant configuration based on the available resources and the selection of optimum working fluid and working conditions based on the energy and exergy analysis.

## CHAPTER – V

### MATHEMATICAL MODELLING

#### 5.1 Energy and Exergy Analysis:

Exergy, also termed as the available energy is the maximum theoretical useful work that can be extracted from the system which is at a specified thermodynamic state relative to its surroundings. If the system is at thermodynamic equilibrium with its surrounding, then it is said to be at a dead state and no useful work can be extracted from it without the expense of work.

Since Exergy Analysis depends upon the second law of thermodynamics and it is also based upon the first law, both laws are combined to get a series of equations for mass, energy and exergy balance of a system at steady state with negligible Kinetic and Potential energy changes. [25, 61, 62]

Mass Balance is given by:

$$\sum \dot{m}_{in} - \sum \dot{m}_{out} = 0$$

Energy Balance is given by:

$$\sum \dot{m} h_{out} - \sum \dot{m} h_{in} = Q - W$$

Exergy balance is given by:

$$\dot{E}x_{heat} - W + \sum \dot{m}_{in} \Psi_{in} - \sum \dot{m}_{out} \Psi_{out} = i$$

Net work in a cycle is given by: [62]

$$W_{net} = W_t + W_p$$

Exergy input to the system is given by: [23, 24, 61 and 64]

$$\dot{E}x_{in} = \dot{m}_{geo}[(h_{geo} - h_o) - T_o(S_{geo} - S_o)]$$

Exergy destroyed in the cycle and the plant are given by [61, 62]

$$I_{cycle} = \sum \text{all components } I_i = I_p + I_{HEs} + I_t + I_c$$

$$I_{plant} = I_{cycle} + I_{rej} + I_{CS} = \dot{E}x_{in} - W_{net}$$

## 5.2 Performance Analysis:

The performance of the system can be analyzed in a number of ways. First and second law efficiency in the based on ambient temperature and inlet state of the geothermal fluid is given by: [23, 24, 61, and 64]

$$\eta_l = \frac{\text{net work output}}{\text{total energy inputs}} = \frac{W_{net}}{\dot{m}_{geo}(h_{geo} - h_o)}$$

$$\eta_{lI} = \frac{\text{net work output}}{\text{total energy inputs}} = \frac{W_{net}}{\dot{m}_{geo}(h_{geo} - h_o) - T_o(S_{geo} - S_o)}$$

Another approach is to calculate the first and second law efficiency on the basis of heat transfer: [23, 24, and 63]

$$\eta_{l,2} = \frac{W_{net}}{\dot{m}_{geo}(h_{geo} - h_{rej})} = \frac{W_{net}}{\dot{m}_{wf}(h_{wf,out} - h_{wf,in})}$$

$$\eta_{lI,2} = \frac{W_{net}}{\dot{m}_{geo}[(h_{geo} - h_{rej}) - T_o(S_{geo} - S_{rej})]}$$

Cycle effectiveness can also be used to analyze the efficiency qualitatively as well as quantitatively, based on the effectiveness of heat transfer to the cycle from the hot geo fluid. [23, 24, 61, 64]

$$\varepsilon = \frac{W_{net}}{\dot{m}_{geo}[(h_{wf,out} - h_{wf,in}) - T_o(S_{wf,out} - S_{wf,in})]}$$

Several dimensionless parameters have been used in the literature to assess the performance of individual cycle components, three of these parameters are: [22, 25]

Relative Irreversibility:



$$\mathcal{X}_i = \frac{\dot{I}_i}{\dot{W}_{net}}$$

Productivity Lack:

$$\xi_i = \frac{\dot{I}_i}{\dot{I}_{plant}}$$

Fuel Depletion Ratio:

$$\delta = \frac{\dot{I}_i}{\dot{E}_{x in}}$$

### **5.3 Optimum Power Plant Configuration Selection:**

Based on the Overview of Geothermal Resources available in Pakistan (Chapter II) and Literature Review (Chapter III), small binary plants operating on geothermal resources in the range on 100°C to 150°C were selected for this study. The ambient conditions were selected to be 25°C and 100 KPa for mathematical modeling.

Four configurations of ORC were analyzed analytically and numerically for finding the optimum power plant configuration. Governing equations of each component for energy and exergy analysis of each configuration are mentioned below.

#### **5.3.1 Basic ORC:**

A Basic ORC is based on the energy transfer from the hot geo fluid to the binary working fluid. A high pressure primary working fluid is pumped to the drilled geothermal sources in the closed piping system and is heated as the temperature increases linearly with depth [64]. Binary working fluid is heated by the heat transfer from the geothermal fluid. By the end of heat transfer the binary working fluid by virtue of its low boiling point and high vapor pressure, vaporizes completely and attains the super-heated state. The binary fluid expands in the turbine and later condenses in the condenser [63].

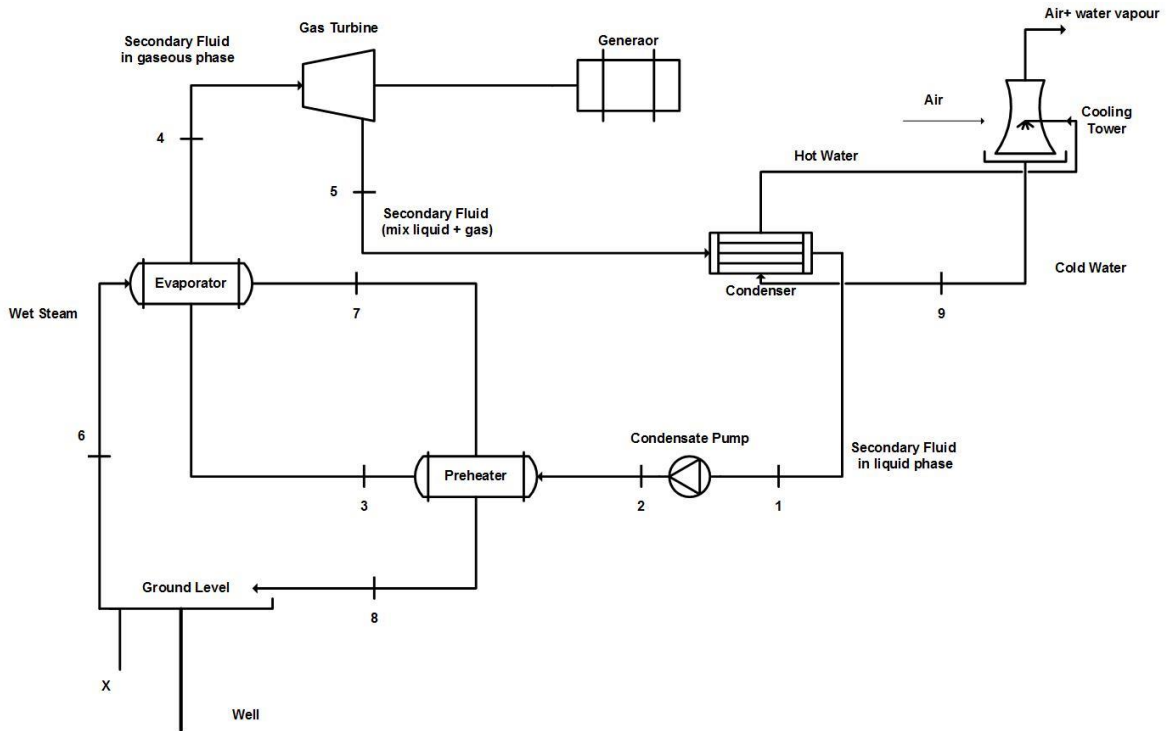


Fig 4.1 Basic Organic Rankine Cycle [8]

In the TS diagram processes 1-2 and 4-2 represents reversible adiabatic pumping and reversible adiabatic expansion respectively, the processes 2-4 and 5-1 refer to constant pressure heat addition and heat rejection respectively.

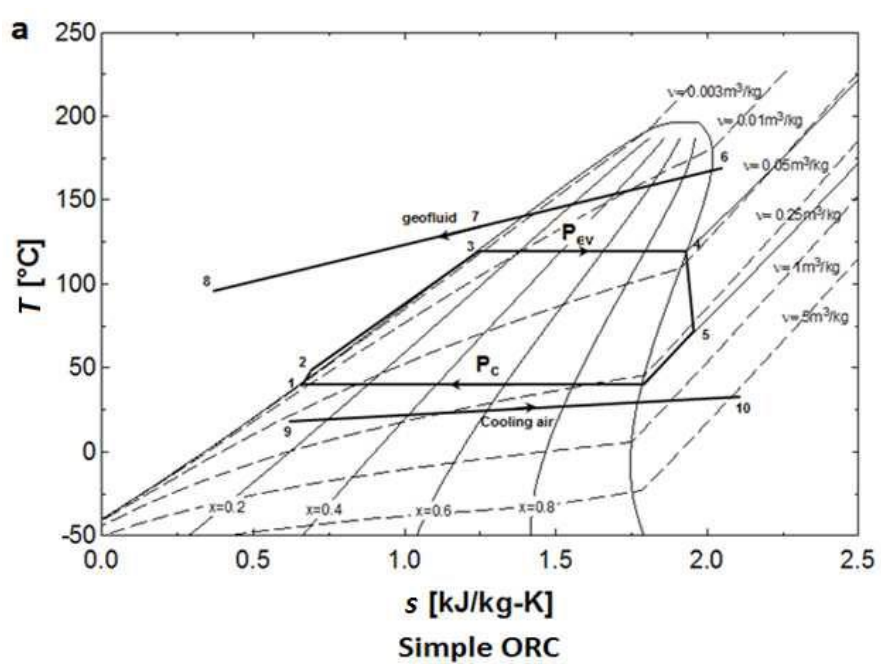


Fig 4.2 T-S Diagram of Basic Organic Rankine Cycle [25]

Governing equations of each component for energy and exergy analysis are mentioned below: [23, 24, 25, 61, 63 and 64]

### Condensate Pump:

**Energy balance:**  $\dot{W}_p = \dot{m}_{wf} (h_{2,s} - h_1) / \eta_p$

**Exergy balance:**  $\dot{I}_p = \dot{E}X_1 - \dot{E}X_2 + \dot{W}_p = \dot{m}_{wf} (\Psi_1 - \Psi_2) + \dot{W}_p$

### Preheater

**Energy balance:**  $\dot{m}_{wf}(h_3 - h_2) = \dot{m}_{geo}(h_7 - h_8)$

**Exergy balance:**  $\dot{I}_{PH} = \dot{E}X_2 + \dot{E}X_7 - \dot{E}X_3 - \dot{E}X_8 = \dot{m}_{wf} (\Psi_2 - \Psi_3) + \dot{m}_{geo} (\Psi_7 - \Psi_8)$

### Evaporator

**Energy balance:**  $\dot{Q}_E = \dot{m}_{wf} (h_4 - h_3) = \dot{m}_{geo} (h_6 - h_7)$

**Exergy balance:**  $\dot{I}_E = \dot{E}X_3 + \dot{E}X_6 - \dot{E}X_4 - \dot{E}X_7 = \dot{m}_{wf} (\Psi_3 - \Psi_4) + \dot{m}_{geo} (\Psi_6 - \Psi_7)$

### Turbine

**Energy balance:**  $\dot{W}_t = \dot{m}_{wf} (h_4 - h_{5,s}). \eta_t$

**Exergy balance:**  $\dot{I}_t = \dot{E}X_4 - \dot{E}X_5 - \dot{W}_t = \dot{m}_{wf} (\Psi_4 - \Psi_5) + \dot{W}_t$

### Condenser

**Energy balance:**  $\dot{Q}_c = \dot{m}_{wf} (h_5 - h_1) = \dot{m}_{ca} (h_{10} - h_9)$

**Exergy balance:**  $\dot{I}_C = \dot{E}X_5 + \dot{E}X_9 - \dot{E}X_1 - \dot{E}X_{10} = \dot{m}_{wf} (\Psi_5 - \Psi_1) + \dot{m}_{ca} (\Psi_9 - \Psi_{10})$

### Reinjection

**Exergy balance:**  $\dot{I}_{rej} = \dot{E}X_8 - \dot{E}X_O = \dot{m}_{geo} (\Psi_8 - \Psi_O)$

### 5.3.2 ORC with IHE:

An internal heat exchanger can be employed when the expansion ends in the super-heated regime. The internal heat exchanger increases the efficiency

utilizes the high temperature binary fluid at the exit of turbine to preheat the binary working fluid before evaporating in the evaporator. [25, 62, 65]

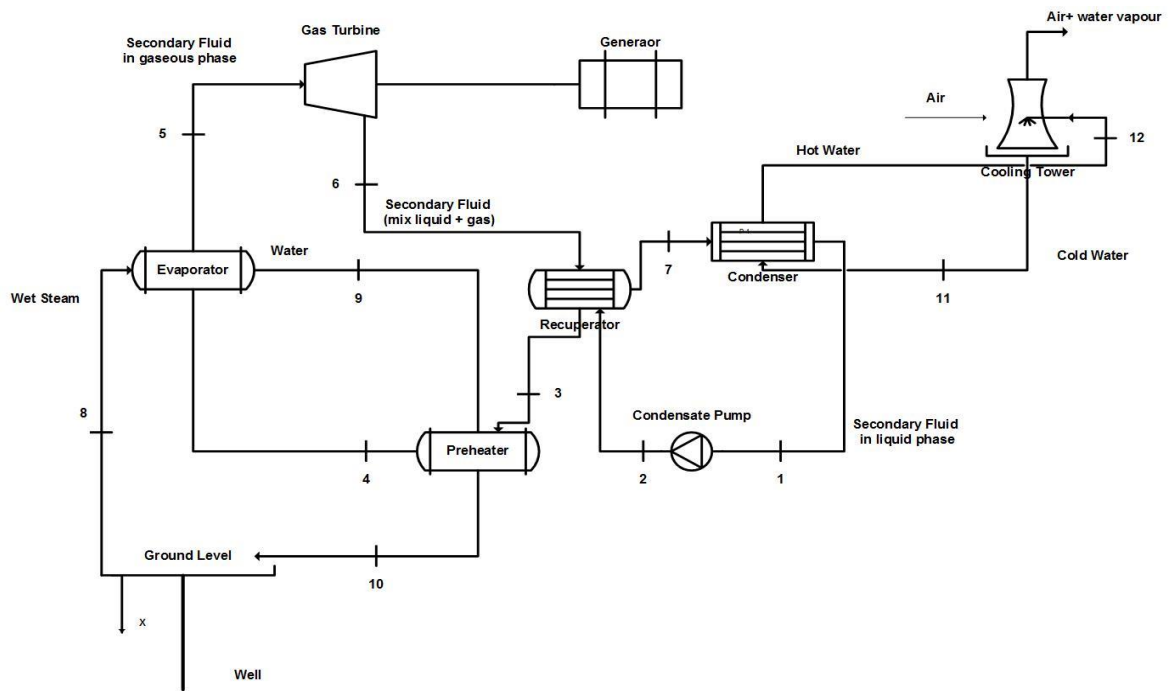


Fig 4.3 Organic Rankine Cycle with IHE [8]

The addition of internal heat exchanger is represented by the states 3 and 7 on the T-S diagram.

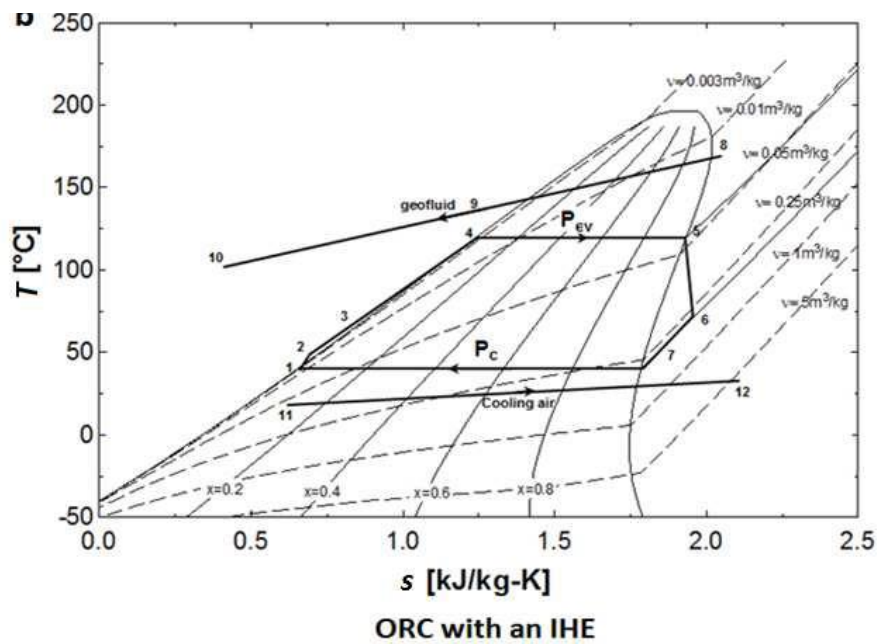


Fig 4.4 T-S Diagram of Organic Rankine Cycle with IHE [25]

Governing equations of each component for energy and exergy analysis are mentioned below: [23, 24, 25, 61, 63 and 64]

### Condensate Pump:

**Energy balance:**  $\dot{W}_p = \dot{m}_{wf} (h_{2,s} - h_1) / \eta_p$

**Exergy balance:**  $\dot{I}_p = \dot{E}x_1 - \dot{E}x_2 + \dot{W}_p = \dot{m}_{wf} (\Psi_1 - \Psi_2) + \dot{W}_p$

### IHE

**Energy balance:**  $h_3 - h_2 = h_6 - h_7$

**Exergy balance:**  $\dot{I}_{IHE} = \dot{E}x_2 + \dot{E}x_6 - \dot{E}x_3 - \dot{E}x_7 = \dot{m}_{wf} [(\Psi_2 - \Psi_3) + (\Psi_6 - \Psi_7)]$

### Preheater

**Energy balance:**  $\dot{m}_{wf}(h_4 - h_3) = \dot{m}_{geo} (h_9 - h_{10})$

**Exergy balance:**  $\dot{I}_{PH} = \dot{E}x_3 + \dot{E}x_9 - \dot{E}x_4 - \dot{E}x_{10} = \dot{m}_{wf} (\Psi_3 - \Psi_4) + \dot{m}_{geo} (\Psi_9 - \Psi_{10})$

### Evaporator

**Energy balance:**  $\dot{Q}_E = \dot{m}_{wf} (h_5 - h_4) = \dot{m}_{geo}(h_8 - h_9)$

**Exergy balance:**  $\dot{I}_E = \dot{E}x_4 + \dot{E}x_8 - \dot{E}x_5 - \dot{E}x_9 = \dot{m}_{wf} (\Psi_4 - \Psi_5) + \dot{m}_{geo}(\Psi_8 - \Psi_9)$

### Turbine

**Energy balance:**  $\dot{W}_t = \dot{m}_{wf} (h_5 - h_{6,s}) \cdot \eta_t$

**Exergy balance:**  $\dot{I}_t = \dot{E}x_5 - \dot{E}x_6 - \dot{W}_t = \dot{m}_{wf} (\Psi_5 - \Psi_6) - \dot{W}_t$

### Condenser

**Energy balance:**  $\dot{Q}_c = \dot{m}_{wf}(h_7 - h_1) = \dot{m}_{ca}(h_{12} - h_{11})$

**Exergy balance:**  $\dot{I}_c = \dot{E}x_7 - \dot{E}x_{11} - \dot{E}x_1 - \dot{E}x_{12} = \dot{m}_{wf} (\Psi_7 - \Psi_1) + \dot{m}_{ca} (\Psi_{11} - \Psi_{12})$

### Reinjection

**Exergy balance:**  $\dot{I}_{rej} = \dot{E}x_{10} - \dot{E}x_0 = \dot{m}_{geo} (\Psi_{10} - \Psi_0)$

### 5.3.3 Regenerative ORC:

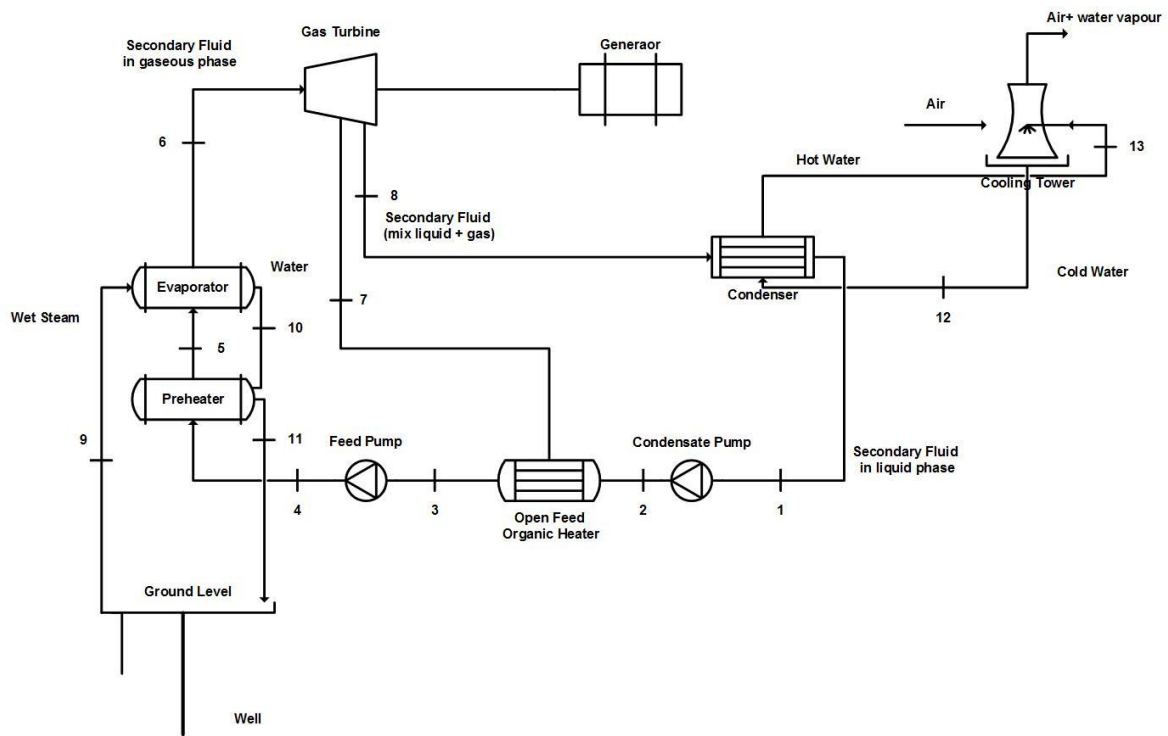


Fig 4.5 Regenerative Organic Rankine Cycle [8]

The cycle performance can also be enhanced by addition of a two phase regenerator. Two phase regenerator utilizes an open feed organic heater to preheat the binary working fluid by heat transfer from the expanded vapors bled from the turbine.[25, 38]

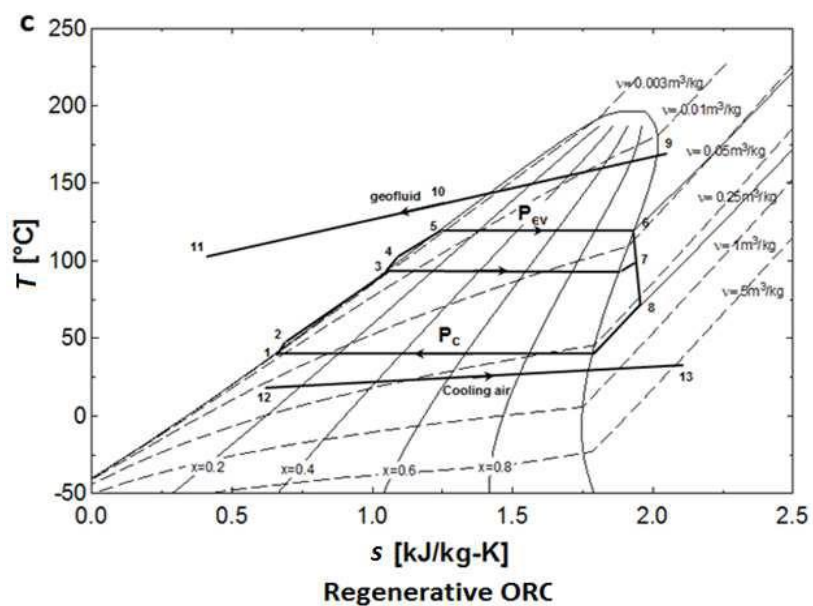


Fig 4.6 T-S Diagram of Regenerative Organic Rankine Cycle [25]

Regenerative Organic Rankine Cycle consists of three constant pressure heat transfer processes. The mixture of turbine bleeding and condensate is ideally assumed to be at evaporator pressure and saturated liquid state at the exit of open feed organic heater [66]

Governing equations of each component for energy and exergy analysis are mentioned below: [23, 24, 25, 61, 63 and 64]

### Condensate Pump:

**Energy balance:**  $\dot{W}_p = \dot{m}_{wf} (h_{2,s} - h_1) / \eta_p$

**Exergy balance:**  $\dot{I}_p = \dot{E}X_1 - \dot{E}X_2 + \dot{W}_p = \dot{m}_{wf} (\Psi_1 - \Psi_2) + \dot{W}_p$

### OFOH:

**Energy balance:**  $(h_3 - h_2) = y(h_7 - h_2)$

**Exergy balance:**  $\dot{I}_{OFOH} = (1 - Y)\dot{E}X_2 + y\dot{E}X_7 - \dot{E}X_3 = \dot{m}_{wf} [(1 - Y)\Psi_2 + y\Psi_7 - \Psi_3]$

### Feed Pump:

**Energy balance:**  $\dot{W}_{P2} = \dot{m}_{wf} (h_{4,s} - h_3) / \eta_p$

**Exergy balance:**  $\dot{I}_P = \dot{E}X_3 - \dot{E}X_4 + \dot{W}_P = \dot{m}_{wf} (\Psi_3 - \Psi_4) + \dot{W}_P$

### Preheater:

**Energy balance:**  $\dot{m}_{wf} (h_5 - h_4) = \dot{m}_{geo} (h_{10} - h_{11})$

**Exergy balance:**  $\dot{I}_{PH} = \dot{E}X_4 + \dot{E}X_{10} - \dot{E}X_5 - \dot{E}X_{11} = \dot{m}_{wf} (\Psi_4 - \Psi_5) + \dot{m}_{geo} (\Psi_{10} - \Psi_{11})$

### Evaporator:

**Energy balance:**  $\dot{Q}_E = \dot{m}_{wf} (h_6 - h_5) = \dot{m}_{geo} (h_9 - h_{10})$

**Exergy balance:**  $\dot{I}_E = \dot{E}X_5 + \dot{E}X_9 - \dot{E}X_6 - \dot{E}X_{10} = \dot{m}_{wf} (\Psi_5 - \Psi_6) + \dot{m}_{geo} (\Psi_9 - \Psi_{10})$

### Turbine:

**Energy balance:**  $W_{t1} = \dot{m}_{wf}(h_6 - h_{7,s})$ .  $\eta_t W_{t2} = \dot{m}_{wf}(h_7 - h_{8,s})$ .  $\eta_t$

**Exergy balance:**  $\dot{I}_t = (\dot{E}X_6 - \dot{E}X_7) + (1-y) = (\dot{E}X_7 - \dot{E}X_8) - W_t = \dot{m}_{wf} [(\Psi_6 - \Psi_7) + (1-y)(\Psi_7 - \Psi_8)] - W_t$

**Condenser:**

**Energy balance:**  $\dot{Q}_c = \dot{m}_{wf}(h_8 - h_1) = \dot{m}_{ca}(h_{13} - h_{12})$

**Exergy balance:**  $\dot{I}_c = \dot{E}X_8 + \dot{E}X_{12} - \dot{E}X_1 - \dot{E}X_{13} = \dot{m}_{wf}(\Psi_8 - \Psi_1) + \dot{m}_{ca}(\Psi_{12} - \Psi_{13})$

**Reinjection:**

**Exergy balance:**  $\dot{I}_{rej} = \dot{E}X_{11} + \dot{E}X_0 = \dot{m}_{wf}(\Psi_{11} - \Psi_0)$

### 5.3.4 Regenerative ORC with IHE:

To further enhance the cycle performance a regenerator with IHE can also be utilized [25].

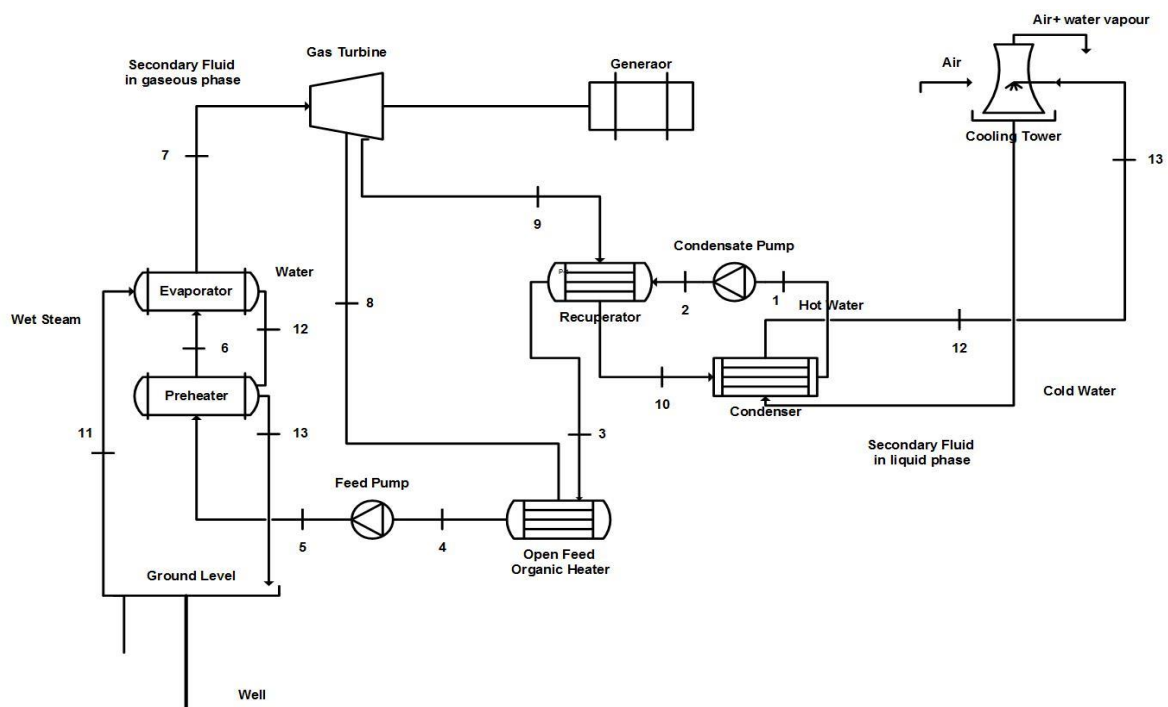


Fig 4.7 Regenerative Organic Rankine Cycle with IHE [8]



Addition of IHE to Regenerative ORC is illustrated by states 3 and 10 on the TS diagram.

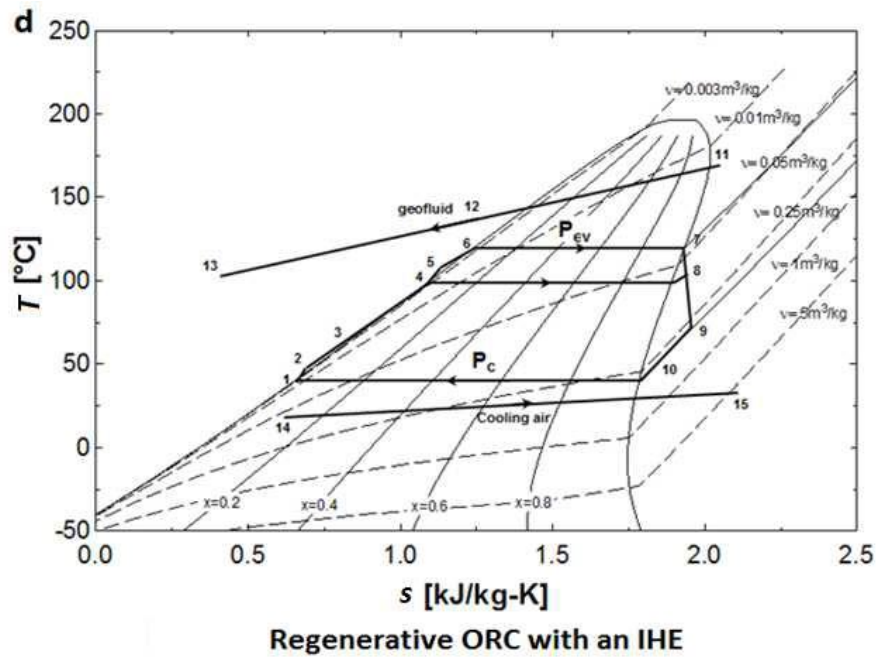


Fig 4.8 T-S Diagram of Regenerative Organic Rankine Cycle with IHE [25]

Governing equations used for energy and exergy analysis for each component are as follows: [23, 24, 25, 61, 63 and 64]

**Condensate Pump:**

**Energy balance:**  $\dot{W}_p = \dot{m}_{wf} (h_{2,s} - h_1) / \eta_p$

**Exergy balance:**  $\dot{I}_p = \dot{E}x_1 - \dot{E}x_2 + \dot{W}_p = \dot{m}_{wf} (\Psi_1 - \Psi_2) + \dot{W}_p$

**IHE:**

**Energy balance:**  $h_3 - h_2 = h_9 - h_{10}$

**Exergy balance:**  $\dot{I}_{IHE} = \dot{E}x_2 + \dot{E}x_9 - \dot{E}x_3 - \dot{E}x_{10} = \dot{m}_{wf} [(\Psi_2 - \Psi_3) + (\Psi_9 - \Psi_{10})]$

**OFOH:**

**Energy balance:**  $(h_4 - h_3) = y(h_8 - h_3)$

**Exergy balance:**  $\dot{I}_{OFOH} = (1-y)\dot{E}x_3 + y\dot{E}x_8 - \dot{E}x_4 = \dot{m}_{wf} [(1-y)\Psi_3 + y\Psi_8 - \Psi_4]$

**Feed Pump:**

**Energy balance:**  $\dot{W}_{P2} = \dot{m}_{wf} (h_{5,S} - h_4) \cdot \eta_P$

**Exergy balance:**  $\dot{I}_P = \dot{E}X_4 - \dot{E}X_5 + W_P = \dot{m}_{wf} (\Psi_4 - \Psi_5) + W_P$

**Preheater:**

**Energy balance:**  $\dot{m}_{wf}(h_6 - h_5) = \dot{m}_{geo} (h_{12} - h_{13})$

**Exergy balance:**  $\dot{I}_{PH} = \dot{E}X_5 + \dot{E}X_{12} - \dot{E}X_6 - \dot{E}X_{13} = \dot{m}_{wf} (\Psi_5 - \Psi_6) + \dot{m}_{geo} (\Psi_{12} - \Psi_{13})$

**Evaporator:**

**Energy balance:**  $\dot{Q}_E = \dot{m}_{wf} (h_7 - h_6) = \dot{m}_{geo}(h_{11} - h_{12})$

**Exergy balance:**  $\dot{I}_E = \dot{E}X_6 + \dot{E}X_{11} - \dot{E}X_7 - \dot{E}X_{12} = \dot{m}_{wf} (\Psi_6 - \Psi_7) + \dot{m}_{geo}(\Psi_{11} - \Psi_{12})$

**Turbine:**

**Energy balance:**  $\dot{W}_{t1} = \dot{m}_{wf} (h_7 - h_{8,S}) \cdot \eta_t$   $\dot{W}_{t2} = \dot{m}_{wf} (h_8 - h_{9,S}) \cdot \eta_t$

**Exergy balance:**  $\dot{I}_t = (\dot{E}X_7 - \dot{E}X_8) + (1-y) (\dot{E}X_8 - \dot{E}X_9) - \dot{W}_t = \dot{m}_{wf} (\Psi_7 - \Psi_8) + (1-y) (\Psi_8 - \Psi_9) \dot{W}_t$

**Condenser:**

**Energy balance:**  $\dot{Q}_c = \dot{m}_{wf}(h_{10} - h_1) = \dot{m}_{ca}(h_{15} - h_{14})$

**Exergy balance:**  $\dot{I}_c = \dot{E}X_{10} + \dot{E}X_{14} - \dot{E}X_1 - \dot{E}X_{15} = \dot{m}_{wf} (10 - \Psi_1) + \dot{m}_{ca} (\Psi_{14} - \Psi_{15})$

**Reinjection:**

**Exergy balance:**  $\dot{I}_{rej} = \dot{E}X_{13} - \dot{E}X_0 = \dot{m}_{geo} (\Psi_{13} - \Psi_0)$

#### **5.4 Selection of Optimal Working Fluid:**

The working fluids are selected on the basis of [67-70]:

1. High Energetic and Exergetic efficiencies.

2. High boiling temperature, latent heat of vaporization, thermal conductivity and density in gaseous state is desired. However, low viscosity, liquid specific heat and liquid density is favorable, moderate critical temperature and pressure is also desired.
3. High chemical stability and compatibility is desired.
4. Low Global Warming Potential (GWP), Ozone Depletion Potential (ODP) & Atmospheric Lifetime (ALT) is highly desirable.
5. Non flammability and Non Toxicity is highly desired.
6. The selected working fluid must be economical to operate and easily available.

This study has considered Refrigerants R113, R245fa, R123, R152a, Iso-pentane and n-pentane as the working fluids of the cycle.

Working fluid	R123	R152a	R600a	R601	R-245fa	R-113
Name	2,2-Dichloro-1,1,1-trifluoroethane	1,1-Difluoroethane	Isobutane	n-Pentane	1,1,1,3,3-pentafluoropropane	1,1,2-trichloro-1,2,2-trifluoroethane
Chemical formula	$\text{CHCl}_2\text{CF}_3$	$\text{CH}_3\text{CHF}_2$	$\text{C}_4\text{H}_{10}$	$\text{C}_5\text{H}_{12}$	$\text{CF}_3\text{CH}_2\text{CF}_2$	$\text{C}_2\text{Cl}_3\text{F}_3$
Type	HCFC	HFC	HC	HC	CFC	CFC
Organic type	Dry	Wet	Dry	Dry	Dry	Dry
Molecular weight	152.93	66.05	58.12	72.15	134	187.38
$T_{\text{bp}}@1\text{atm} [\text{C}]$	27.82	-24.02	-11.67	36	15.3	47.59
$T_{\text{cr}}[\text{C}]$	183.68	113.26	134.67	196.55	154.05	214.06
$C_{\text{pv}} [\text{J/Kg.K}]$	738.51	1456.02	181.42	1824.12	980.9	1524.06

P <sub>cr</sub> [MPa]	3.662	4.517	3.62	3.37	3.64	3.392
ALT [year]	1.3	1.4	0.02	1	7.2	85
ODP	0.02	0	0	0	0	0.9
GWP [100 years]	77	120	~20	11	1050	6130

Table 5.1: Properties of selected Refrigerants [68, 71 and 72]

### 5.5 **Methodology:**

For the study, small ORC power plants operating on geothermal resources in the range on 100°C to 150°C were selected. The ambient conditions were selected to be 25°C and 100KPa.

The study encompasses the thermodynamic analysis of different types of ORC configurations. The goals of the study were to find the energetic and energetic efficiencies of plant and to find the components with highest loss of energy to maximize the power output. The analysis is carried out for a set of working fluids to check for the most viable working fluid for the cycle operating in this range of temperature.

### 5.6 **Assumptions:**

1. Water has been used as the geo fluid for all cases. The geo fluid outlet temperature varies in the range of 100°C to 150°C.
2. The geo fluid mass flow rate of 1kg/s is assumed for all cases.
3. The ambient temperature is assumed to be 25°C and an ambient pressure of 100KPa is assumed.
4. Air has been used as the cooling fluid in the condenser, the condensing temperature is assumed to be 40°C and the pinch point temperature is assumed to be 5°C.

5. The working fluid pump efficiency is assumed to be 90% and the turbine efficiency is assumed to be 80% for all working fluids and all configurations of ORC considered.
6. Wall heat flux is assumed to be constant in the down hole heat exchanger as the increase in underground temperature with depth is almost linear.
7. The effectiveness of heat exchanger is assumed to be constant.
8. Heat loss through the piping system is neglected.
9. All the heat exchangers and associated components are insulated from atmosphere.
10. Only effect of conduction mode of the heat transfer is considered as natural convection and radiation heat transfer modes were neglected.
11. Kinetic and Potential energy losses are neglected.
12. Fully developed flow of fluids is considered.
13. The system is assumed to be working under steady state control volume model.
14. The pressure and temperature losses in the pump are negligible.
15. The heat transfer coefficients are assumed to be constant.
16. Pressure drop in the condenser, evaporator and piping system is neglected.

## 5.7 Reference Conditions:

In order to select the optimum working fluid and cycle configuration, reference conditions were selected which are also used in the literature. The basic design conditions considered for this study are:

### 1. **Ambient Pressure and Temperature:**

The ambient pressure is taken to be 100KPa and ambient temperature is taken to be 25°C.

### 2. **Condenser Temperature:**

The condenser temperature is taken to be 40°C.

### 3. **Geothermal Fluid Temperature:**

The temperature of geothermal fluid is assumed to vary in the range of 100°C to 150°C.

### 4. **Efficiency:**

The efficiency of pump is assumed to be constant at 90% whereas the efficiency of turbine is assumed to be 80%.

### 5. **Heat Exchanger Effectiveness:**

The effectiveness of internal heat exchanger (IHE) is assumed to be 90%.

## 5.8 Mathematical Model Validation:

The mathematical model developed in section is validated by comparing the results with published result [25]. Reference conditions used in our calculations are similar to the one used by Mortaza Yari [25] i.e.; ambient pressure 100 KPa, ambient temperature 25°C, Condenser Temperature 40°C, Evaporator Inlet temperature 120°C, geothermal fluid temperature 180°C, pump efficiency 90%, turbine efficiency 80% and pinch point temperature 10°C.

$$\text{Relative Error} = \frac{| \text{Present Work Value} - \text{Reference Paper Value} | * 100}{\text{Reference Paper Value}}$$

The comparison table exhibits that the results of mathematical model are in concurrence with the reference paper.

Performance parameters	R123		
	Mortaza Yari [25]	Present Work	Relative Error
$\dot{W}_{net}$ [kJ/kg]	50.38	50.29	0.18%
$\dot{I}_{plant}$ [kJ/kg]	80.25	79.68	0.71%
$\eta_{I,1}$ [%]	7.65	7.369	3.67%
$\eta_{I,2}$ [%]	13.28	13.06	1.66%
$\eta_{II,1}$ [%]	38.76	37.84	2.37%
$\eta_{II,2}$ [%]	49.06	48.56	1.02%
$\xi$ [%]	64.33	63.28	1.63%

Table 5.2: Model Validation for Basic ORC using R123 as working fluid

Table 5.2 compares the Net Work Output, Overall Plant Irreversibility, First Law Efficiencies, Second Law Efficiencies and Cycle Effectiveness obtained from the EES Simulation of Basic ORC Mathematical Model devised in Section 5.3.1 using R123 as working fluid with Mortaza Yari [25]. It is found that the results are in very good comparison with the reference paper.

Performance parameters	n-Pentane		
	Mortaza Yari [25]	Present Work	Relative Error
$\dot{W}_{net}$ [kJ/kg]	48.57	49.23	1.36%
$\dot{I}_{plant}$ [kJ/kg]	81.11	80.74	0.46%
$\eta_{I,1}$ [%]	7.376	7.213	2.21%
$\eta_{I,2}$ [%]	12.6	12.64	0.32%
$\eta_{II,1}$ [%]	37.37	37.04	0.88%
$\eta_{II,2}$ [%]	46.8	47.15	0.75%
$\xi$ [%]	61.3	61.73	0.7%

Table 5.3: Model Validation for Basic ORC using n-Pentane as working fluid

Table 5.3 compares the Net Work Output, Overall Plant Irreversibility, First Law Efficiencies, Second Law Efficiencies and Cycle Effectiveness obtained from the EES Simulation of Basic ORC Mathematical Model devised in Section 5.3.1 using n-Pentane as working fluid with Mortaza Yari [25]. It is found that the results are in very good comparison with the reference paper.

Performance parameters	R113		
	Mortaza Yari [25]	Present Work	Relative Error
$\dot{W}_{net}$ [kJ/kg]	50.38	48.12	4.49%
$\dot{I}_{plant}$ [kJ/kg]	80.25	81.85	1.99%
$\eta_{I,1}$ [%]	7.65	7.05	7.84%
$\eta_{I,2}$ [%]	13.28	12.97	2.33%
$\eta_{II,1}$ [%]	38.76	36.2	6.60%
$\eta_{II,2}$ [%]	49.06	47.66	2.85%
$\xi$ [%]	64.33	62.23	3.26%

Table 5.4: Model Validation for Basic ORC using R113 as working fluid

Table 5.4 compares the Net Work Output, Overall Plant Irreversibility, First Law Efficiencies, Second Law Efficiencies and Cycle Effectiveness obtained from the EES Simulation of Basic ORC Mathematical Model devised in Section 5.3.1 using R113 as working fluid with Mortaza Yari [25]. It is found that the results are in very good comparison with the reference paper.

Performance parameters	R123		
	Mortaza Yari [25]	Present Work	Relative Error
$\dot{W}_{net}$ [kJ/kg]	50.38	50.29	0.18%
$\dot{I}_{plant}$ [kJ/kg]	80.25	79.68	0.71%
$\eta_{I,1}$ [%]	7.65	7.369	3.67%
$\eta_{I,2}$ [%]	14.2	13.97	1.62%
$\eta_{II,1}$ [%]	38.76	37.84	2.37%
$\eta_{II,2}$ [%]	51.4	50.91	0.95%
$\xi$ [%]	65.82	64.75	1.63%

Table 5.5: Model Validation for ORC with IHE using R123 as working fluid

Table 5.5 compares the Net Work Output, Overall Plant Irreversibility, First Law Efficiencies, Second Law Efficiencies and Cycle Effectiveness obtained from the EES Simulation of ORC with IHE Mathematical Model devised in Section 5.3.2 using R123 as working fluid with Mortaza Yari [25]. It is found that the results are in very good comparison with the reference paper.



Performance parameters	n-Pentane		
	Mortaza Yari [25]	Present Work	Relative Error
$\dot{W}_{net}$ [kJ/kg]	48.57	49.23	1.36
$\dot{I}_{plant}$ [kJ/kg]	81.11	80.74	0.46
$\eta_{I,1}$ [%]	7.376	7.213	2.21
$\eta_{I,2}$ [%]	14.06	14.15	0.64
$\eta_{II,1}$ [%]	37.37	37.04	0.88
$\eta_{II,2}$ [%]	50.52	51.08	1.11
$\eta_{II,3}$ [%]	64.21	64.42	0.33

Table 5.6: Model Validation for ORC with IHE using n-Pentane as working fluid

Table 5.6 compares the Net Work Output, Overall Plant Irreversibility, First Law Efficiencies, Second Law Efficiencies and Cycle Effectiveness obtained from the EES Simulation of ORC with IHE Mathematical Model devised in Section 5.3.2 using n-pentane as working fluid with Mortaza Yari [25]. It is found that the results are in very good comparison with the reference paper.

Performance parameters	R113		
	Mortaza Yari [25]	Present Work	Relative Error
$\dot{W}_{net}$ [kJ/kg]	47.87	48.12	0.52%
$\dot{I}_{plant}$ [kJ/kg]	82.48	81.85	0.76%
$\eta_{I,1}$ [%]	7.27	7.051	3.01%
$\eta_{I,2}$ [%]	14.45	14.29	1.11%
$\eta_{II,1}$ [%]	36.83	36.2	1.71%
$\eta_{II,2}$ [%]	51.33	51.14	0.37%
$\xi$ [%]	65.84	64.6	1.88%

Table 5.7: Model Validation for ORC with IHE using R113 as working fluid

Table 5.7 compares the Net Work Output, Overall Plant Irreversibility, First Law Efficiencies, Second Law Efficiencies and Cycle Effectiveness obtained from the EES Simulation of ORC with IHE Mathematical Model devised in Section 5.3.2 using R113 as working fluid with Mortaza Yari [25]. It is found that the results are in very good comparison with the reference paper.

Performance parameters	R123		
	Mortaza Yari [25]	Present Work	Relative Error
$\dot{W}_{net}$ [kJ/kg]	43.361	44.13	1.77
$\dot{I}_{plant}$ [kJ/kg]	85.98	85.84	0.16
$\eta_{I,1}$ [%]	6.623	6.466	2.37
$\eta_{I,2}$ [%]	14.52	14.48	0.28
$\eta_{II,1}$ [%]	33.56	33.2	1.07
$\eta_{II,2}$ [%]	50.39	50.64	0.5
$\xi$ [%]	62.67	62.49	0.29

Table 5.8: Model Validation for regenerative ORC using R123 as working fluid

Table 5.8 compares the Net Work Output, Overall Plant Irreversibility, First Law Efficiencies, Second Law Efficiencies and Cycle Effectiveness obtained from the EES Simulation of regenerative ORC Mathematical Model devised in Section 5.3.3 using R123 as working fluid with Mortaza Yari [25]. It is found that the results are in very good comparison with the reference paper.

Performance parameters	n-Pentane		
	Mortaza Yari [25]	Present Work	Relative Error
$\dot{W}_{net}$ [kJ/kg]	42.55	39.3	7.64
$\dot{I}_{plant}$ [kJ/kg]	87.11	90.67	4.09
$\eta_{I,1}$ [%]	6.462	5.758	10.89
$\eta_{I,2}$ [%]	14.06	13.91	1.07
$\eta_{II,1}$ [%]	32.74	29.57	9.68
$\eta_{II,2}$ [%]	48.85	47.87	2.01
$\xi$ [%]	60.83	58.9	3.17

Table 5.9: Model Validation for regenerative ORC using n-Pentane as working fluid

Table 5.9 compares the Net Work Output, Overall Plant Irreversibility, First Law Efficiencies, Second Law Efficiencies and Cycle Effectiveness obtained from the EES Simulation of regenerative ORC Mathematical Model devised in Section 5.3.3 using n-pentane as working fluid with Mortaza Yari [25]. It is found that the results are in fair comparison with the reference paper.

Performance parameters	R113		
	Mortaza Yari [25]	Present Work	Relative Error
$\dot{W}_{net}$ [kJ/kg]	41.89	34.43	17.81
$\dot{I}_{plant}$ [kJ/kg]	87.87	95.53	8.72
$\eta_{I,1}$ [%]	6.362	5.045	20.7
$\eta_{I,2}$ [%]	14.34	13.82	3.63
$\eta_{II,1}$ [%]	32.23	25.91	19.61
$\eta_{II,2}$ [%]	49.45	46.49	5.99
$\xi$ [%]	62	57.38	7.45

Table 5.10: Model Validation for regenerative ORC using R113 as working fluid

Table 5.10 compares the Net Work Output, Overall Plant Irreversibility, First Law Efficiencies, Second Law Efficiencies and Cycle Effectiveness obtained from the EES Simulation of regenerative ORC Mathematical Model devised in Section 5.3.3 using R113 as working fluid with Mortaza Yari [25]. It is found that the results are in fair comparison with the reference paper.

Performance parameters	R123		
	Mortaza Yari [25]	Present Work	Relative Error
$\dot{W}_{net}$ [kJ/kg]	44.02	43.88	0.32
$\dot{I}_{plant}$ [kJ/kg]	86.59	86.09	0.58
$\eta_{I,1}$ [%]	6.685	6.429	3.83
$\eta_{I,2}$ [%]	15.35	15.08	1.76
$\eta_{II,1}$ [%]	33.87	33.01	2.54
$\eta_{II,2}$ [%]	52.73	52.2	1.01
$\xi$ [%]	65.41	64.24	1.79

Table 5.11: Model Validation for regenerative ORC with IHE using R123 as working fluid

Table 5.11 compares the Net Work Output, Overall Plant Irreversibility, First Law Efficiencies, Second Law Efficiencies and Cycle Effectiveness obtained from the EES Simulation of regenerative ORC with IHE Mathematical Model devised in Section 5.3.4 using R123 as working fluid with Mortaza Yari [25]. It is found that the results are in very good comparison with the reference paper.

Performance parameters	n-Pentane		
	Mortaza Yari [25]	Present Work	Relative Error
$\dot{W}_{net}$ [kJ/kg]	42.31	39.97	5.53
$\dot{I}_{plant}$ [kJ/kg]	87.38	89.99	2.99
$\eta_{I,1}$ [%]	6.425	5.857	8.84
$\eta_{I,2}$ [%]	14.96	14.97	0.07
$\eta_{II,1}$ [%]	32.24	30.08	6.7
$\eta_{II,2}$ [%]	51.24	50.97	0.53
$\xi$ [%]	63.57	62.71	1.35

Table 5.12: Model Validation for regenerative ORC with IHE using n-Pentane as working fluid

Table 5.12 compares the Net Work Output, Overall Plant Irreversibility, First Law Efficiencies, Second Law Efficiencies and Cycle Effectiveness obtained from the EES Simulation of regenerative ORC with IHE Mathematical Model devised in Section 5.3.4 using n-pentane as working fluid with Mortaza Yari [25]. It is found that the results are in fair comparison with the reference paper.

Performance parameters	R113		
	Mortaza Yari [25]	Present Work	Relative Error
$\dot{W}_{net}$ [kJ/kg]	42.28	34.53	18.33
$\dot{I}_{plant}$ [kJ/kg]	88.06	95.44	8.38
$\eta_{I,1}$ [%]	6.42	5.059	21.2
$\eta_{I,2}$ [%]	15.34	14.69	4.24
$\eta_{II,1}$ [%]	32.53	25.98	20.14
$\eta_{II,2}$ [%]	52.34	48.98	6.42
$\xi$ [%]	65.35	60.8	6.96

Table 5.13: Model Validation for regenerative ORC with IHE using R113 as working fluid

Table 5.13 compares the Net Work Output, Overall Plant Irreversibility, First Law Efficiencies, Second Law Efficiencies and Cycle Effectiveness obtained from the EES Simulation of regenerative ORC with IHE Mathematical Model devised in Section 5.3.4 using R113 as working fluid with Mortaza Yari [25]. It is found that the results are in fair comparison with the reference paper.

The difference in the readings may be attributed by the employment of Preheater and Evaporator unit in present work as compared to the evaporator alone in the reference paper, the effect of which are complemented by the high boiling point temperature properties of R113.

## CHAPTER –VI

### ANALYSIS

#### 6.1 Performance Analysis of Organic Binary Fluids:

A performance Analysis is performed to find the optimum working fluid for the conditions and variables of the analysis.

The effect of variation in turbine inlet temperature on several parameters is analyzed. When the net power output per unit mass flow rate of geo fluid is plotted against the turbine inlet temperature, it is observed that all the binary fluids demonstrated similar behavior for the Basic ORC and ORC with IHE, whereas for the regenerative cycles the behavior is quite different. The optimum Turbine Inlet Temperature corresponding to maximum net work output is also elicited from this plot. The comparison of cycles shows that the isobutene exhibits similar net power output for both basic and regenerative cycles, while other refrigerants exhibit significant reduction in power when used with Regenerative Cycles i.e., an average reduction of 27% for R123, 19% for R152a, 45% for n-pentane, 10% for R245fa and 63% for R113.

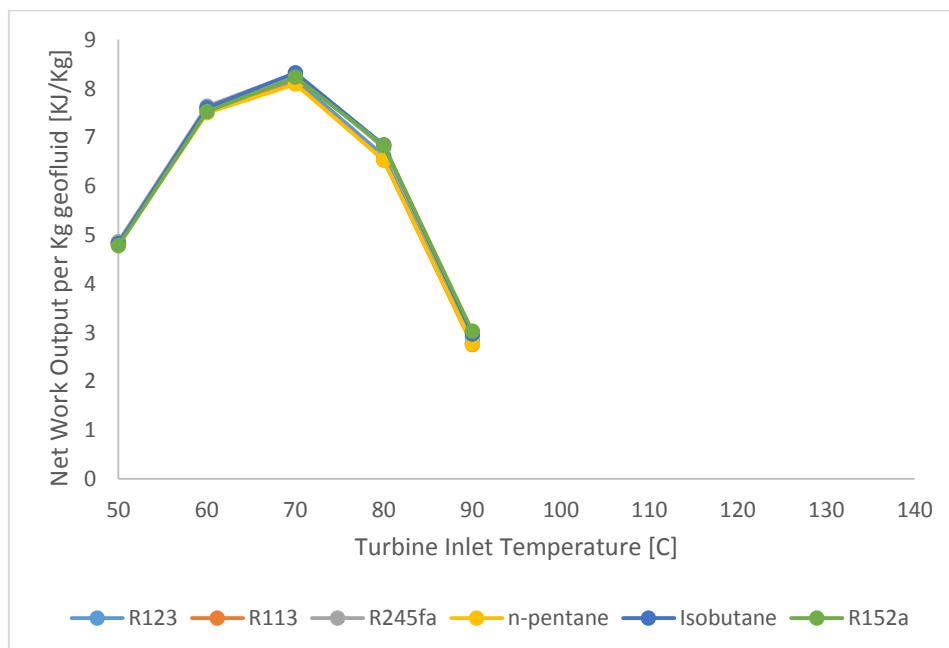


Fig 6.1 Net Work output per Kg of geo fluid at the temperature of 100 °C for Basic Organic Rankine Cycle

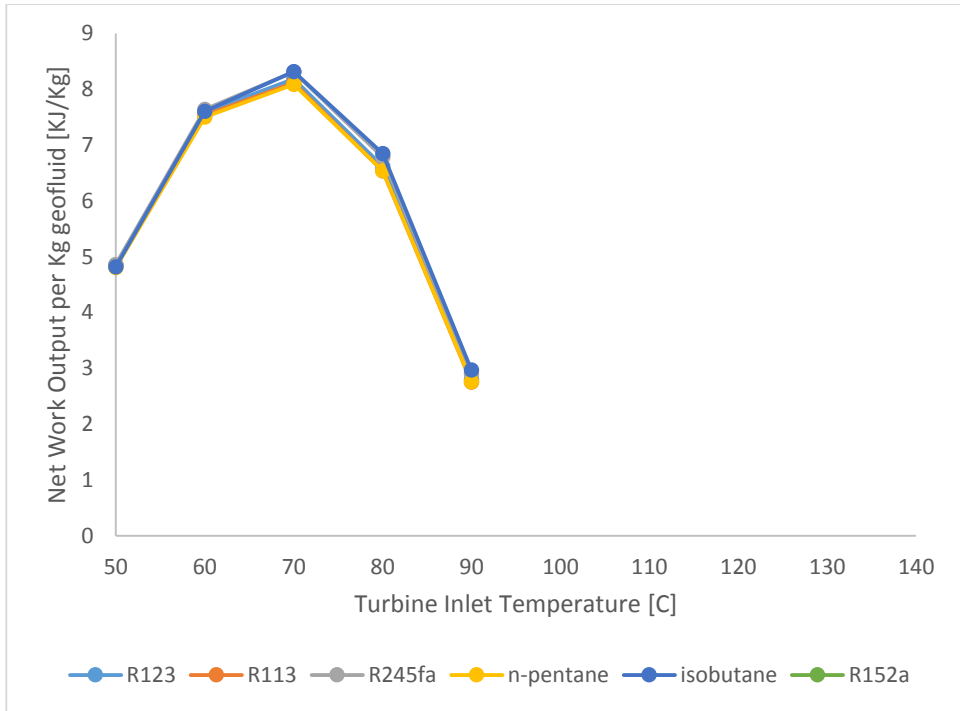


Fig 6.2 Net Work output per Kg of geo fluid at the temperature of 100 °C for Organic Rankine Cycle with IHE

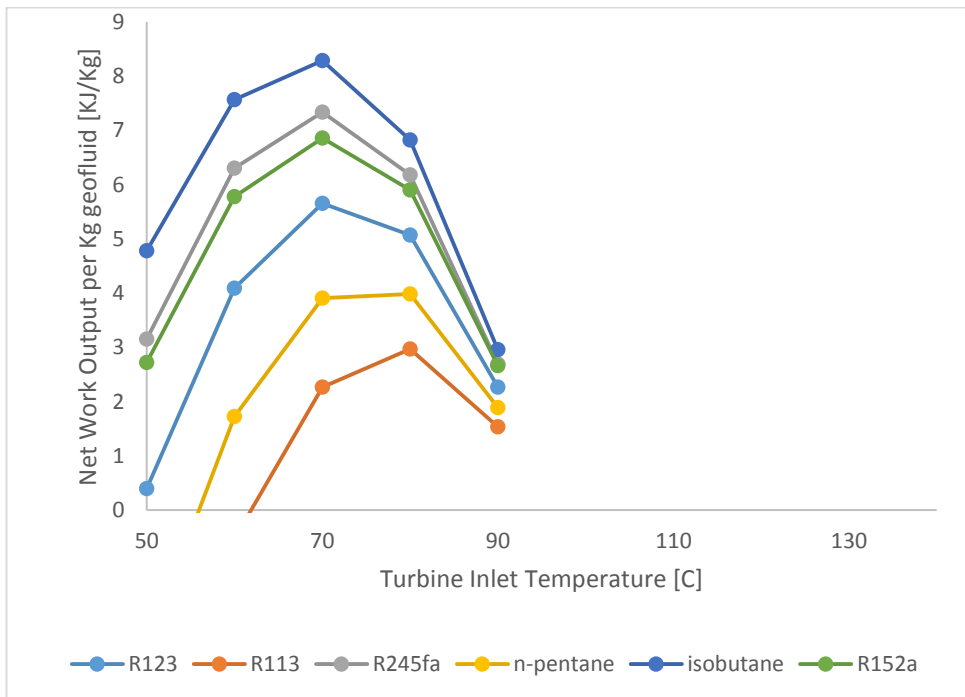


Fig 6.3 Net Work output per Kg of geo fluid at the temperature of 100 °C for Regenerative Rankine Cycle

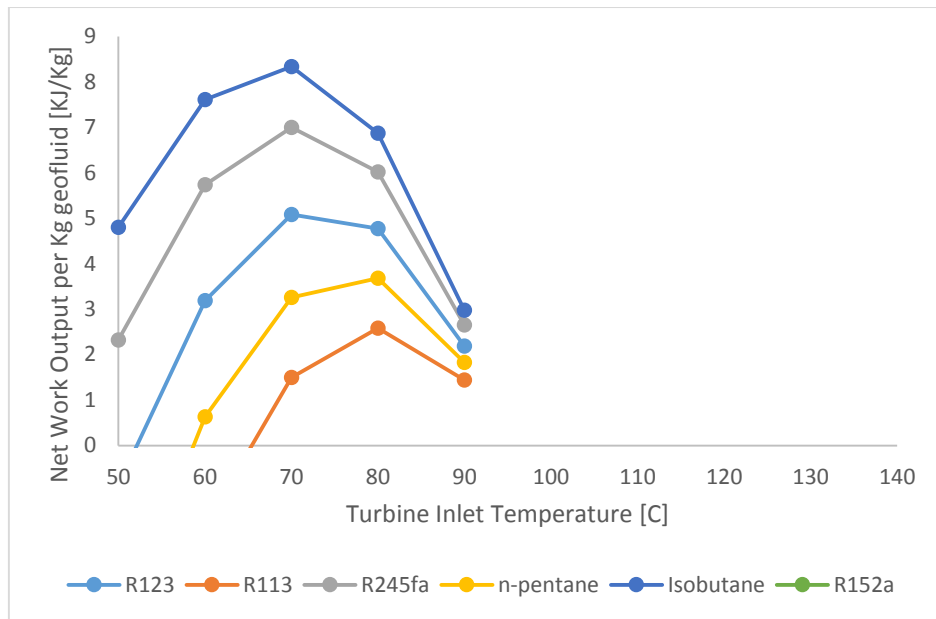


Fig 6.4 Net Work output per Kg of geo fluid at the temperature of 100 °C for Regenerative Rankine Cycle with IHE

It is also observed that the Net Work Output increases exponentially with increase in geo fluid temperature under sub critical pressure operating conditions and turbine inlet temperature increases linearly with increase in geo fluid temperature. An increase of 50% in the temperature of geo fluid from 100 °C to 150 °C will result in an average increment of 367% in Net Work Output per Kg geo fluid for both basic and regenerative cycles.

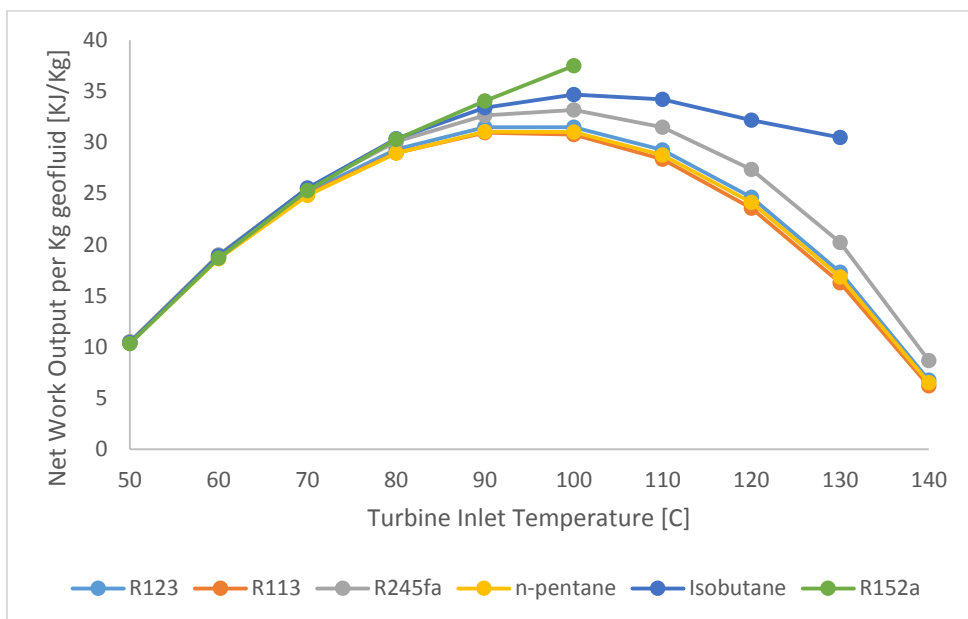


Fig 6.5 Net Work output per Kg of geo fluid at the temperature of 150 °C for Basic Organic Rankine Cycle



Since the binary fluids with higher boiling point temperature or lower specific heat capacity have relatively lower optimum turbine inlet temperature corresponding to maximum work output which reduces extra capital cost, higher boiling point organic fluids like n-pentane, R123 and R113 are recommended for Basic ORC configuration, whereas organic fluids with lower vapor specific heat capacity like iso-butane and R245fa are recommended for Regenerative ORC as low specific heat capacity binary fluids have relatively lower optimum turbine inlet temperature corresponding to maximum work output.

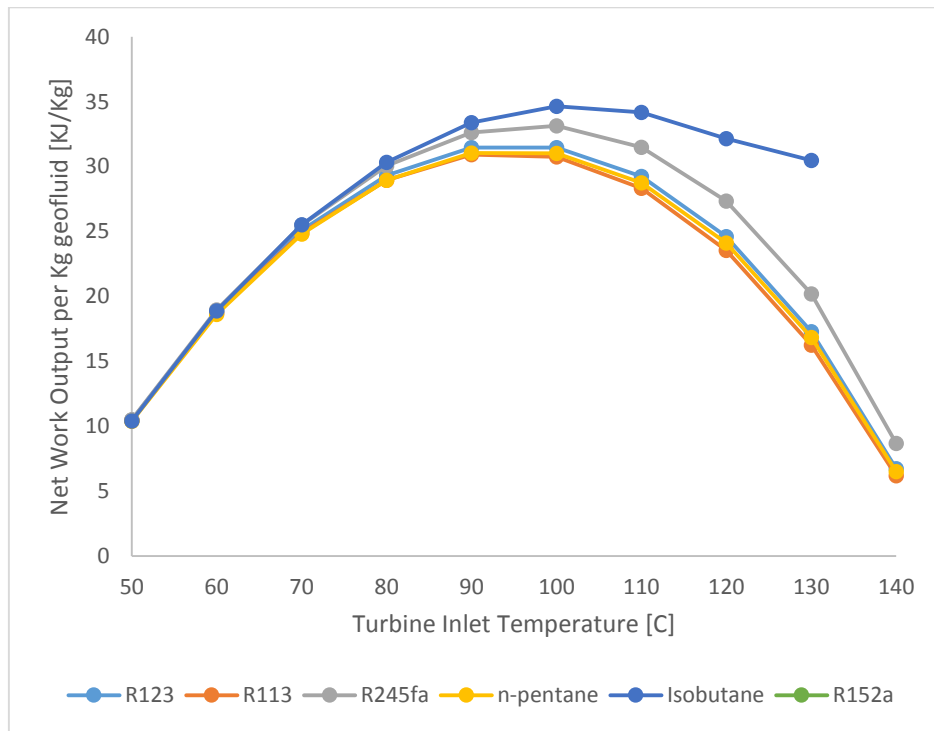


Fig 6.6 Net Work output per Kg of geo fluid at the temperature of 150 °C for Organic Rankine Cycle with IHE

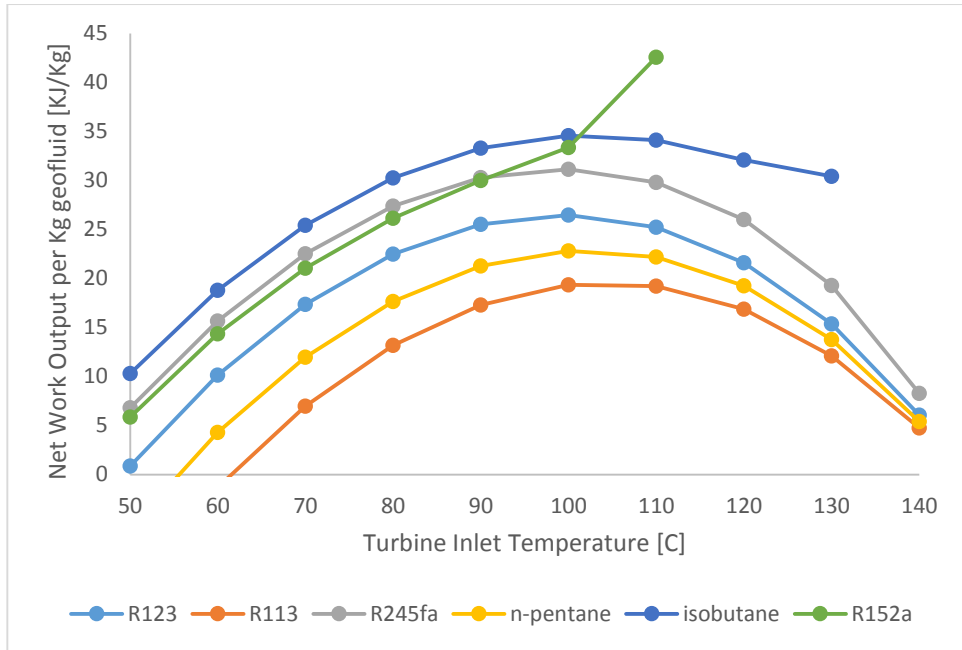


Fig 6.7 Net Work output per Kg of geo fluid at the temperature of 150 °C for Regenerative Rankine Cycle

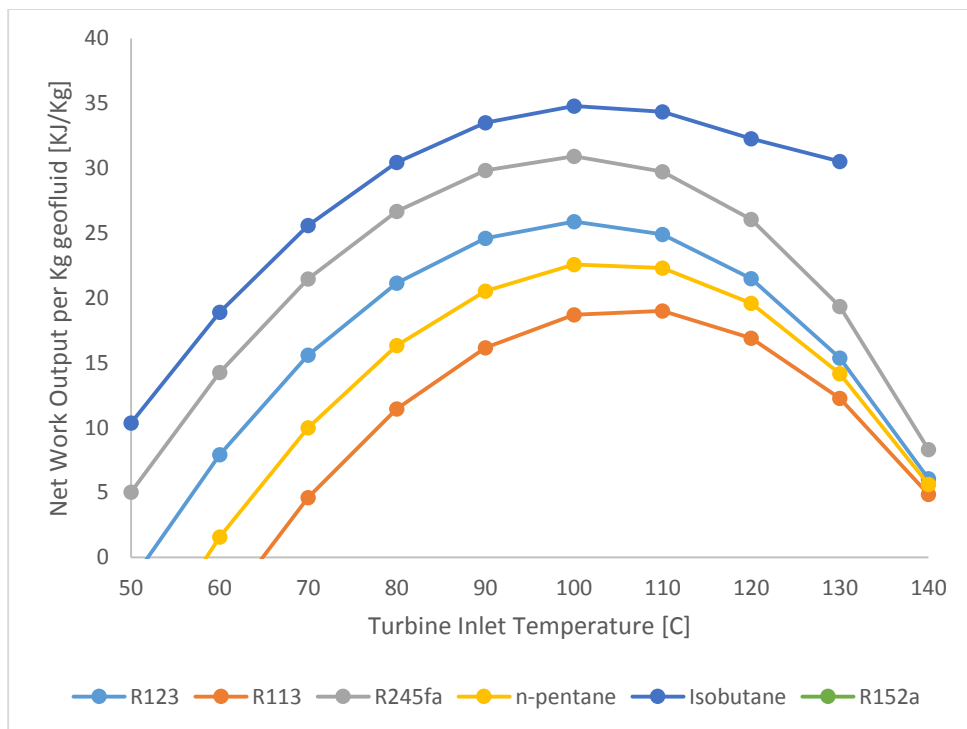


Fig 6.8 Net Work output per Kg of geo fluid at the temperature of 150 °C for Regenerative Rankine Cycle with IHE

Fig 6.9 to Fig 6.12 depicts the effect of Turbine Inlet Temperature on Thermal Efficiency. It is found that in general the thermal efficiency increases with increase in Turbine Inlet Temperature.

Furthermore the working fluids with higher boiling point i.e.; R123, n-pentane and R113 showed better Thermal Efficiency as compared to working fluids with lower boiling points.

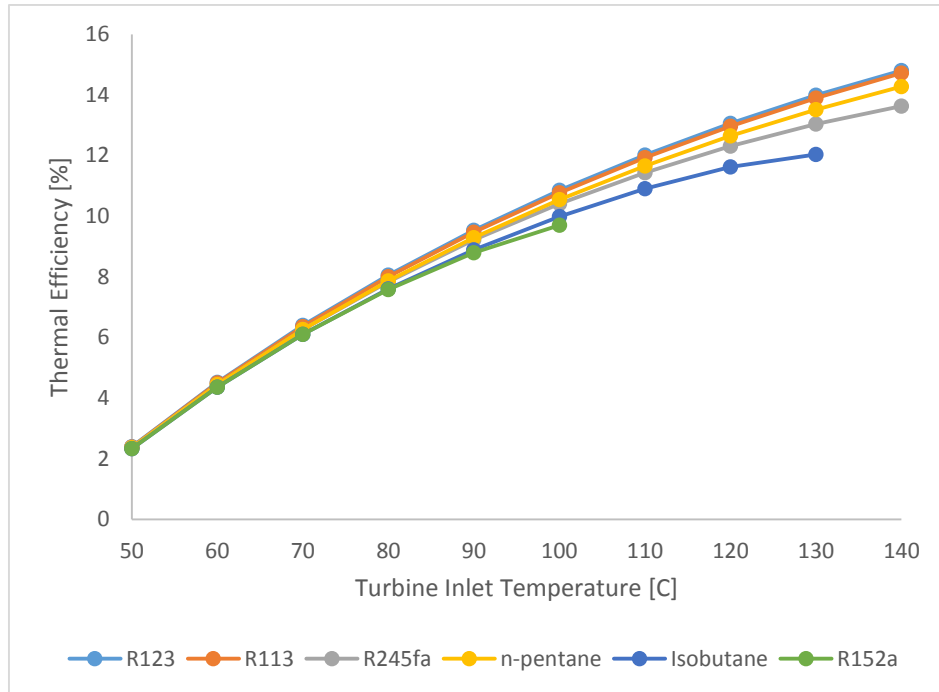


Fig 6.9 Cycle thermal efficiency for geo fluid at the temperature of 150 °C for Basic Organic Rankine Cycle

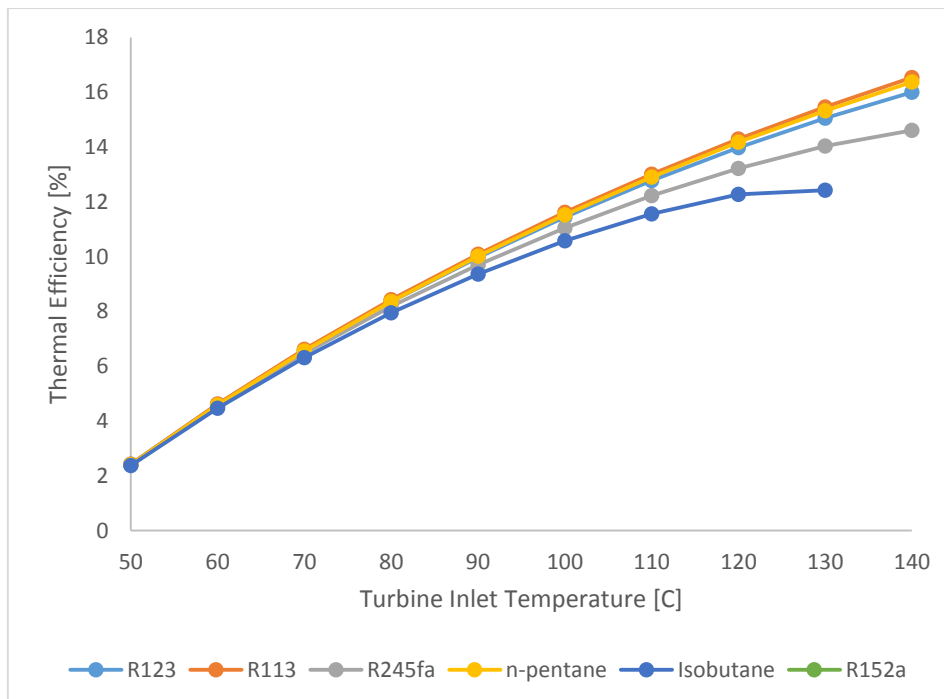


Fig 6.10 Cycle thermal efficiency for geo fluid at the temperature of 150 °C for Organic Rankine Cycle with IHE

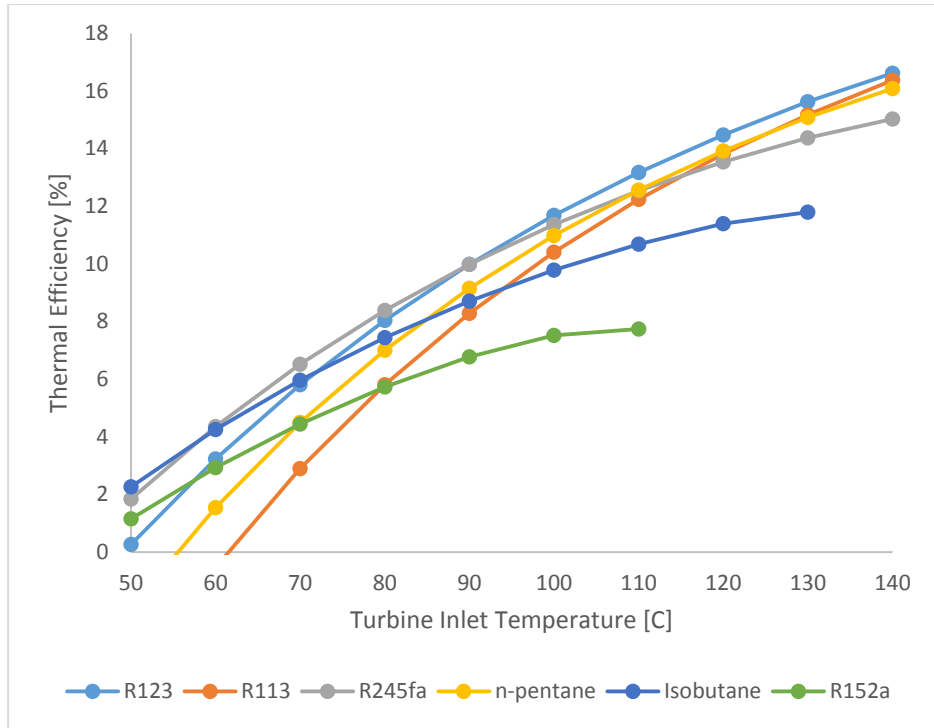


Fig 6.11 Cycle thermal efficiency for geo fluid at the temperature of 150 °C for Regenerative Organic Rankine Cycle

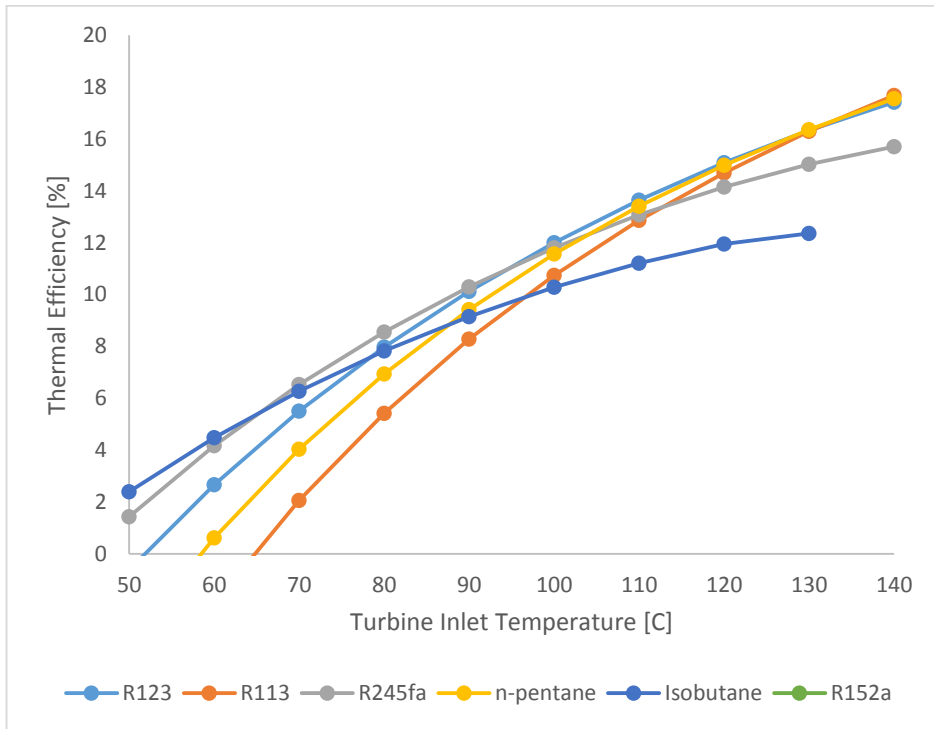


Fig 6.12 Cycle thermal efficiency for geo fluid at the temperature of 150 °C for Regenerative Organic Rankine Cycle with IHE

Fig 6.13 to Fig 6.16 portrays the effect of Turbine Inlet Temperature on the first law efficiency based on geo fluid inlet conditions that is a measure of the

efficiency of conversion of available geothermal energy into the useful work. First law efficiency provides a basis of selection of optimum Turbine Inlet Temperature. It is found that working fluids with lower boiling point like iso-butane and R152a provide a better first law efficiency but due to lower Critical Temperature, they cannot be used with systems with higher geo fluid temperatures. R152a being a wet refrigerant exhibits linear increase in efficiency with increase in Turbine Inlet Temperature, which upon reaching the maximum efficiency is truncated due to the low critical temperature.

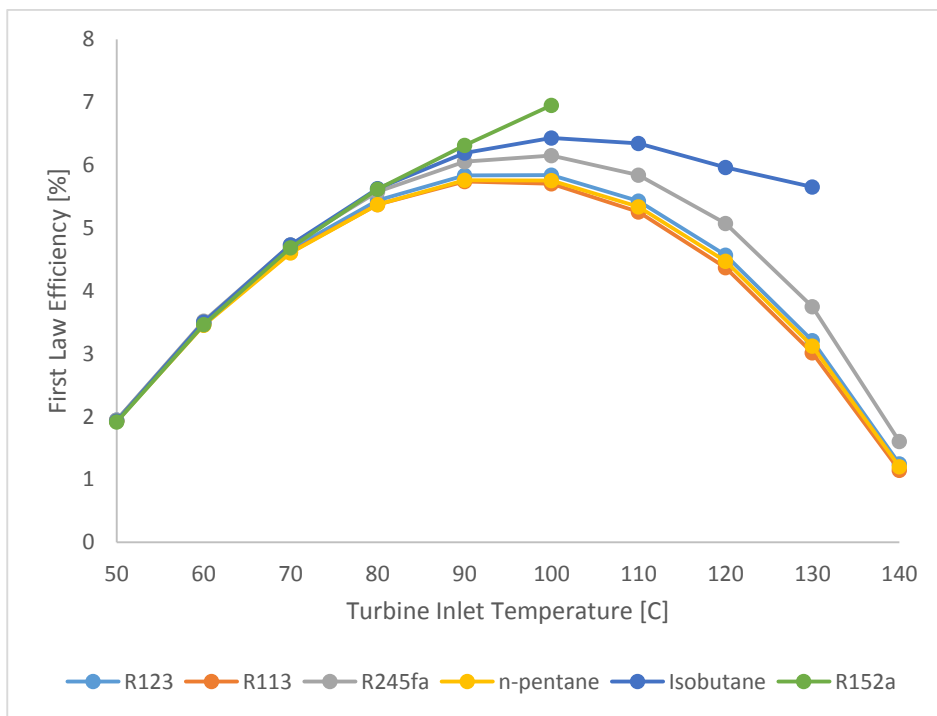


Fig 6.13 First Law Efficiency (based on geo fluid inlet state conditions) for geo fluid at the temperature of 150 °C for Basic Organic Rankine Cycle

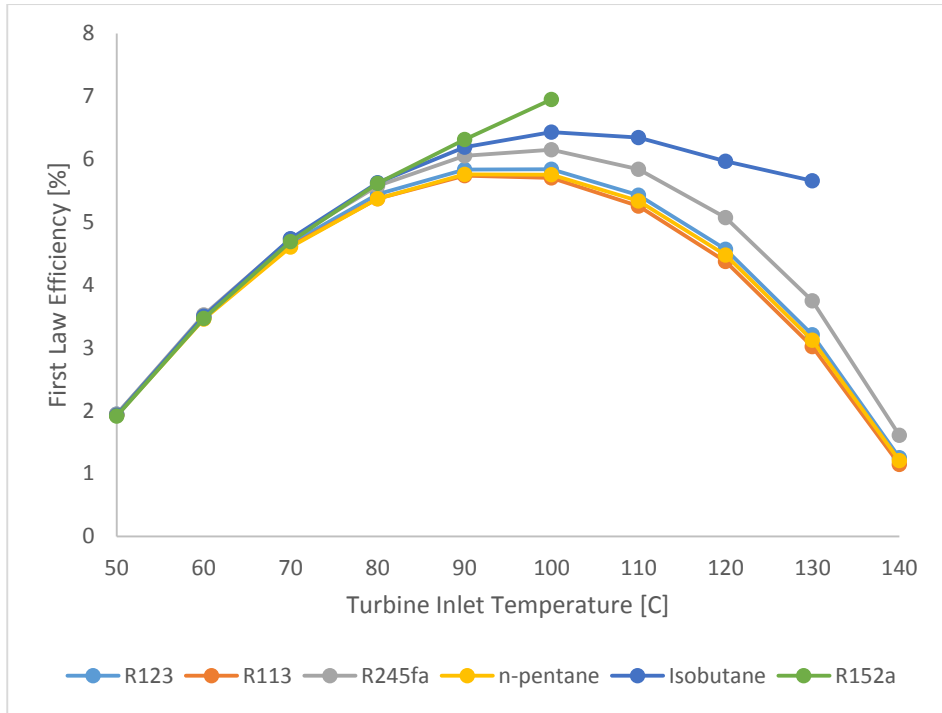


Fig 6.14 First Law Efficiency (based on geo fluid inlet state conditions) for geo fluid at the temperature of 150 °C for Organic Rankine Cycle with IHE

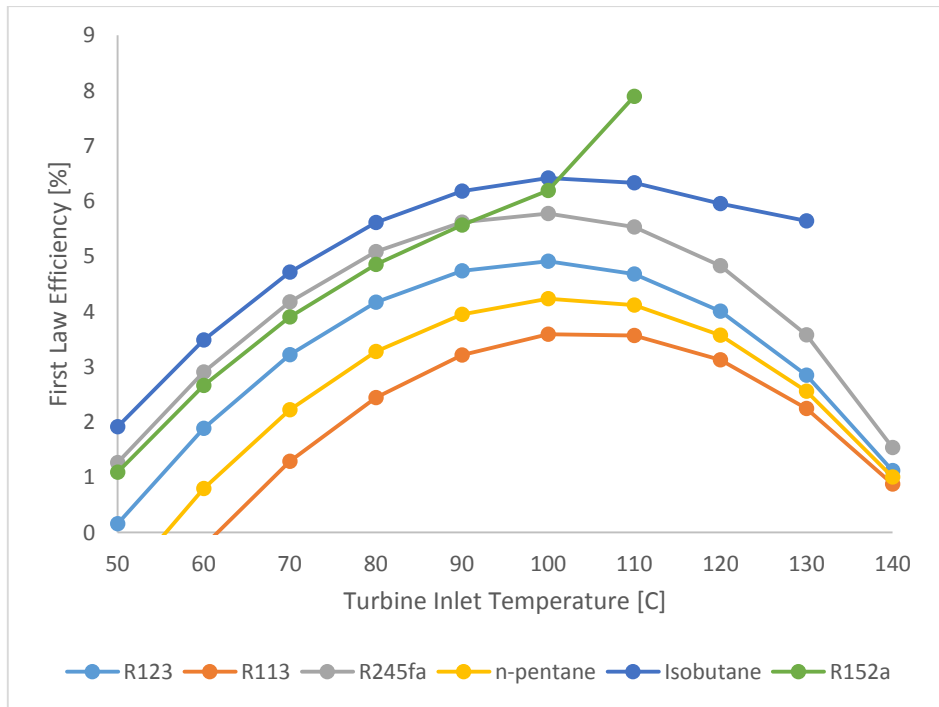


Fig 6.15 First Law Efficiency (based on geo fluid inlet state conditions) for geo fluid at the temperature of 150 °C for Regenerative Organic Rankine Cycle

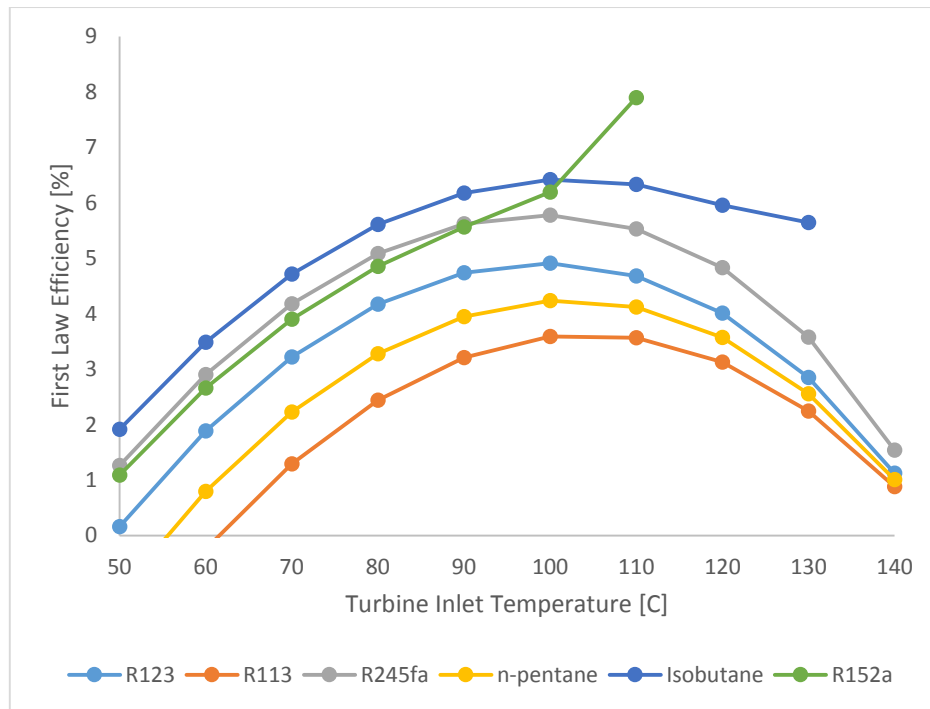


Fig 6.16 First Law Efficiency (based on geo fluid inlet state conditions) for geo fluid at the temperature of 150 °C for Regenerative Organic Rankine Cycle with IHE

Fig 6.17 to Fig 6.20 exhibits effect of Turbine Inlet Temperature on Second Law Efficiency based on geo fluid inlet state. It is found that working fluids with lower boiling point like iso-butane and R152a provide a better first law efficiency but due to lower Critical Temperature, iso-butane and R152a cannot be used with systems with higher geo fluid temperatures.

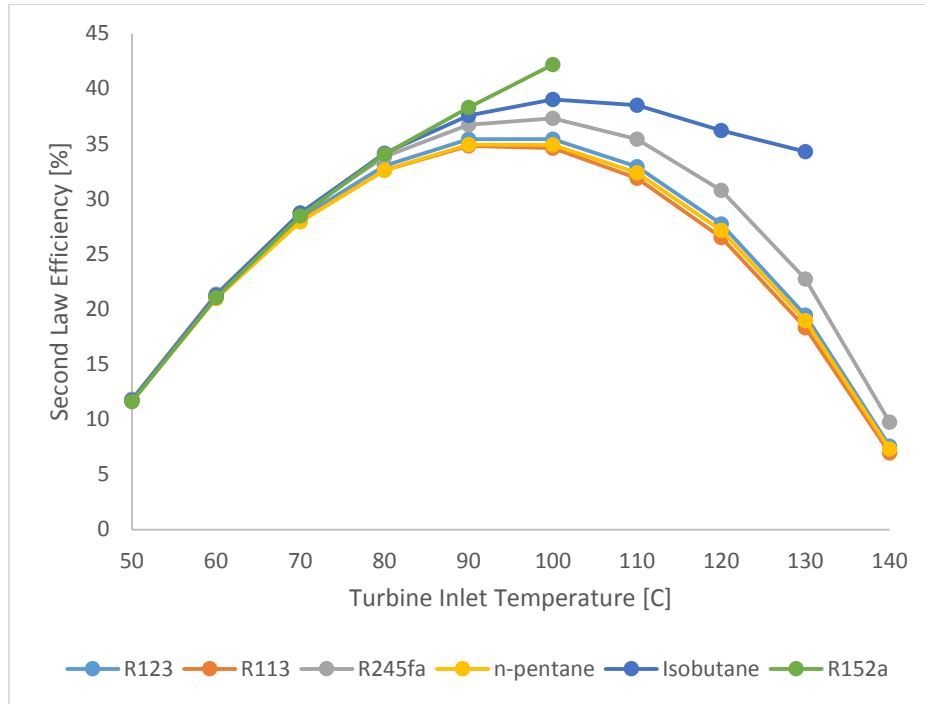


Fig 6.17 Second Law Efficiency (based on geo fluid inlet state) for geo fluid at the temperature of 150 °C for Basic Organic Rankine Cycle

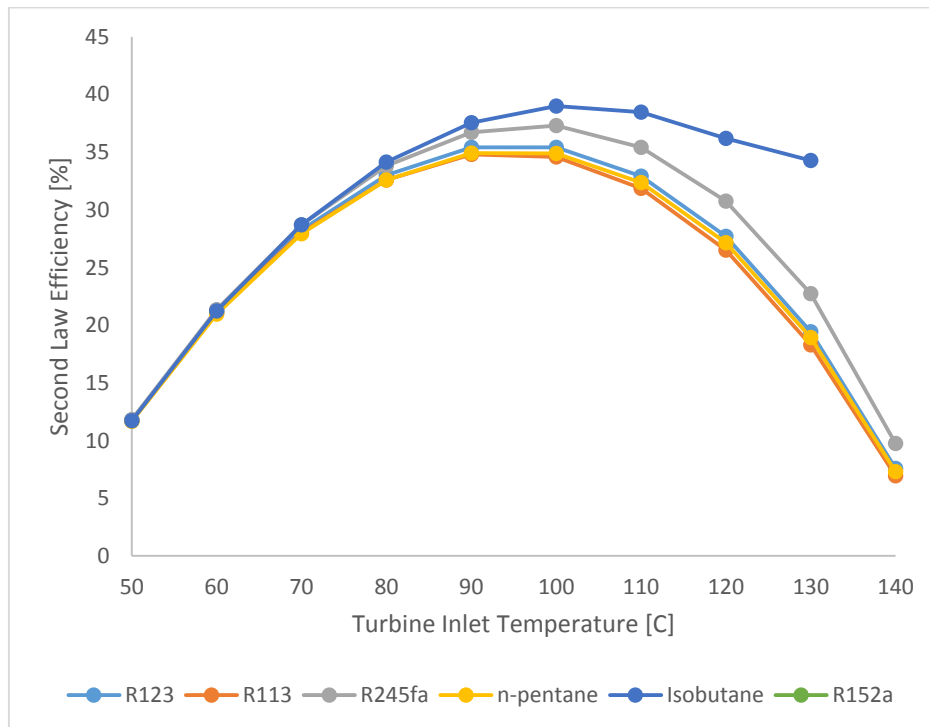


Fig 6.18 Second Law Efficiency (based on geo fluid inlet state) for geofluid at the temperature of 150 °C for Organic Rankine Cycle with IHE



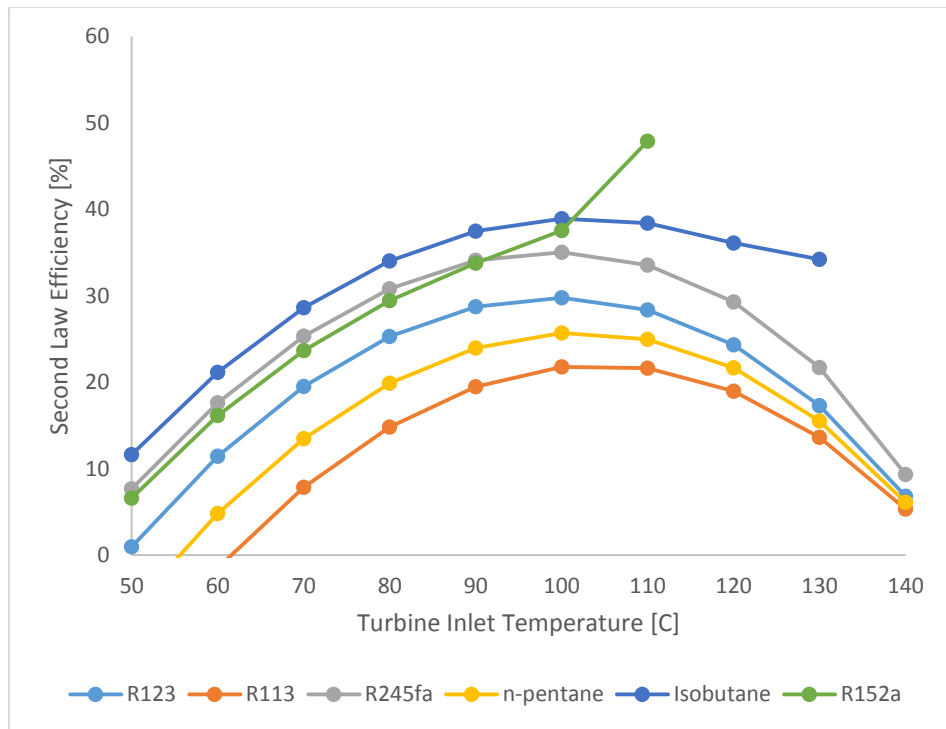


Fig 6.19 Second Law Efficiency (based on geo fluid inlet state) for geo fluid at the temperature of 150 °C for Regenerative Organic Rankine Cycle

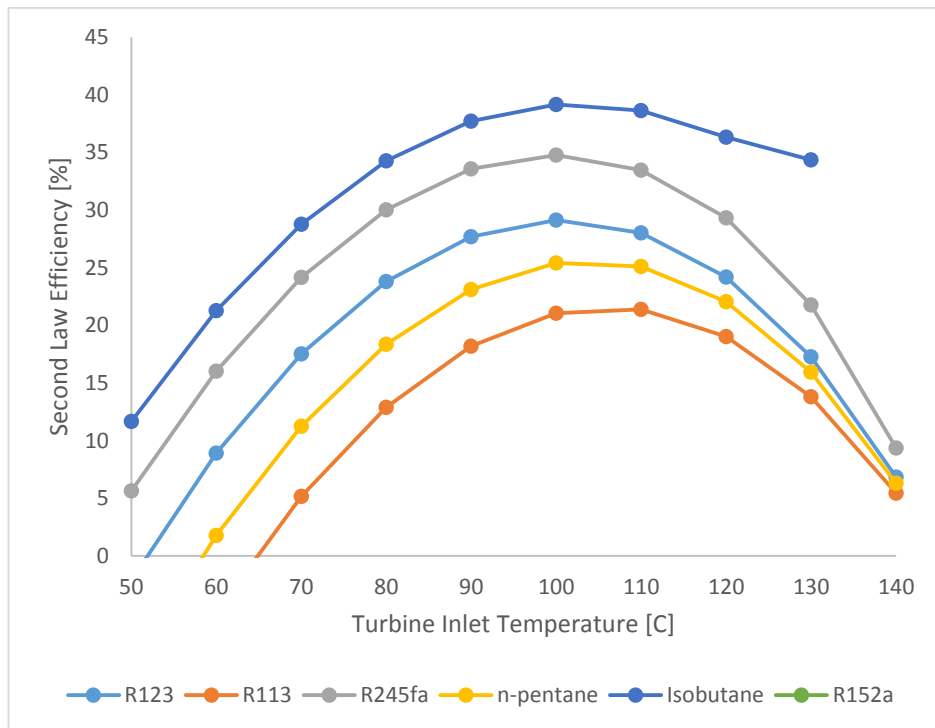


Fig 6.20 Second Law Efficiency (based on geo fluid inlet state) for geo fluid at the temperature of 150 °C for Regenerative Organic Rankine Cycle with IHE

Fig 6.21 to Fig 6.24 exhibits effect of Turbine Inlet Temperature on Second Law Efficiency based on energy input to the system. It is found that beyond an optimum turbine inlet temperature there is not any substantial increase in second law efficiency. All working fluid exhibited similar efficiency for the basic ORC. However for regenerative cycles the working fluids showed substantially lower efficiency at low turbine inlet temperatures below 100 °C. It is also noted that the second law efficiency for regenerative cycle is higher than basic ORC for higher Turbine Inlet temperatures.

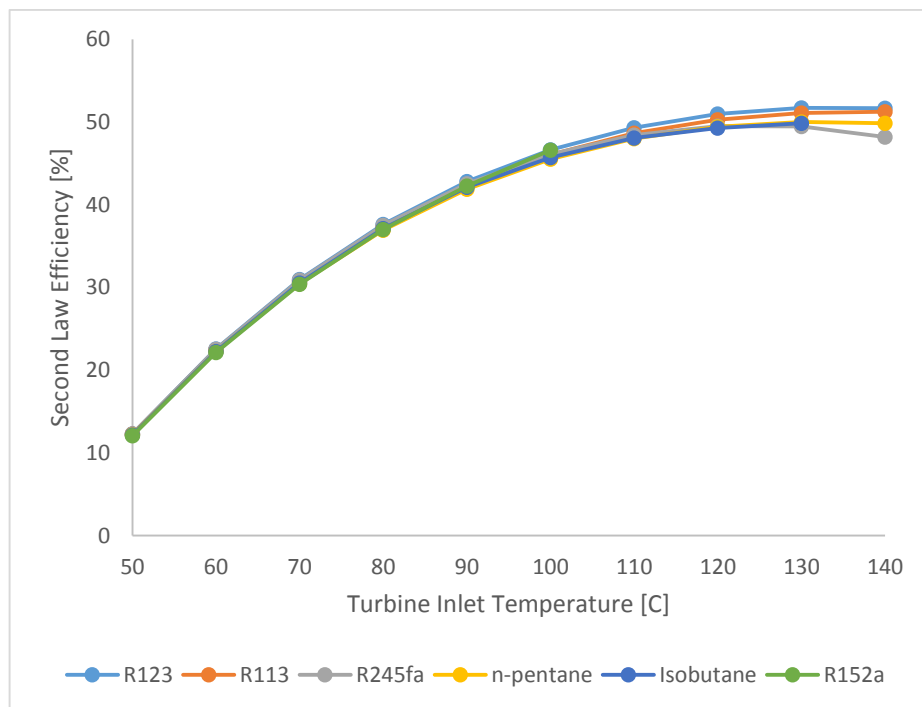


Fig 6.21 Second Law Efficiency (based on energy input) for geo fluid at the temperature of 150 °C for Basic Organic Rankine Cycle

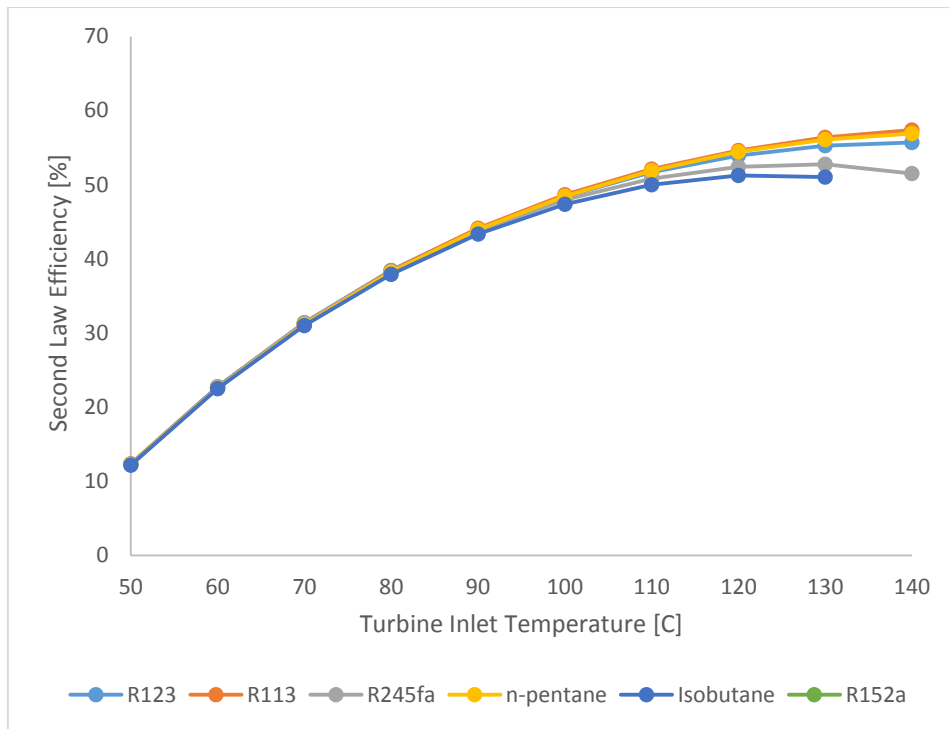


Fig 6.22 Second Law Efficiency (based on energy input) for geo fluid at the temperature of 150 °C for Organic Rankine Cycle with IHE

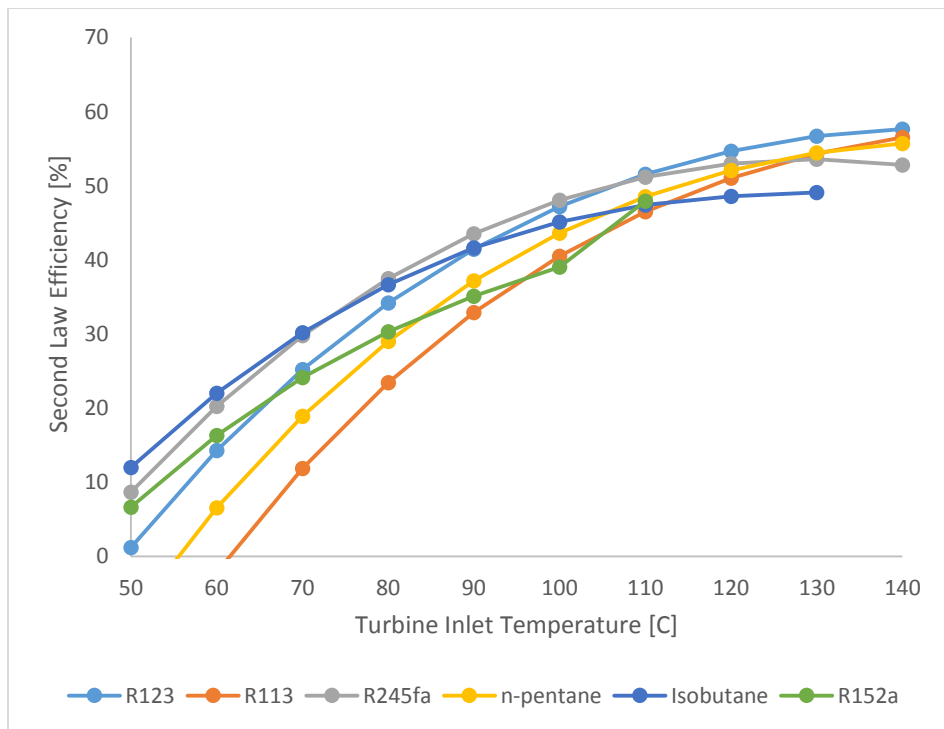


Fig 6.23 Second Law Efficiency (based on energy input) for geo fluid at the temperature of 150 °C for Regenerative Organic Rankine Cycle

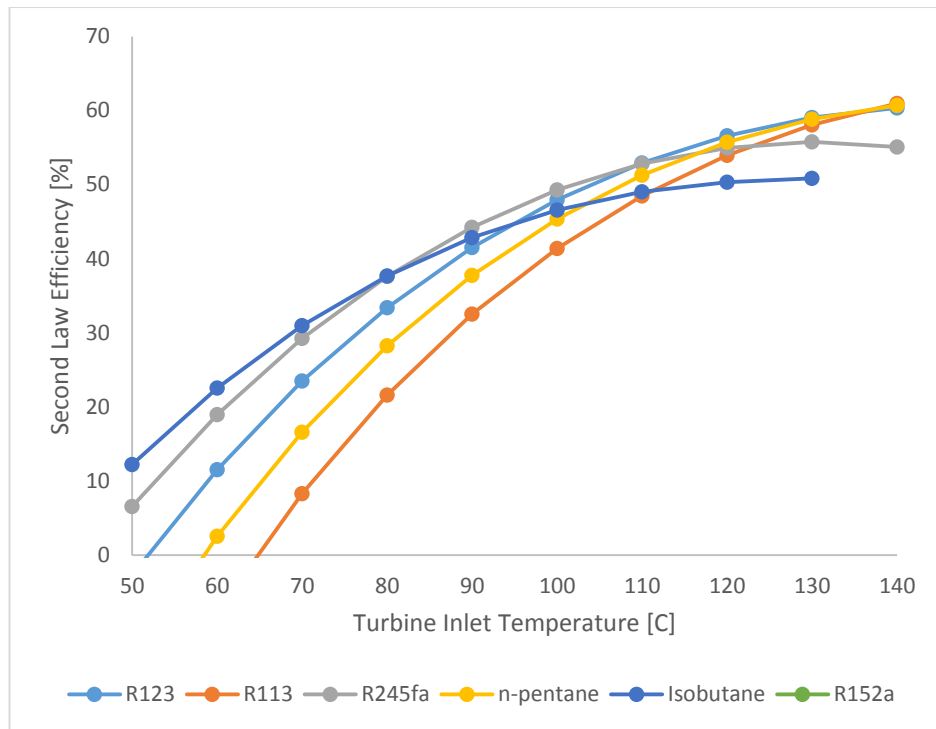


Fig 6.24 Second Law Efficiency (based on energy input) for geo fluid at the temperature of 150 °C for Regenerative Organic Rankine Cycle with IHE

Cycle effectiveness measures qualitatively as well as quantitatively the amount of available energy transferred from the geo fluid to the working fluid. It is found that like Second Law Efficiency beyond an optimum turbine inlet temperature there is not any substantial increase in Cycle Effectiveness. For basic ORC a marginal difference in Cycle Effectiveness is noted among the working fluids, however for the Regenerative ORC n-pentane, R123, R 113 and R152a showed substantial decrease in Cycle Effectiveness at temperatures lower than 100 °C.

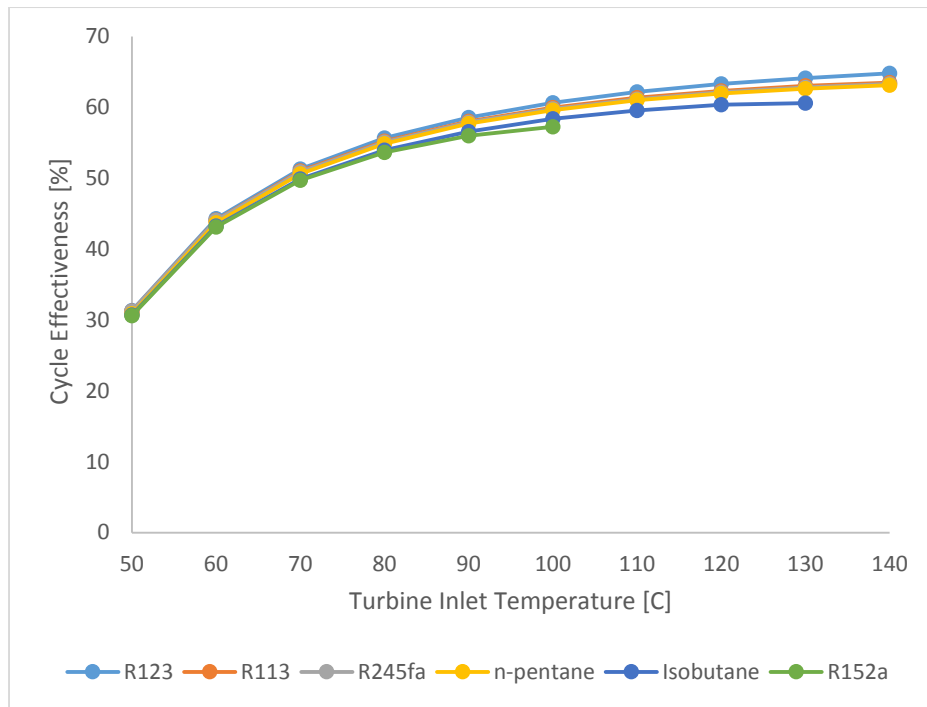


Fig 6.25 Cycle Effectiveness for geo fluid at the temperature of 150 °C for Basic Organic Rankine Cycle

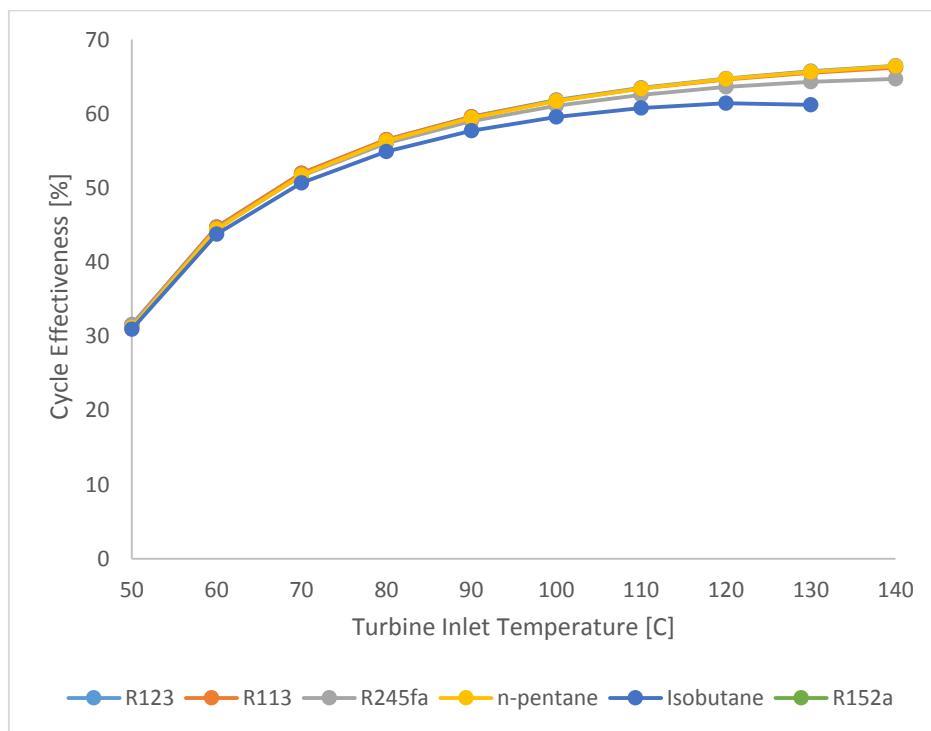


Fig 6.26 Cycle Effectiveness for geo fluid at the temperature of 150 °C for Organic Rankine Cycle with IHE

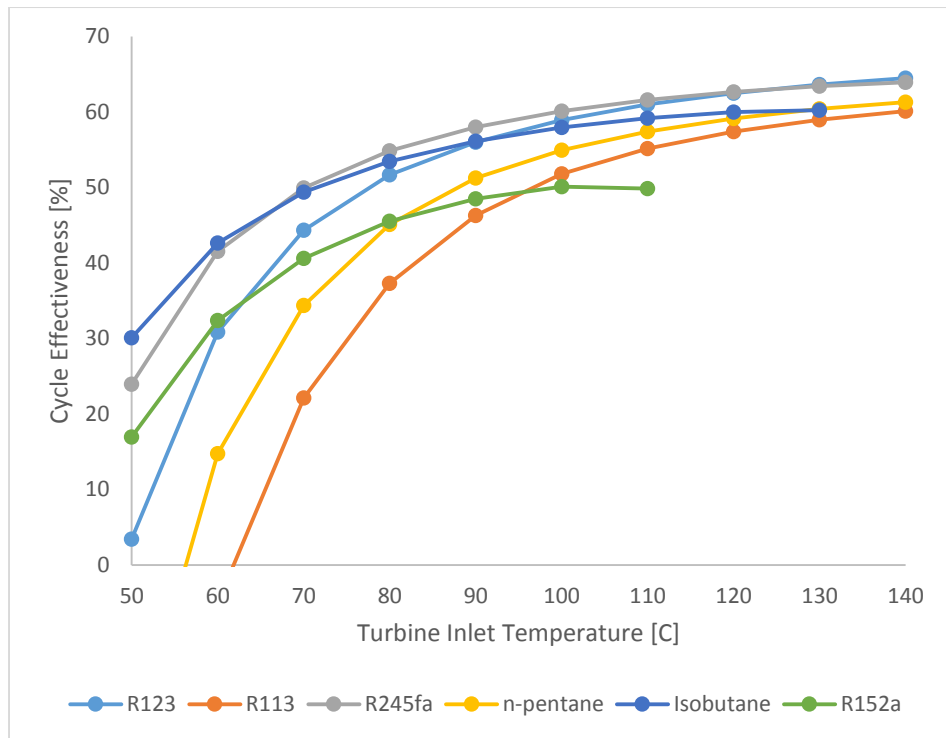


Fig 6.27 Cycle Effectiveness for geo fluid at the temperature of 150 °C for Regenerative Organic Rankine Cycle

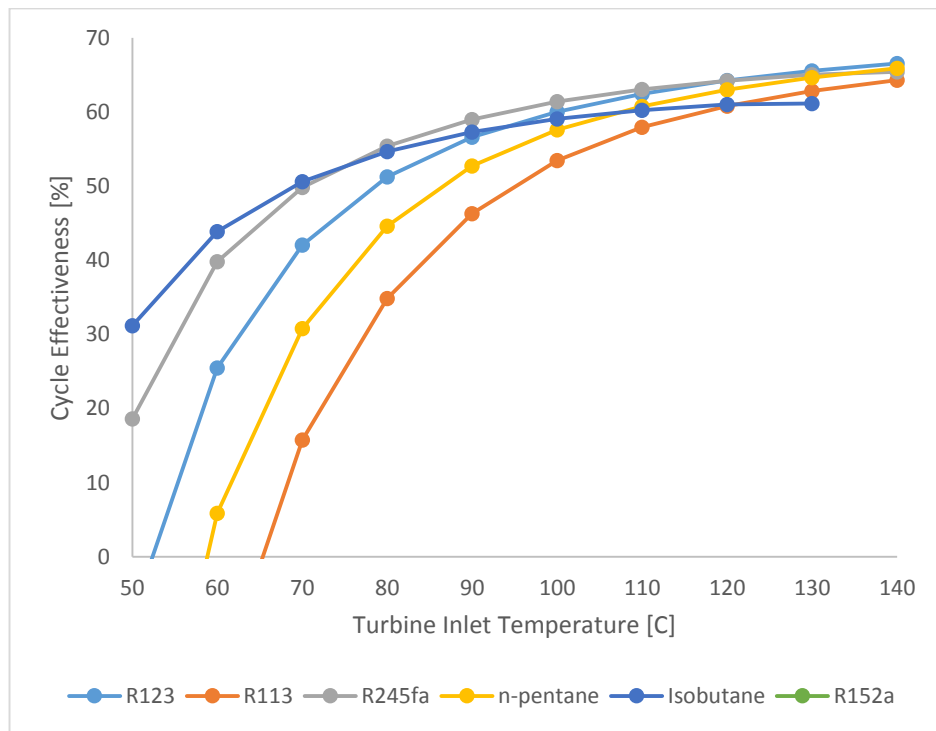


Fig 6.28 Cycle Effectiveness for geo fluid at the temperature of 150 °C for Regenerative Organic Rankine Cycle with IHE

Fig 6.29 to Fig 6.32 shows the variation of Mass flow rate of binary fluid per unit mass flow rate of geo fluid with Turbine Inlet temperature, it is found that mass flow rate of binary working fluid except the wet working fluid R152a decreases with increase in Turbine Inlet temperature with a higher rate particularly for R113, R123 and R245fa. R113 and R123 have the highest mass flow rate and n-pentane has the lowest mass flow rate for having the highest heat capacity among the refrigerants under study.

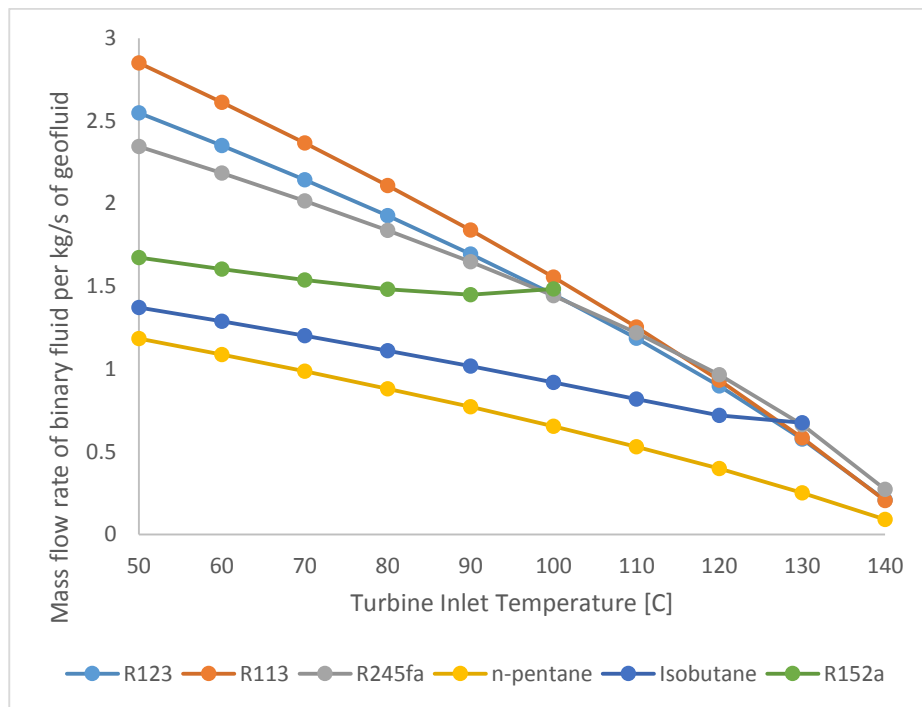


Fig 6.29 Mass flow rate of binary fluid per kg/s of geo fluid at the temperature of 150 °C for Basic Organic Rankine Cycle

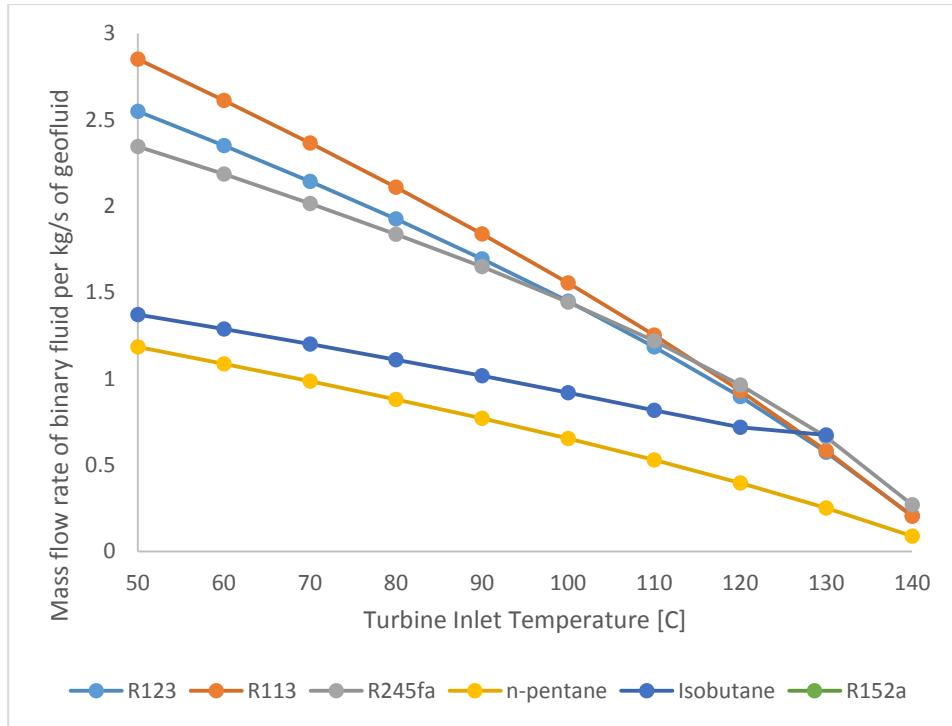


Fig 6.30 Mass flow rate of binary fluid per kg/s of geo fluidat the temperature of 150 °C for Basic Organic Rankine Cycle with IHE

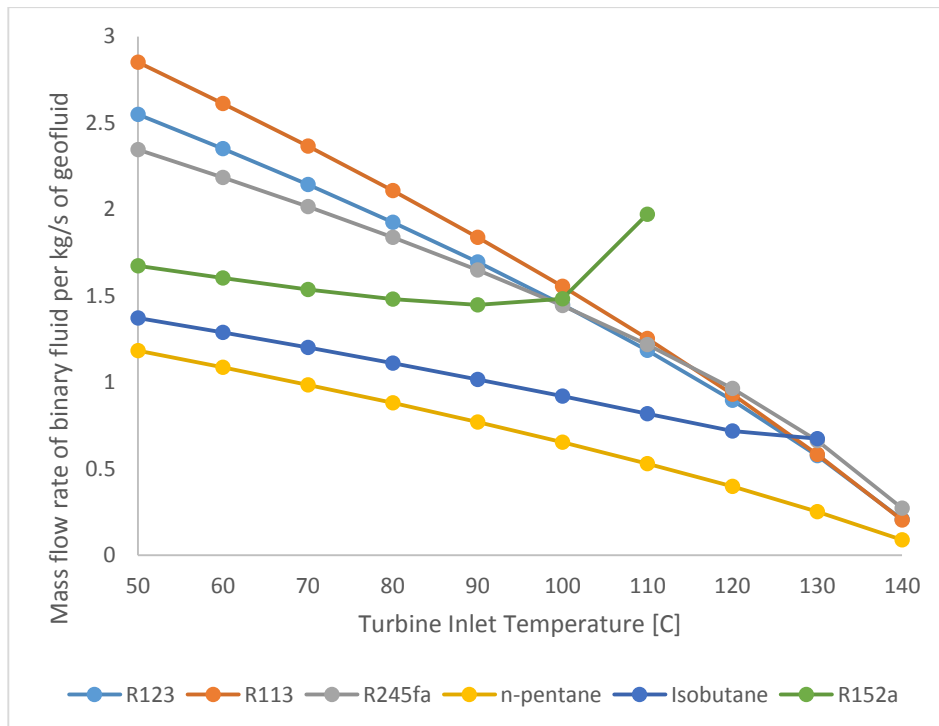


Fig 6.31 Mass flow rate of binary fluid per kg/s of geo fluidat the temperature of 150 °C for Regenerative Organic Rankine Cycle



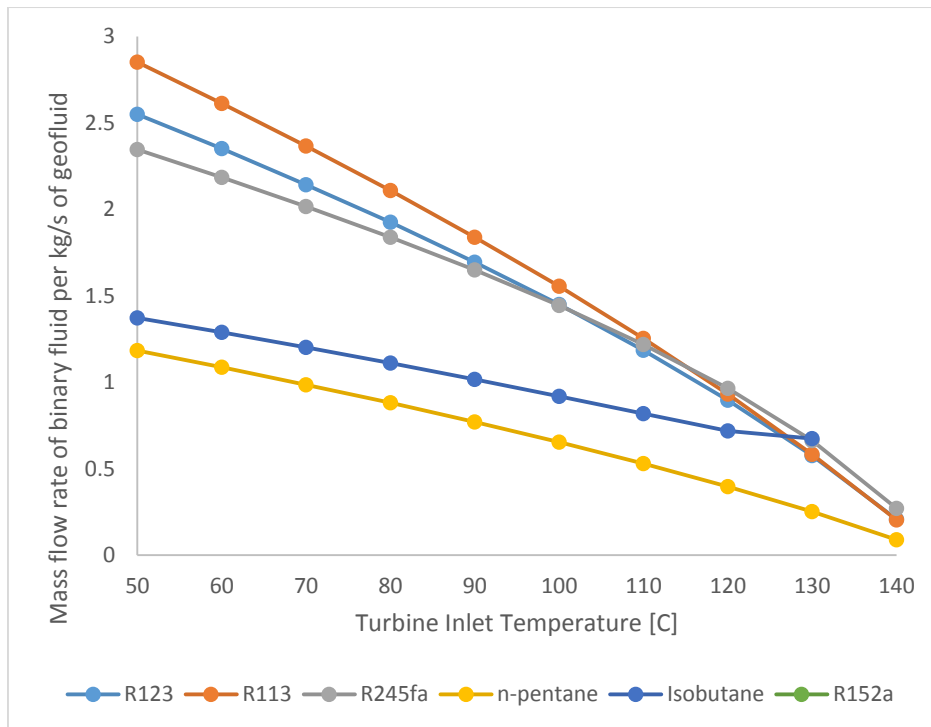


Fig 6.32 Mass flow rate of binary fluid per kg/s of geofluid at the temperature of 150 °C for Regenerative Organic Rankine Cycle with IHE

Overall Plant Irreversibility is the sum of exergy loss in all the components of ORC. Fig 6.33 to Fig 6.36 represent the Overall Plant Irreversibility as a function of turbine inlet temperature. It is found that R152a has the lowest Overall Plant Irreversibility followed by isobutene. R113 and n pentane exhibit the highest amount of Overall Plant Irreversibility. It is also observed that an optimum turbine inlet temperature can be obtained where the overall plant irreversibility is minimum, maximum First- and Second-law efficiencies also occur at the same point.

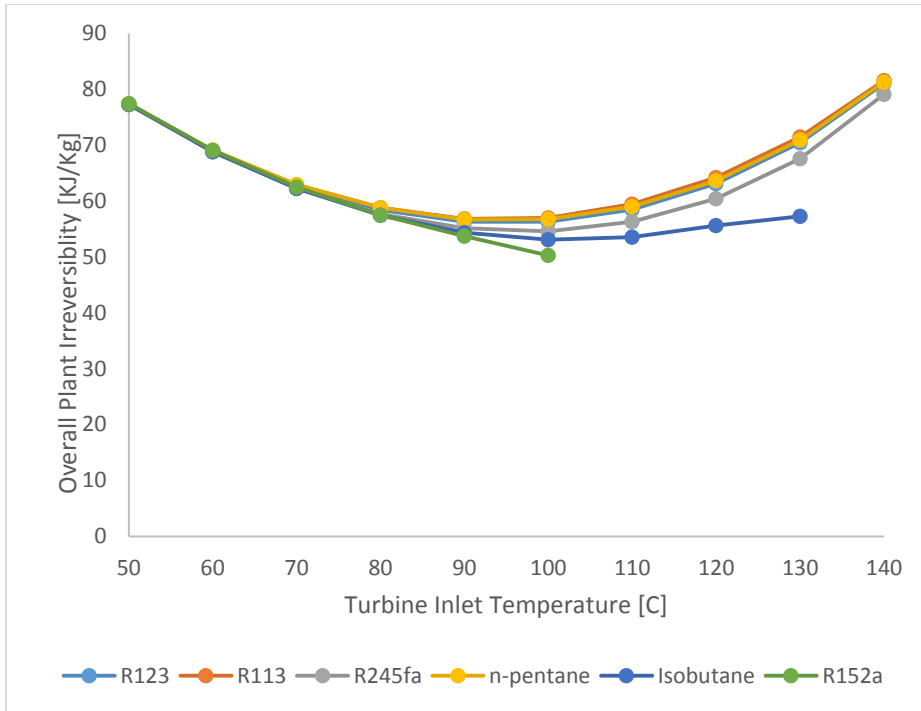


Fig 6.33 Overall Plant Irreversibility at the geo fluidtemperature of 150 °C for Basic Organic Rankine Cycle

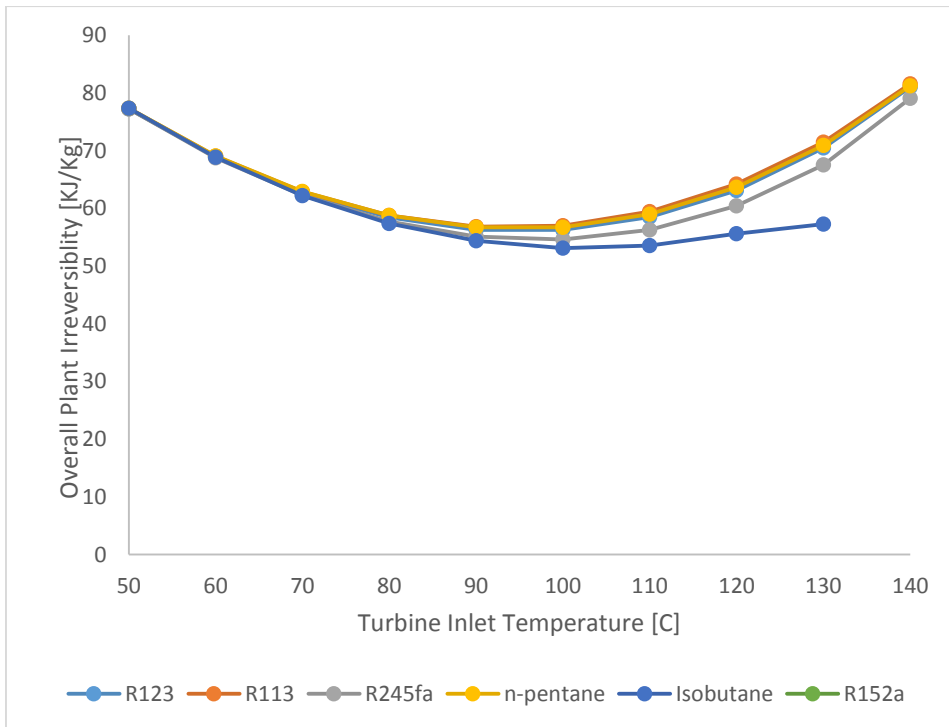


Fig 6.34 Overall Plant Irreversibility at the geo fluidtemperature of 150 °C for Basic Organic Rankine Cycle with IHE

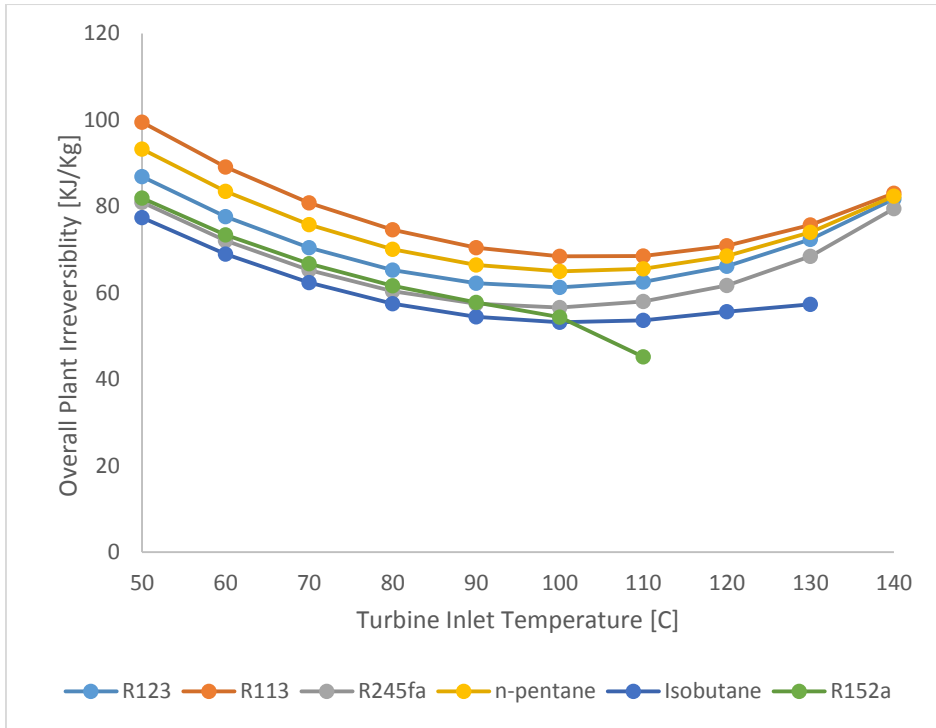


Fig 6.35 Overall Plant Irreversibility at the geo fluidtemperature of 150 °C for Regenerative Organic Rankine Cycle

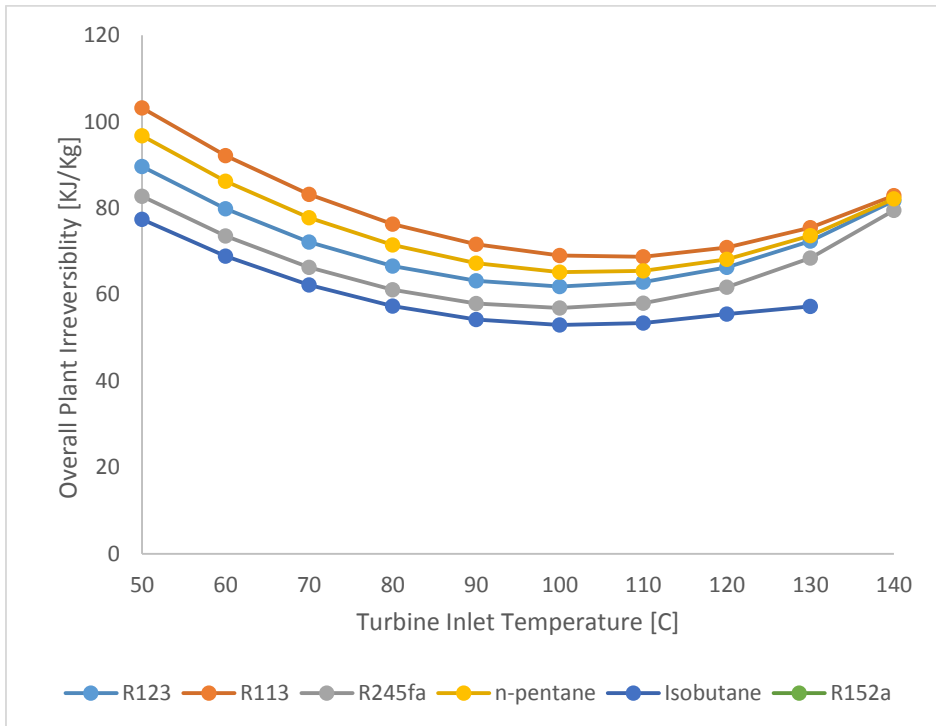


Fig 6.36 Overall Plant Irreversibility at the geo fluidtemperature of 150°C for Regenerative Organic Rankine Cycle with IHE

From the analysis of binary fluids, it is concluded that since R245fa provides the best combination of selection parameters with a higher efficiency

and effectiveness complemented with a lower overall Plant Irreversibility and mass flow rate of binary fluid per unit mass flow rate of geo fluid. R245fa has been selected as the reference fluid for the selection of optimum cycle configuration.

## 6.2 Performance Analysis of ORC configurations:

Fig 6.37 compares the net work output of different Organic Rankine Cycle Configurations. It is found that the net work output of the ORC doesn't change by the addition of IHE to basic configuration, however it decreases by 10% on average on addition of OFOH and by 13% on addition of a combination of OFOH and IHE.

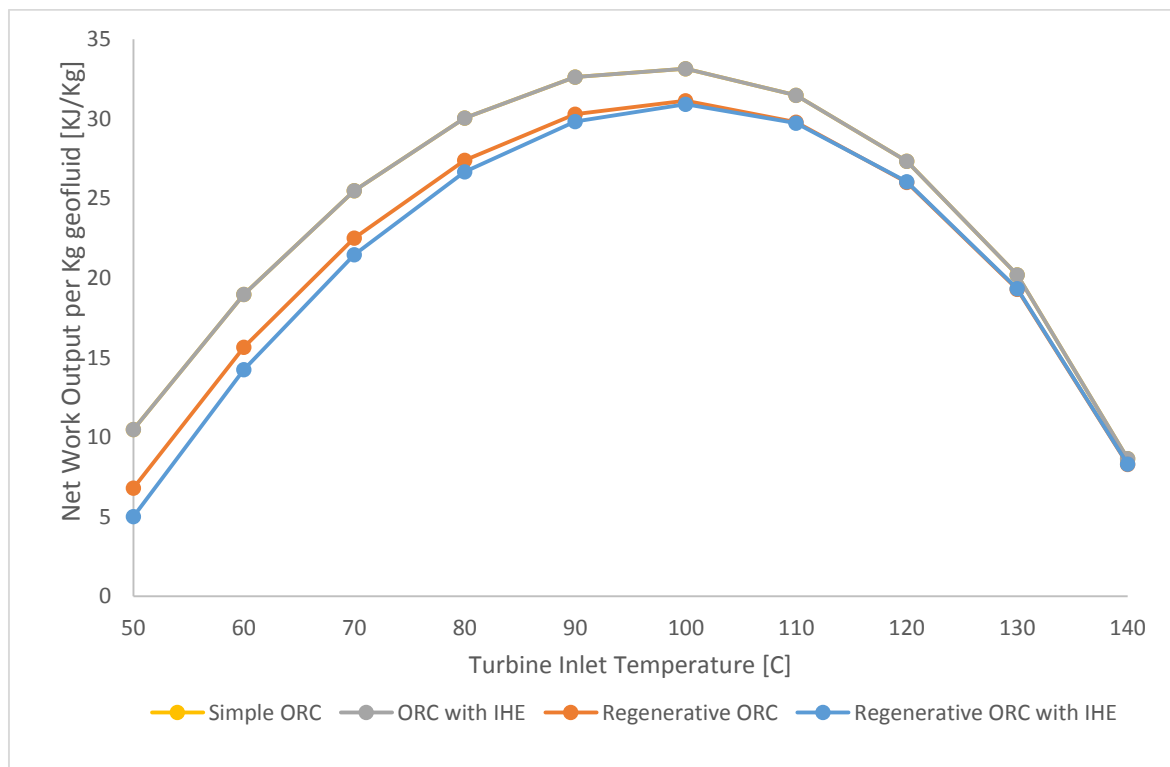


Fig 6.37 Comparison of net work output of different Organic Rankine Cycle Configurations.

Fig 6.38 exhibits the effect of change in turbine inlet temperature over thermal efficiency (which is also equal to first law efficiency based on energy input ) for different ORC configurations, it is observed that the thermal efficiency increases with increase in turbine inlet temperature for all configurations but Basic

ORC are more efficient at lower turbine inlet temperatures as the turbine inlet temperature increases the regenerative cycles become more efficient. At higher temperatures addition of IHE to basic ORC increases the thermal efficiency by 5% on average, addition of OFOH increases the thermal efficiency by 7% and addition of OFOH and IHE by 10%. The lower thermal efficiency is attributed to the large difference in the temperatures of working of fluid and geo fluid in the primary heat exchanger.

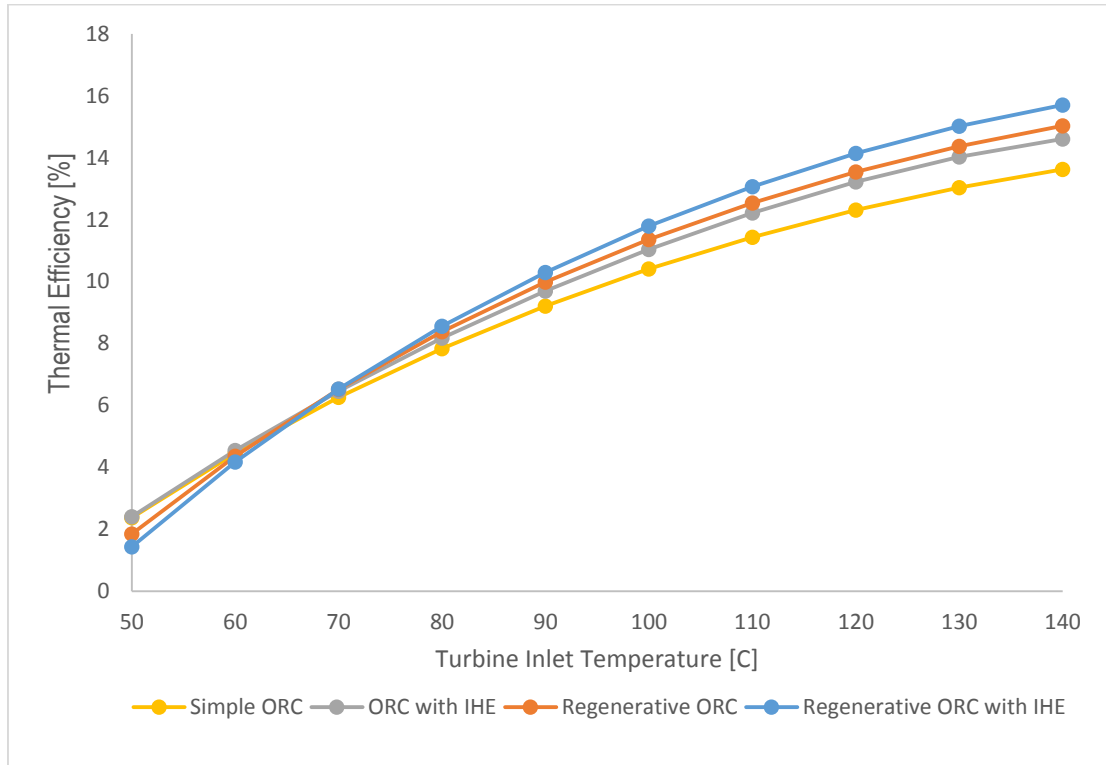


Fig 6.38 Comparison of Thermal Efficiency of different Organic Rankine Cycle Configurations.

Fig 6.39 describes the effects of turbine inlet temperature on First Law efficiency that is a measure of energy conversion efficiency. Basic ORC and ORC with IHE were found to have similar first law efficiency, however the first law efficiency is slightly lower for regenerative cycles at lower temperatures but the difference minimizes with increase in turbine inlet temperature.

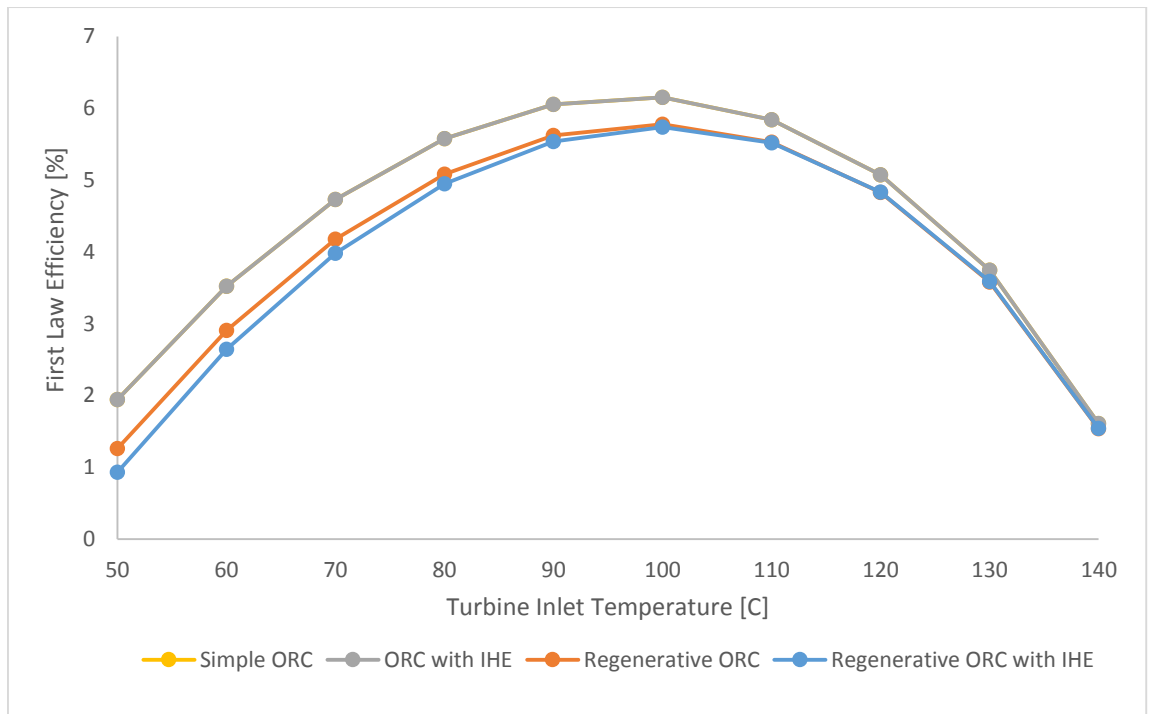


Fig 6.39 Comparison of First Law Efficiency of different Organic Rankine Cycle Configurations.

Fig 6.40 exhibits the effects of Turbine inlet temperature on Second law efficiency based on Geo fluid inlet state, which is a measure on efficiency on conversion of available energy (exergy). Basic ORC and ORC with IHE were found to have similar second law efficiency, however the second law efficiency is slightly lower for regenerative cycles at lower temperatures but this difference minimizes with increase in turbine inlet temperature.

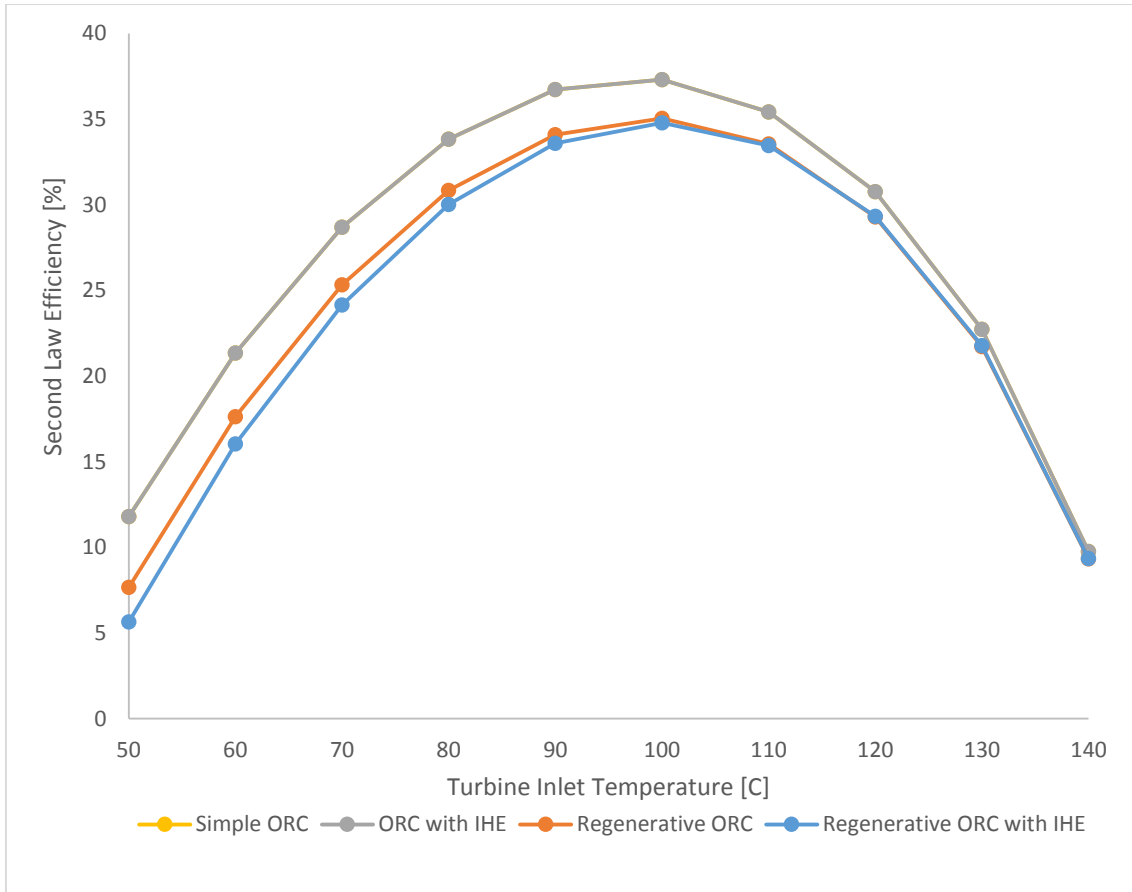


Fig 6.40 Comparison of Second Law Efficiency (based on geo fluid inlet state) of different Organic Rankine Cycle Configurations.

Fig 6.41 compares the Second Law Efficiency based on heat transfer of different Organic Rankine Cycle Configurations. At low turbine inlet temperatures basic ORC exhibits better performance however as the temperatures increase regenerative ORC with IHE becomes most efficient due to the ability to reduce the irreversibility during the heat transfer processes. In Fig 6.41 the temperatures in the range of 85-90 °C are the points where the phenomenon of linear increase in efficiency with increase in temperature changes to increase with a declining rate due to increasing losses in heat transfer process.

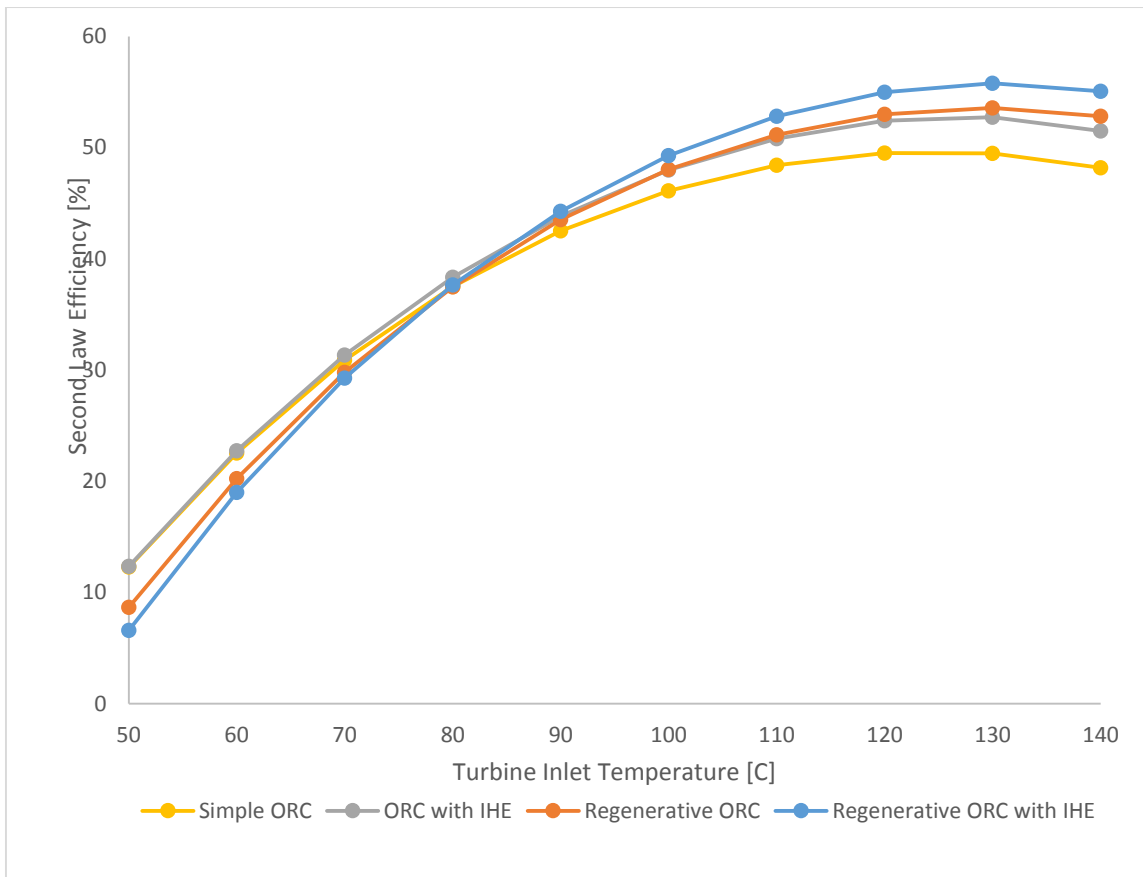


Fig 6.41 Comparison of Second Law Efficiency (based on exergy input) of different Organic Rankine Cycle Configurations.

Fig 6.42 compares the behavior of cycle effectiveness of different ORC configurations on increasing the turbine inlet temperature, it is observed that beyond a certain optimum temperature, there is no significant increase in cycle effectiveness, furthermore, basic ORC configurations were found to be more efficient at lower temperatures whereas the regenerative ORC with IHE is found most effective at higher temperatures due to reduction in irreversibility in the heat transfer processes.



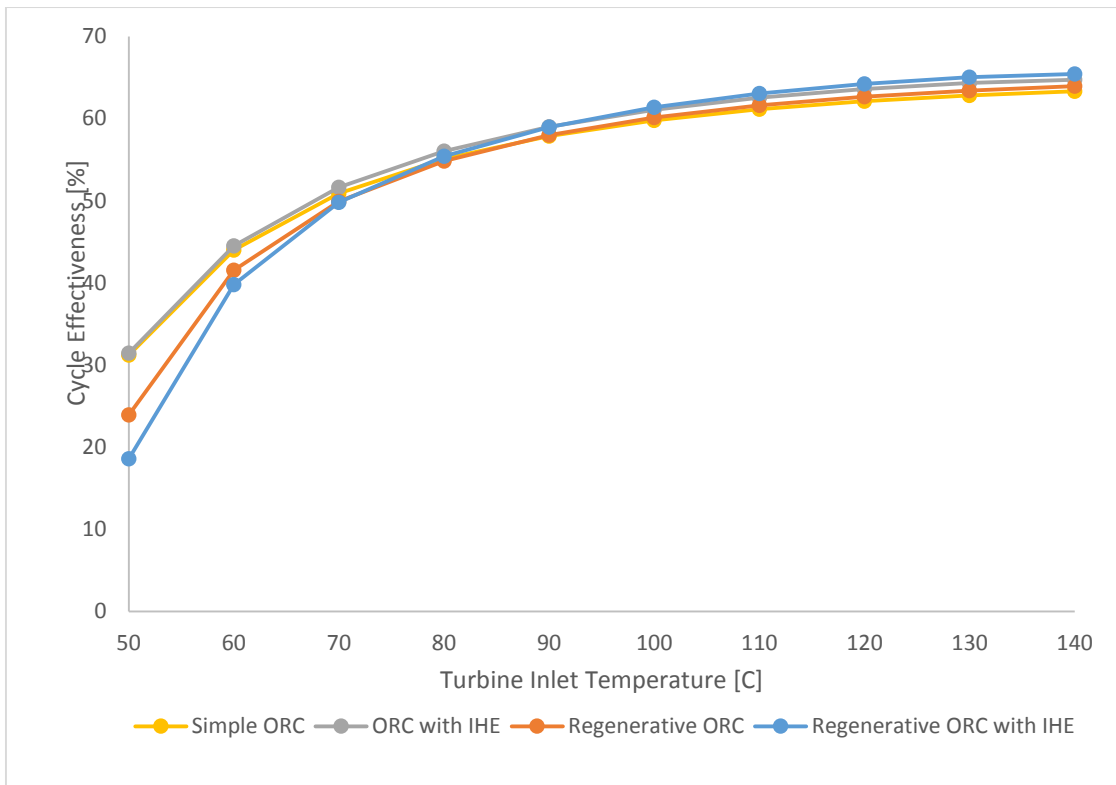


Fig 6.42 Comparison of Cycle Effectiveness of different Organic Rankine Cycle Configurations.

Fig 6.43 shows comparison of Overall Plant Irreversibility of different Organic Rankine Cycle Configurations as a function of turbine inlet temperature. An optimum temperature corresponding to the minimum overall plant irreversibility can be elicited from the plot. It is also observed that at lower temperatures basic ORC exhibited the overall plant irreversibility, but with the increase in temperature the irreversibility of basic ORC approaches irreversibility of regenerative ORC.

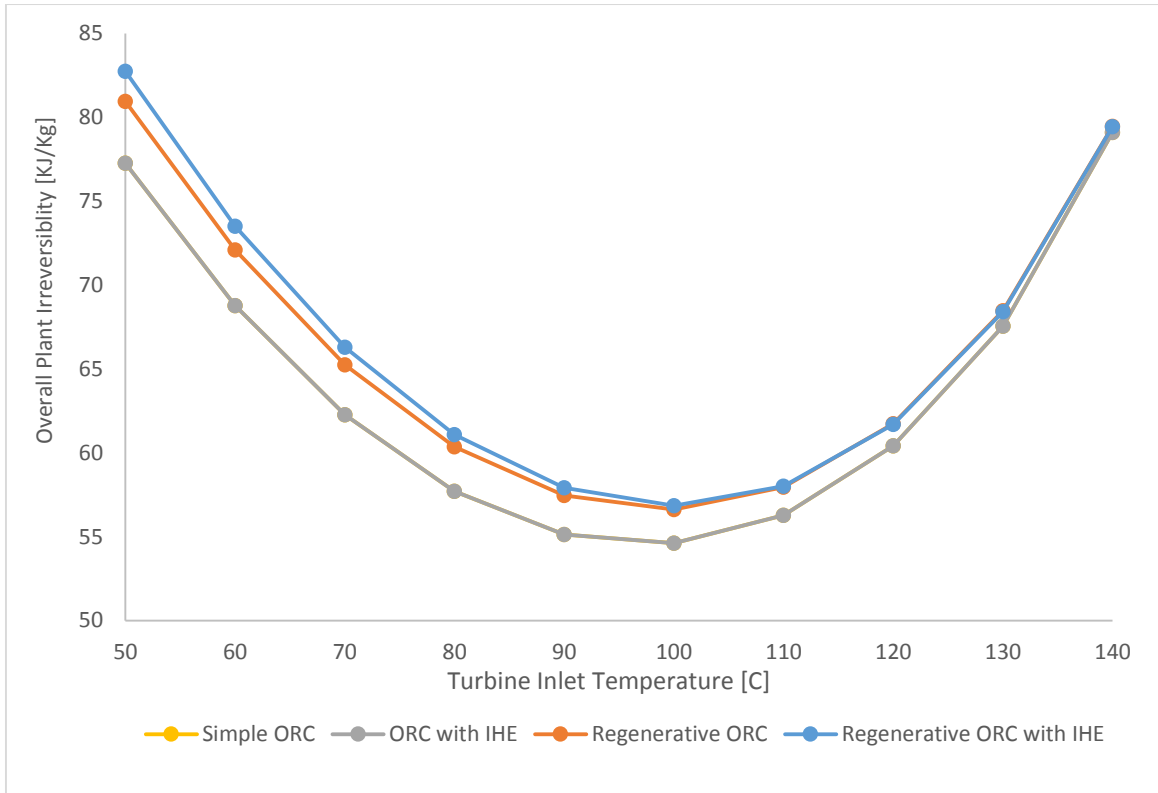


Fig 6.43 Comparison of Overall Plant Irreversibility of different Organic Rankine Cycle Configurations.

Fuel depletion ratio is the thermodynamic parameter defined in Section 5.2 that measures the ratio of exergy destruction in the individual components to total exergy input to the ORC. Fig 6.44 to Fig 6.46 describes the fuel depletion ratio of different ORC configurations at three different turbine inlet temperatures. The processes involving major exergy destruction were found to be rejection, evaporation, condensation and expansion in turbine.

It is also observed that with increase of 10 °C in turbine inlet temperature, the rejection exergy loss increases by 22% on average for regenerative cycle with IHE, 24% for regenerative cycle, 37% for ORC with IHE and 38% for basic ORC Configuration. However, the exergy destruction in the evaporator is reduced by 20% on average; the exergy loss in the condenser is reduced by 15%-18% on average.

The addition of IHE to basic configuration resulted in a substantial decrease in exergy loss in the Preheater and evaporator. The exergy loss in the Preheater evaporator unit and condenser are reduced by 28% and 11% on average respectively.

The addition of OFOH to a basic ORC results in substantial reduction in exergy loss in all the components of ORC particularly 65% on average for Preheater Evaporator Unit, 25% on average for pumping system, 14% on average for Turbine and 37% on average for Condenser and cooling air.

The addition of a combination of OFOH and IHE to a basic ORC results in substantial reduction in exergy loss in all the components of ORC particularly 78% on average for Preheater Evaporator Unit, 61% on average for pumping system, 17% on average for Turbine and 41% on average for Condenser and cooling air.

However, these reductions in exergy losses is quelled by the increase in rejection exergy loss, which increase by 9% , 25% and 33% on average on addition of IHE, OFOH and a combination of OFOH and IHE respectively.

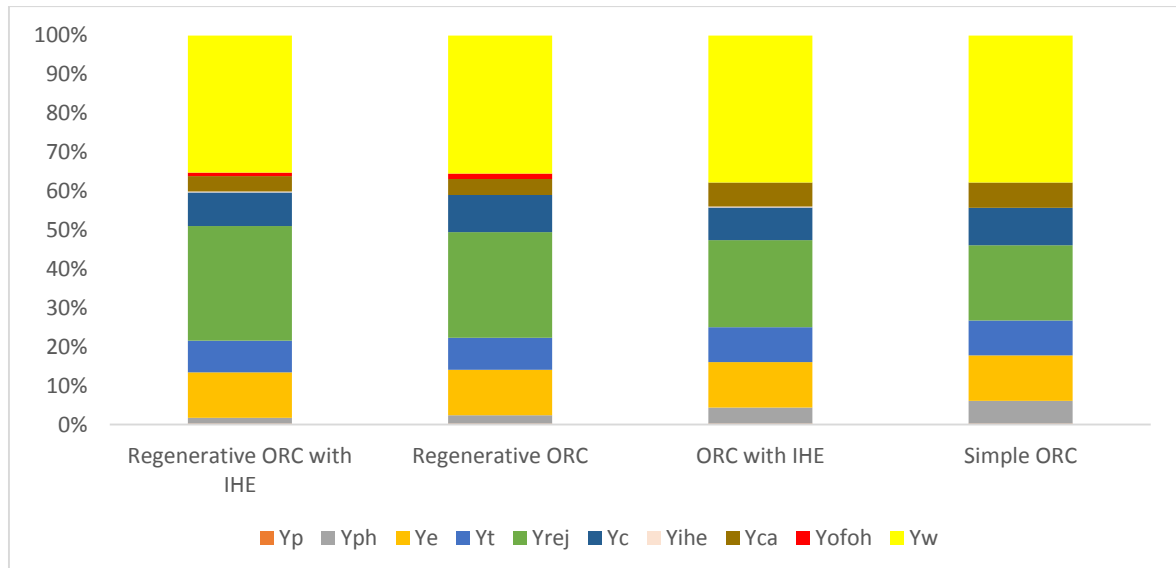


Fig 6.44 Comparison of Fuel Depletion Ratio of different Organic Rankine Cycle Configurations at turbine inlet temperature of 100°C

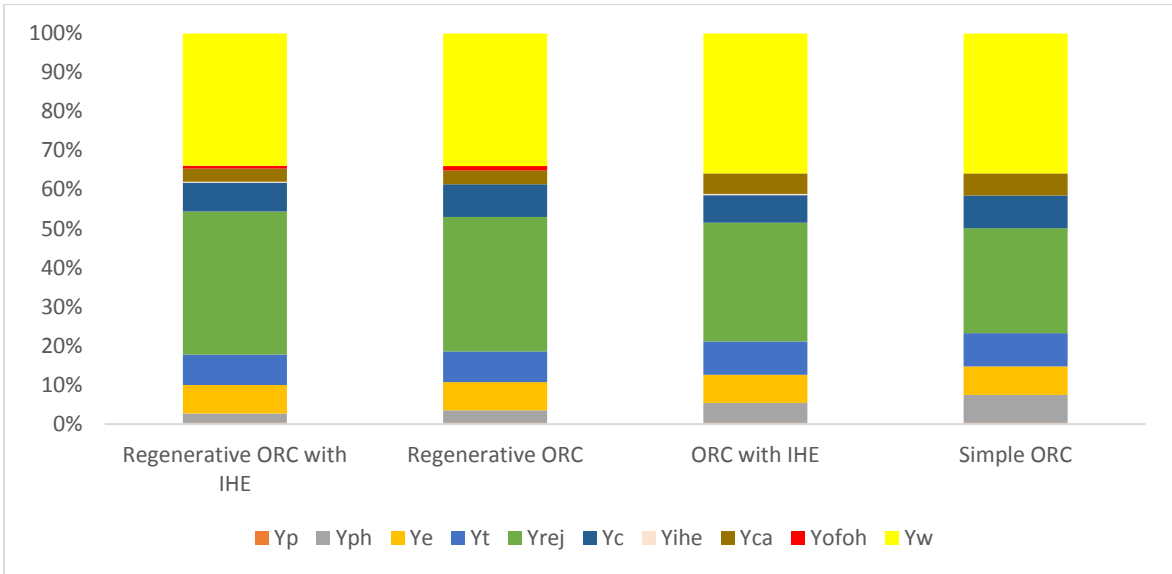


Fig 6.45 Comparison of Fuel Depletion Ratio of different Organic Rankine Cycle Configurations at turbine inlet temperature of 110°C

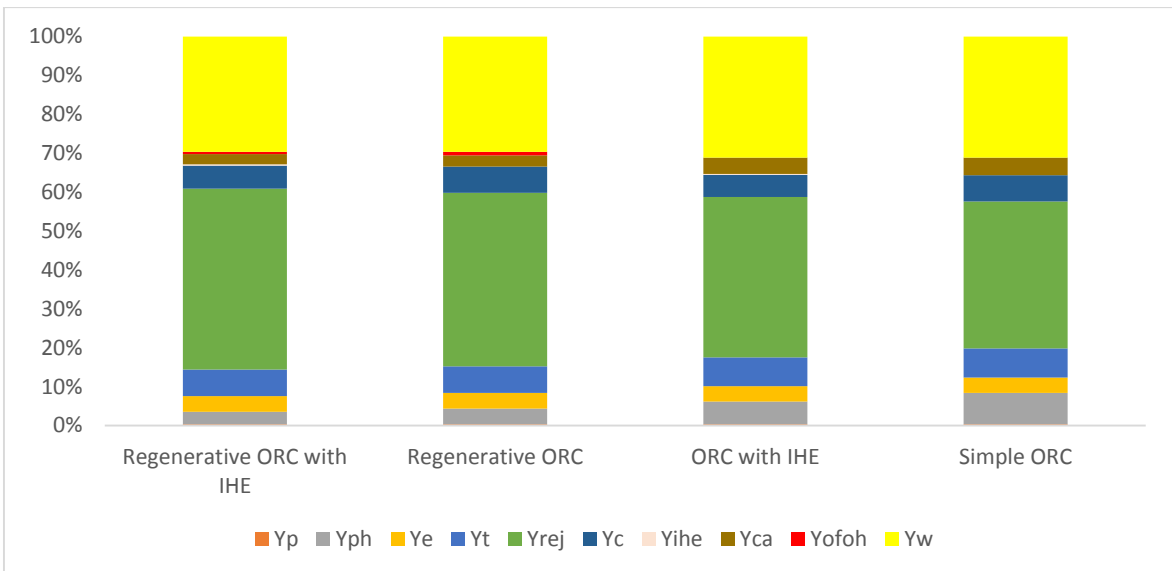


Fig 6.46 Comparison of Fuel Depletion Ratio of different Organic Rankine Cycle Configurations at turbine inlet temperature of 120°C

Fig 6.47 to Fig 6.49 shows the comparison of relative irreversibility of different ORC configurations at three different turbine inlet temperatures. Relative irreversibility is the ratio of individual plant component irreversibility to the overall plant irreversibility.

It is observed that with increase of 10 °C in turbine inlet temperature, the rejection relative irreversibility increases by 22% on average for regenerative

cycle with IHE, 24% for regenerative cycle, 37% for ORC with IHE and 38% for basic ORC Configuration. However, the relative irreversibility of the evaporator is reduced by 30% on average for Basic ORC and 28% on average for Regenerative ORC, the relative irreversibility of the condenser is reduced by 15%-18% on average due to recovery of heat transfer losses in IHE and OFOH.

The addition of IHE to basic configuration resulted in a substantial decrease in relative irreversibility of the Preheater and evaporator. The relative irreversibility of the Preheater evaporator unit and condenser are reduced by 28% and 11% on average respectively.

The addition of OFOH to a basic ORC results in substantial reduction in relative irreversibility of all the components of ORC particularly 65% on average for Preheater Evaporator Unit, 25% on average for pumping system, 14% on average for Turbine and 37% on average for Condenser and cooling air.

The addition of a combination of OFOH and IHE to a basic ORC results in substantial reduction in relative irreversibility of all the components of ORC particularly 78% on average for Preheater Evaporator Unit, 61% on average for pumping system, 17% on average for Turbine and 41% on average for Condenser and cooling air.

However, these reductions in relative irreversibility is quelled by the increase in rejection exergy loss, which increase by 9% , 25% and 33% on average on addition of IHE, OFOH and a combination of OFOH and IHE respectively.

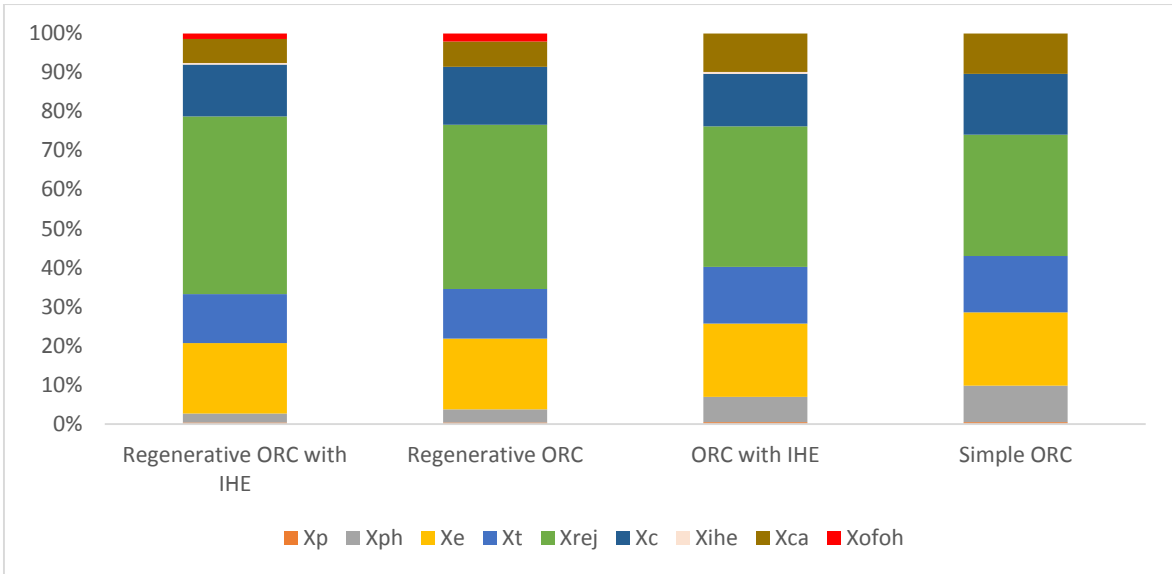


Fig 6.47 Comparison of Relative Irreversibility of different Organic Rankine Cycle Configurations at turbine inlet temperature of 100°C.

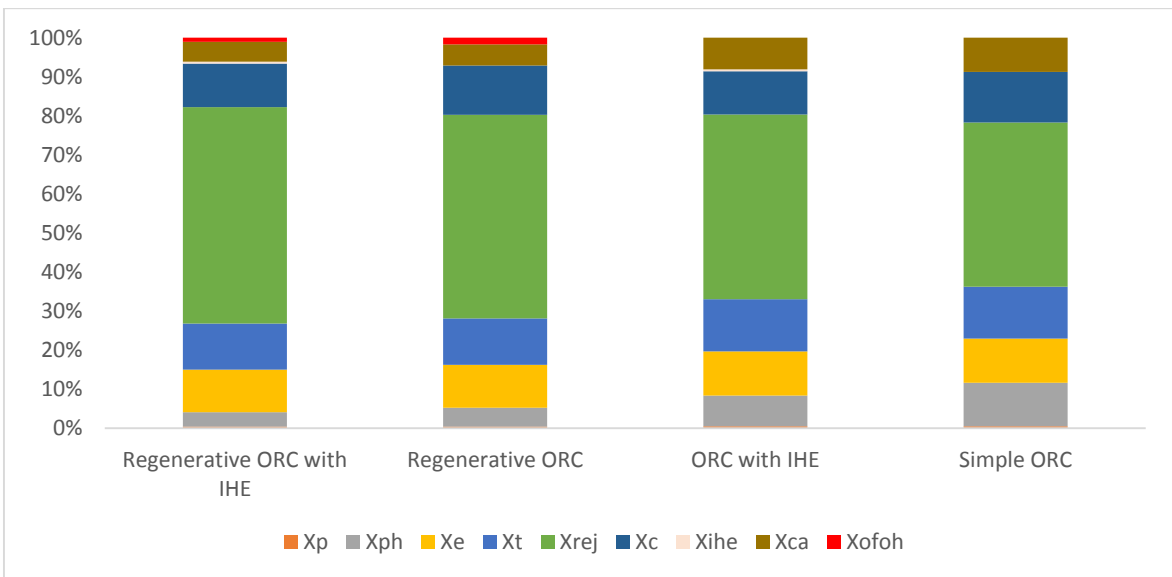


Fig 6.48 Comparison of Relative Irreversibility of different Organic Rankine Cycle Configurations at turbine inlet temperature of 110°C

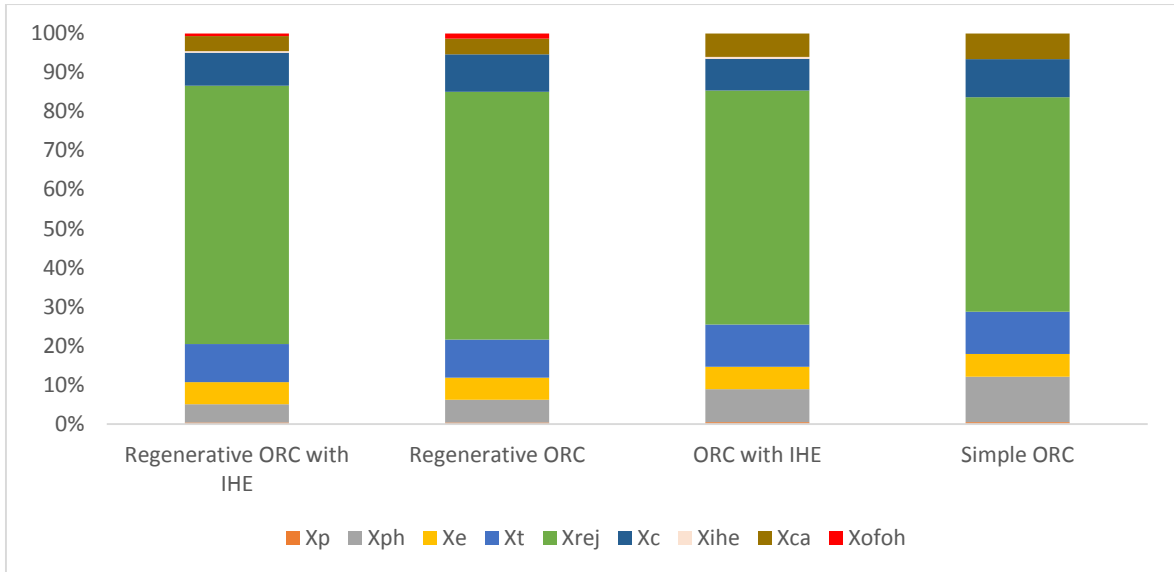


Fig 6.49 Comparison of Relative Irreversibility of different Organic Rankine Cycle Configurations at turbine inlet temperature of 120°C

Productivity lack is another parameter defined in Section 5.2 which measures the Exergy Destruction in the individual cycle component in relation to net work output per Kg of geo fluid. Fig 6.50 to Fig 6.52 shows the Productivity lack of cycle components.

It is observed that with increase of 10 °C in turbine inlet temperature, the productivity lack in the pump reduces by 16% on average, productivity lack in the pre heater reduces by 30-33% on average for Basic ORC and 48%-57% for regenerative cycles. However, the productivity lack of the evaporator is increased by 37% on average; the productivity lack of the condenser is increased by 7%-9% on average.

The addition of IHE to basic configuration resulted in a substantial decrease in productivity lack of the pre heater and condenser. The productivity lack is reduced by 29% on average and 15% on average for the pre heater and condenser respectively which is substantial as compared to the increase in overall productivity lack due to addition of IHE.

The addition of OFOH to a basic ORC results in substantial reduction in productivity lack of the pre heater. The productivity lack of the pre heater is

reduced by 53% on average which is very low as compared to the increase in overall productivity lack due to addition of IHE and 4% on average increase in productivity lack of condenser.

The addition of a combination of OFOH and IHE to a basic ORC results in substantial reduction in productivity lack of the pre heater. The productivity lack of the pre heater is reduced by 64% on average which is very low as compared to the increase in overall productivity lack due to addition of OFOH and IHE. The addition of a combination of OFOH and IHE to a basic ORC also results in marginal reduction by 6% in productivity lack of the condenser.

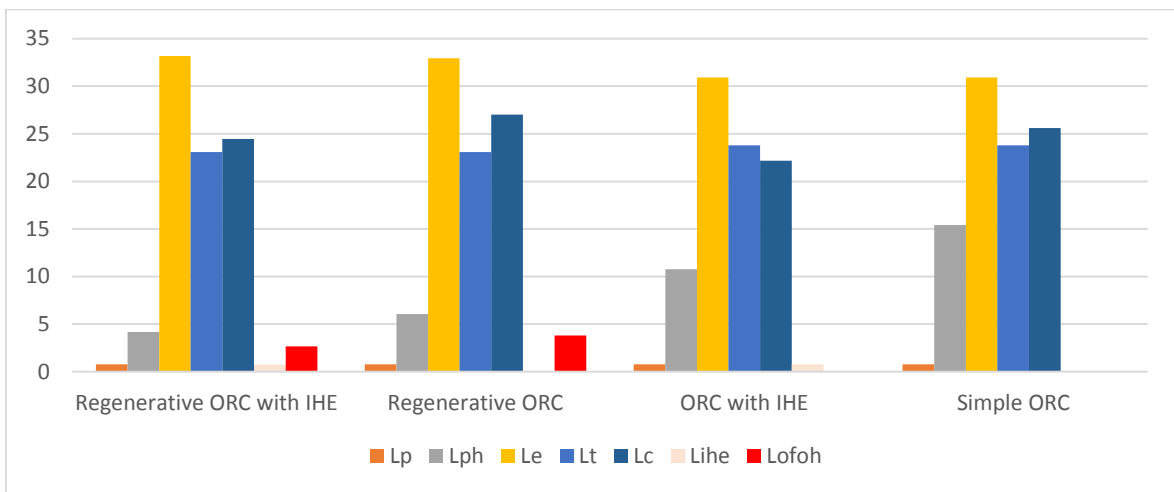


Fig 6.50 Comparison of Productivity lack of different Organic Rankine Cycle Configurations at turbine inlet temperature of 100°C

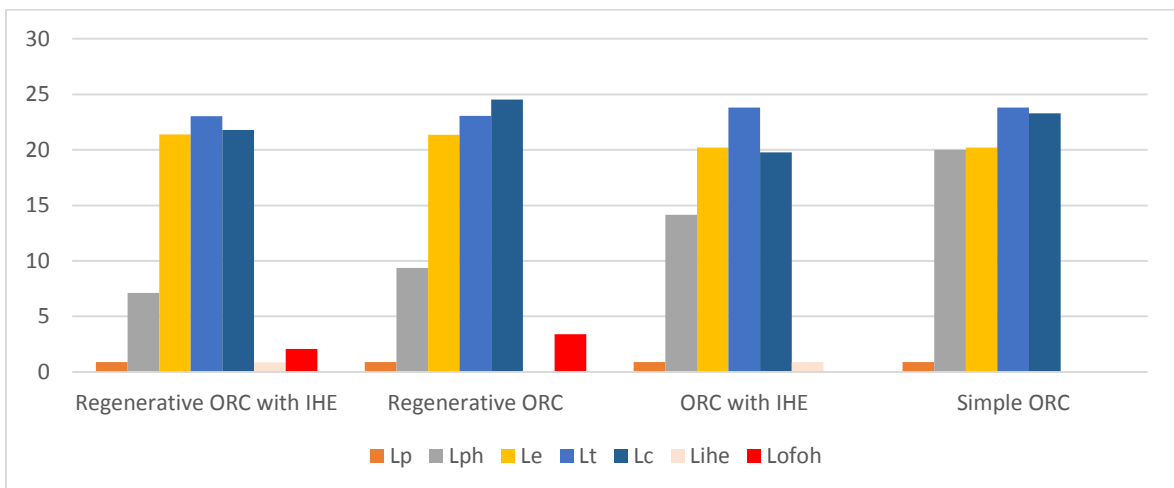


Fig 6.51 Comparison of Productivity lack of different Organic Rankine Cycle Configurations at turbine inlet temperature of 110°C



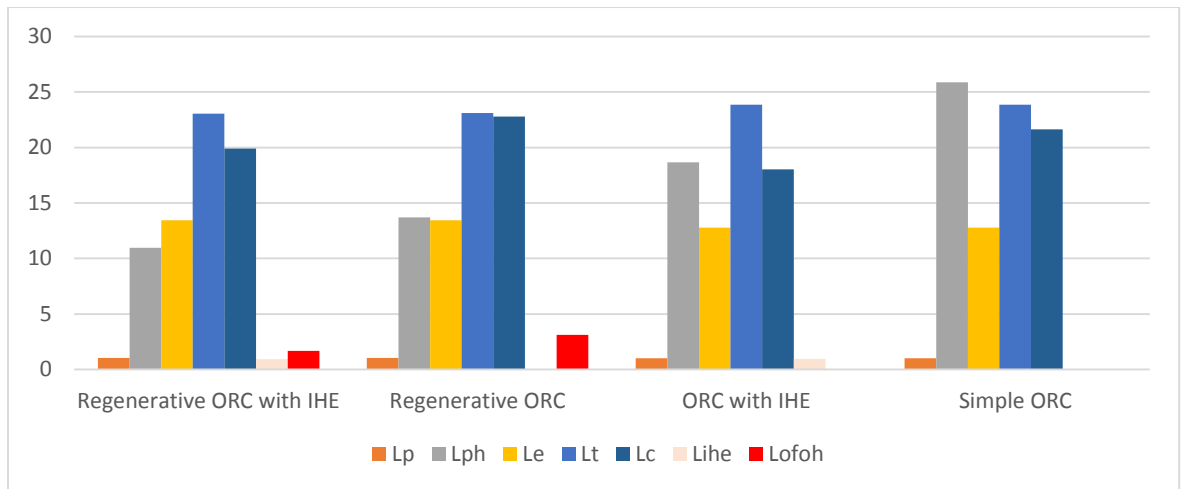


Fig 6.52 Comparison of Productivity lack of different Organic Rankine Cycle Configurations at turbine inlet temperature of 120°C

Analysis were also performed to study effects of change in geo fluid temperature, condenser temperature and pinch point temperature on the performance of ORC. Fig 6.53 shows the effect of changing geo fluid temperature on the net work output per unit mass flow rate of geo fluid. Net Work Output increases with increase in geo fluid temperature and it is found that an increase of 10°C will bring an increase of 18% net work out put on average.

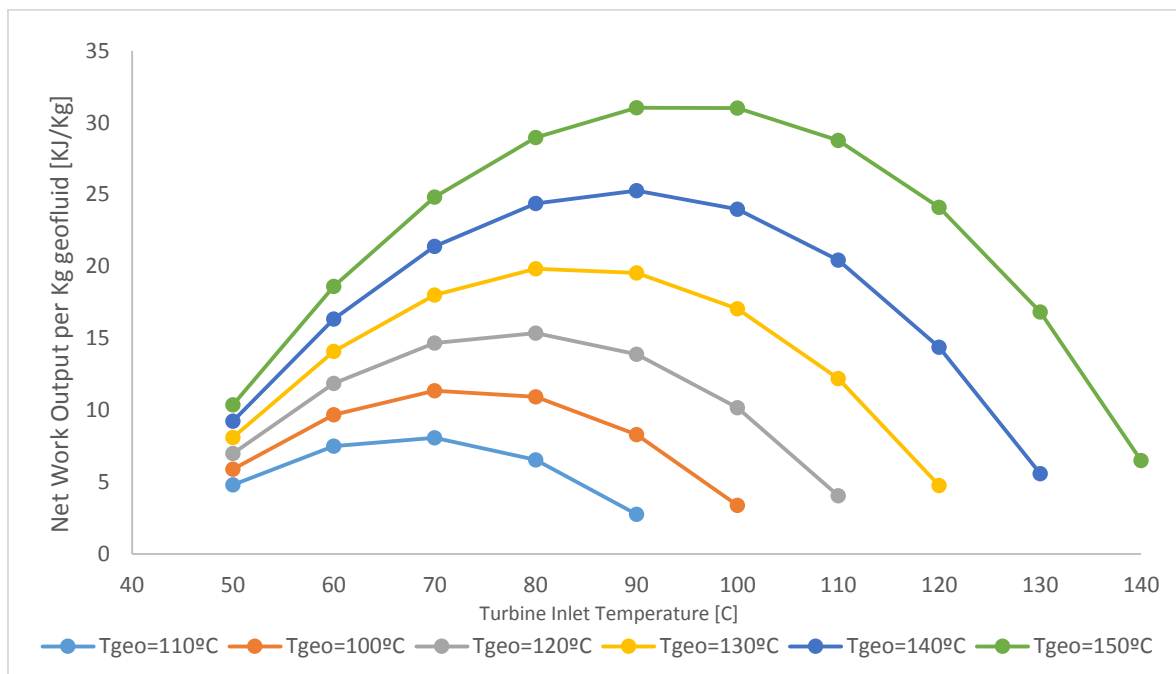


Fig 6.53 Comparison of Net Work Output at different geo fluid temperatures

Fig 6.54 shows the effect of changing condenser temperature on the net work output per unit mass flow rate of geo fluid. The reduction in condensing temperature results in higher net work output corresponding a lower optimum turbine inlet temperature. However, the reduction in condensing temperature is limited by the choice of binary fluid, capital cost of condenser and ambient conditions.

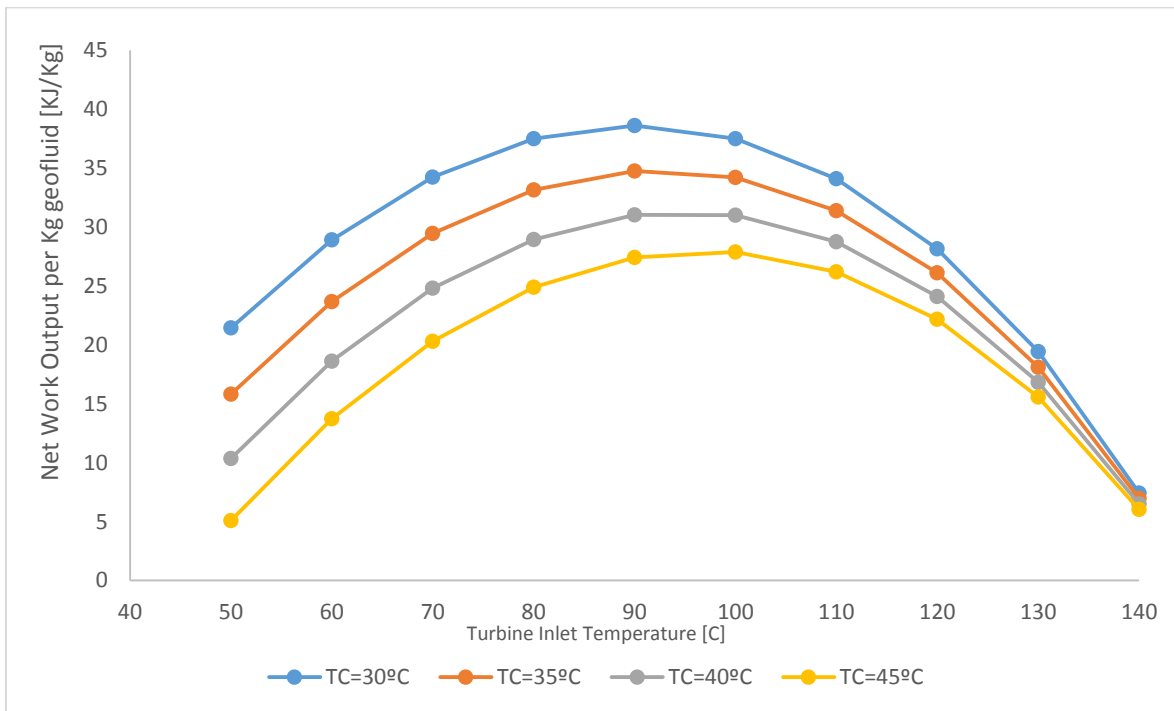


Fig 6.54 Comparison of Net Work Output at different Condenser temperatures

The net work output is found to decrease with increase in pinch point temperature as shown in Fig 6.55. Heat transfer losses owing to increase in temperature difference between geo fluid and organic binary fluid in the evaporator cause the net work output to decrease with increase in pinch point temperature. However a very low pinch point temperature cannot be justified owing to high capital cost due to increase in optimum temperature corresponding a marginal increase in net work output.

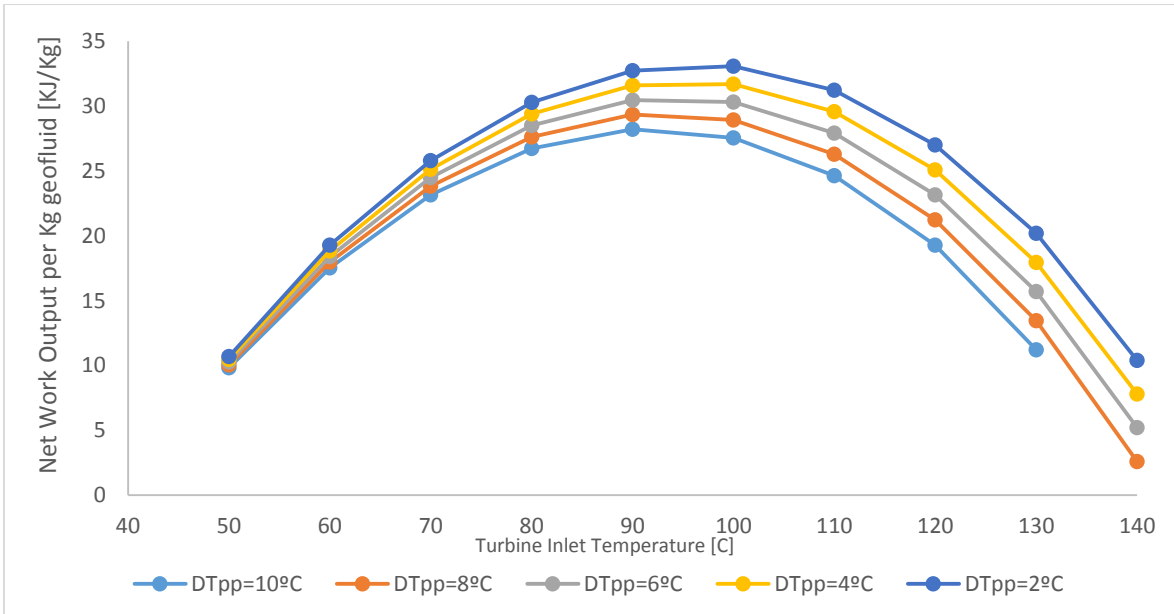


Fig 6.55 Comparison of Net Work Output at different Pinch Point temperatures

## CHAPTER –VI

### CONCLUSION

Geothermal energy being abundantly available on the Earth surface pose as a viable future energy solution but its exploitation for the power generation is still an immature technology. Pakistan an energy deprived developing country has tremendous potential for geothermal power generation. Geological research underlines presence of several geothermal resources in country. Most of the geothermal resources of the world lie near the seismic belts and Pakistan too is situated in the western rifted margin of Indo-Pakistan sub continental plate. The presence of exploitable geo thermal resources in Pakistan is strengthened by the development of alteration zones and fumaroles, presence of hot springs and indication of quaternary volcanism in different regions of the country. There exist several medium and low temperature geothermal sources up to geo fluid temperatures of 200°C in different areas of Pakistan.

Present work presents an analysis of possibilities of exploiting this resource in Pakistan and addresses the idea of power generation from geothermal energy sources in Pakistan. It encompasses energy and exergy analysis and performance optimization of small Organic Rankine Cycle Power Plants with geo fluid temperature in the range of 100°C to 150°C, as to available geothermal resources in the Pakistan are moderate to low temperature, water dominated sources. Cycles incorporated in present work are basic Organic Rankine Cycle (ORC), Organic Rankine Cycle with an Internal Heat Exchanger, Regenerative Organic Rankine Cycle & Regenerative Organic Rankine Cycle with an Internal Heat Exchanger. Present work has considered Refrigerants R113, R245fa, R123, R152a, Iso-pentane and n-pentane as the binary working fluids of the cycle.

It was found that the binary fluids with higher boiling point temperature or lower specific heat capacity have relatively lower optimum turbine inlet temperature corresponding to maximum work output. Therefore, higher boiling point organic fluids like n-pentane are recommended for Basic ORC

configurations, whereas organic fluids with lower vapor specific heat capacity like iso-butane are recommended for Regenerative ORC.

Optimal operating conditions corresponding maximum cycle output and efficiencies and minimum overall plant irreversibility were elicited by analyzing the variations of these parameters with Turbine Inlet Temperature. It is observed that the increase in geothermal fluid temperature results in an exponential increase in maximum cycle output and a linear increase in turbine inlet temperature. The addition of an IHE and/or an OFOH improved significantly the effectiveness of the ORC by reduction in irreversibility in the heat transfer processes, therefore it is recommended to use Regenerative ORC with IHE. The Regenerative ORC with IHE was found to be 3.7%, 2.4% and 1.8% more effective on average as compared to Basic ORC, ORC with IHE and Regenerative ORC respectively. The processes involving major Exergy destruction were found to be rejection, evaporation, condensation and expansion in turbine. The addition of OFOH and IHE to a basic ORC results in substantial reduction in relative irreversibility and Productivity lack of the processes involving major Exergy destruction.

## **References**

[1] IEA 2013, Key World Energy Statistics 2013.

[2] IEA 2013, CO<sub>2</sub> Emissions from Fuel Combustion Highlights 2013.

[3] IEA 2013, World Energy Outlook 2013, Renewable Energy Outlook 2013, Chapter 6, p192-232

[4] Ministry of Petroleum and Natural Resources, Hydrocarbon Development Institute of Pakistan 2013, Pakistan Energy Year Book 2012 p81-91

[5] Bassfeld Technology Transfer 2009, Geothermal Power Generation: Economically viable electricity generation through advanced geothermal energy technologies, Switzerland.

[6] Pollack, HN, Hurter, SJ & Johnson, JR 1993, 'Heat flow from the Earth's interior: Analysis of the Global Data Set', Reviews of Geophysics Volume 31, Issue 3, pages 267–280, August 1993

[7] 'Joint Programme on Geothermal Energy' of the Europe's Energy Research Alliance (EERA), TNO ThermoGIS, <<http://www.thermogis.nl/worldaquifer.html>>

[8] DiPippo, R 2008, Geothermal power plants principles, applications, case studies and environmental impact, Butterworth-Heinemann, London.

[9] Lund, JW 2006, and geothermal energy focus: tapping the earth's natural heat, refocus.

[10] Bertani, R 2012, 'Geothermal power generation in the world 2005-2010 update report', Geothermics, vol. 41, no.1, pp. 1-29.

- [11] Lund JW, Freeston DH, Boyd TL. Direct utilization of geothermal energy 2010 worldwide review. In: Proceedings world geothermal congress, Bali, Indonesia. Paper number 0007. Session: 0. Keynote; April 25–30, 2010
- [12] Muffler P, Cataldi R. Methods for regional assessment of geothermal resources. *Geothermics* 1978; 7:53–89.
- [13] Hochstein MP. Classification and assessment of geothermal resources. In: Dickson MH, Fanelli M, editors. *Small geothermal resources: a guide to development and utilization*. New York: UNITAR; 1990. p. 31–57.
- [14] Benderitter Y, Cormy G. Possible approach to geothermal research and relative cost. In: Dickson MH, Fanelli M, editors. *Small geothermal resources: a guide to development and utilization*. New York: UNITAR; p. 59–69.
- [15] Haenal R, Rybach L, Stegena L. Fundamentals of geothermics. In: Haenal R, Rybach L, Stegena L, editors. *Handbook of terrestrial heat flow-density determination*. Dordrecht: Kluwer Academic Publishers; 1988. p. 9–57.
- [16] EPRI 2010, *Geothermal Power: Issues, Technologies, and Opportunity for Research, Development, Demonstration, and Deployment*.
- [17] Alfe, D, Gillan, MJ & Price, GD 2003, 'Thermodynamics from first principles: temperature and composition of the Earth's core', *Mineralogical Magazine*, vol. 67, no. 1, pp. 113–123.
- [18] Clauser C. Geothermal energy. In: Heinloth K, editor, *Landolt-Bornstein. Group VIII: advanced materials and technologies, vol. 3: Energy technologies, Subvol.C: renewable energies*. Springer Verlag, Heidelberg-Berlin; 2006. p. 493–604.
- [19] The NEED project 2010, *Secondary Energy Infobook*, viewed on 10 December, 2010, <[www.NEED.org](http://www.NEED.org)>.

[20] Chen, H, Goswami, DY & Stefanakos, EK 2010, 'A review of thermodynamic cycles and working fluids for the conversion of low-grade heat', *Renewable and sustainable energy reviews*, vol. 14, no. 1, pp. 3059-3067.

[21] DiPippo, R 1998, 'Geothermal Power Systems', in Elliott, TC, Chen, K & Swanekamp, RC, *Standard handbook of power plant engineering*, 2nd edn, MacGraw-Hill, New York, pp. 8.27 - 8.60.

[22] Hepbasli, A 2008, 'A key review on exergetic analysis and assessment of renewable energy resources for a sustainable future', *Renewable and Sustainable Energy Reviews*, vol. 12, pp. 593-661.

[23] Subbiah, S & Natarajan, R 1988, 'Thermodynamic analysis of binary-fluid rankine cycles for geothermal power plants', *Energy Conversion and Management*, vol. 28, no. 1, pp. 47-52.

[24] DiPippo, R 2004, 'Second Law assessment of binary plants generating power from low temperature geothermal fluids', *Geothermics*, vol. 33, no.1, pp. 565–86.

[25] Yari, M 2010, 'Exergetic analysis of various types of geothermal power plants', *Renewable Energy*, vol. 35, no. 1, pp. 112-121.

[26] ZvonimirGuzovic´ , Boris Majcen , Svetislav Cvetkovic´ 2012, Possibilities of electricity generation in the Republic of Croatia from medium-temperature geothermal sources, *Applied Energy* 98 (2012) 404–414

[27] RamazanKose 2005, Research on the generation of electricity from the geothermal resources in Simav region, Turkey, *Renewable Energy* 30 (2005) 67–79

[28] Chao Luo, Lichang Huang , Yulie Gong , WeibinMaa, 2012, Thermodynamic comparison of different types of geothermal power plants systems and case studies in China, *Renewable Energy* 48 (2012) 155-160



[29] [4r] Daniël Walraven , Ben Laenen, William D'haeseleerm 2012, Comparison of thermodynamic cycles for power production from low-temperature geothermal heat sources, Energy Conversion and Management (2012) In Press

[30] Carlos Eymel Campos Rodríguez , José Carlos Escobar Palacio , Osvaldo J. Venturini ,Electo E. Silva Lora , Vladimir Melián Cobas , Daniel Marques dos Santos b, Fábio R. Lofrano Dotto , Vernei Gialluca, Exergetic and economic comparison of ORC and Kalina cycle for low temperature enhanced geothermal system in Brazil, Applied Thermal Engineering 52 (2013) 109-119

[31] Florian Heberle, Dieter Brüggemann, 2010, Exergy based fluid selection for a geothermal Organic Rankine Cycle for combined heat and power generation, Applied Thermal Engineering 30 (2010) 1326-1332

[32] Fu-Zhen Zhang, Pei-Xue Jiang 2012, Thermodynamic analysis of a binary power cycle for different EGS geo fluid temperatures, Applied Thermal Engineering 48 (2012) 476-485

[33] T. Guo, H.X. Wang, S.J. Zhang, 2011, Fluids and parameters optimization for a novel cogeneration system driven by low-temperature geothermal sources, Energy 36 (2011) 2639-2649

[34] Franco, A 2011, 'Power production from a moderate temperature geothermal resource with regenerative Organic Rankine Cycles', Energy for Sustainable Development, vol. 15, pp. 411-419.

[35] Tester J, Anderson B, Batchelor A, Blackwell D, DiPippo R, Drake E, et al. The future of geothermal energy: impact of enhanced geothermal systems (EGSs) on the United States in the 21st century. Tech. Rep., Massachusetts, USA: Massachusetts Institute of Technology; 2006.

[36] Kanoglu, M 2002, 'Exergy analysis of a dual-level binary geothermal power plant', Geothermics, vol. 31, pp. 709–24.

[37] Gnutek, Z & Bryszewska-Mazurek, A 2001, 'The thermodynamic analysis of multicycle ORC engine', *Energy*, vol. 26, no. 1, pp. 1075-1082.

[38] Desai, N & Bandyopadhyay, S 2009, 'Process integration of organic Rankine cycle', *Energy*, vol. 34, no. 1, pp. 1674-86.

[39] Madhawa, HD, Mihajlo, G, Worek, WM & Yasuyuki, I 2007, 'Optimum design criteria for an organic Rankine cycle using low temperature geothermal heat sources', *Energy*, vol. 32, no.1, pp. 1698–706.

[40] Franco, A & Villani, M 2009, 'Optimum design of binary cycle power plants for water dominated, medium-temperature geothermal fields', *Geothermics*, vol. 38, no.1, pp. 379-391.

[41] Muslim M, Das B. A preliminary report on suitable springs for bottling mineral water in Sindh and part of Baluchistan. Geological Survey of Pakistan 1988; p304-12.

[42] Shuja TA. Geothermal areas in Pakistan. *Geothermics* 1986; 15: 719–23.

[43] Arthurton RS, Farah A, Ahem W. The late Cretaceous-Cenozoic history of western Baluchistan, Pakistan, the northern margin of the Makran subduction complex. In: Leggett JK, editor. *Trench-fore arc geology (Special Publication 10)*. London, 1982. p. 373–85.

[44] Arthurton RS, Alam GS, Ahmed A, Seed I. Geological history of the Alamreg-MashkiChah area, Chagai District, Baluchistan. In: Farah A, DeJong KE, editors. *Dynamics of Pakistan*. Quetta: Geological Survey of Pakistan; 1979. p. 325–31.

[45] Muslim M. Koh-e-Sultan sulphur evaluation. GSP Report—5, vol. 21, Baluchistan, Pakistan, 1972. 8pp.

[46] HSC. Reconnaissance geology of part of West Pakistan: Colombo Plan Cooperative project for Government of Pakistan. Government of Canada, 1960. 550pp.

[47] NayyerAlam Zaigham, Zeeshan Alam Nayyar, Noushaba Hisamuddin, 2009, Review of geothermal energy resources in Pakistan, Renewable and Sustainable Energy Reviews 13 (2009) 223–232

[48] Armstead HC. Geothermal energy. London: Spon Ltd.; 1979.

[49] Eickhoff G, Alam S. On the petroleum geology and prospectivity of Kirthar range, Kirthar depression and Sibi trough, southern Indus basin, Pakistan. Islamabad: Hydrocarbon Development Institute of Pakistan; 1991.

[50] Kazmi AH. Active fault systems in Pakistan. In: Farah A, Dejong KA, editors. Geodynamics of Pakistan. Quetta: Geological Survey of Pakistan; 1979. p. 286–94.

[51] Oldham T. Thermal springs of India. GeolSurv India Mem1882; 19(2):63.

[52] Bakr MA. Thermal springs of Pakistan. GeolSurv Pak Rec 1965; 16:3–4.

[53] Zaigham NA. Belaophiolites and associated mineralizations in southern part of axial-belt of Pakistan. PhD thesis, University of Karachi, 1991.

[54] Khan MA, Raza HA. Role of geothermal gradients in hydrocarbon exploration in Pakistan. J Petro Geol 1986; 9(3):245–58.

[55] Zaigham NA, Ahmed M, Hissam N. Thar-rift and its significance for hydrocarbon. Special Publication of SPE & PAPG, 2000. p. 117–30.

[56] Calkins JA, Jamiluddin S, Bhuyan K, Hussain A. Geology and mineral resources of Chitral-Partsan area, Hindu Kush Range, northern Pakistan. USGS Paper, vol. 716-G, 1981. 33pp.

[57] Shuja TA, Khan AL. Prospects of geothermal energy in Pakistan. GSP Info Rel 1984; 242. 22pp.

[58] Shuja TA, Sheikh MI. A study of geothermal resources of Gilgit and Hunza agencies, northern Pakistan. GeolSurv Pak Info Rel 1983; 179. 22pp.

[59] Todaka N, Shuja TA, Jamiluddin S, Khan NA, Pasha MA, Iqbal M. A preliminary study of geothermal energy resources of Pakistan. GSP Info Rel 1999; 407. 93pp.

[60] Quittmeyer RC, Farah A, Jacob KH. The seismicity of Pakistan and its relation to surface faults. In: Farah A, Dejong KA, editors. Geodynamics of Pakistan. Quetta: Geological Survey of Pakistan; 1979. p. 271–84.

[61] Kanoglu, M & Bolatturk, A 2008, 'Performance and parametric investigation of a binary geothermal power plant by exergy', Renewable Energy, vol. 33, no. 1, pp. 2366–74.

[62] Aljundi, IH 2011, 'Effect of dry hydrocarbons and critical point temperature on the efficiencies of organic Rankine cycle', Renewable Energy, vol. 36, no.1, pp. 1196-1202.

[63] Kanoglu, M 2002, 'Exergy analysis of a dual-level binary geothermal power plant', Geothermics, vol. 31, no. 1, pp. 709-724.

[64] Bejan, A 1993, Heat transfer, Wiley, New York.

[65] Demuth, OJ & Kochan, RJ 1981, Analyses of mixed hydrocarbon binary thermodynamic cycles for moderate temperature geothermal resources using regeneration techniques, INELRep. EGG-GTH-05710, Idaho Falls, ID.

[66] Mago, PJ, Chamra, LM, Srinivasan, K & Somayaji, C, 2008, 'An examination of regenerative organic Rankine cycles using dry fluids', Applied Thermal Engineering, vol. 28, no.1, pp. 998-1007.

[67] Tchanche, BF, Lambrinos, Gr, Frangoudakis, A & Papadakis G 2011, 'Low-grade heat conversion into power using organic Rankine cycles- A review of various applications', Renewable and Sustainable Energy Review, vol. 15, no.1, pp. 3963-3979.

[68] Saleh, B, Koglbauer, G, Wendland M & Fischer, J 2007, 'Working fluids for low temperature organic Rankine cycles', Energy, vol. 32, no. 7, pp. 1210-1221.

[69] DiPippo, R 1999, 'Small geothermal power plants: Design, performance and economics', Geothermal Resources Council BULLETIN, pp. 1-8.

[70] Maizza, V & Maizza, A 1996, 'Working fluids in non-steady flows for waste energy recovery systems', Applied Thermal Engineering, vol. 16, no. 1, pp. 579–90.

[71] Calm, JM & Hourahan, GC, 2001, 'Refrigerant Data Summary', Engineered Systems, vol.18, no. 11, pp. 74-88.

[72] Calm JM, Hourahan GC, 2011. "Physical, Safety, and Environmental Data for Current and Alternative Refrigerants," Refrigeration for Sustainable Development (proceedings of the 23rd International Congress of Refrigeration (ICR 2011, Prague, Czech Republic, 2011.08.21-26), International Institute of Refrigeration (IIR/IIF), Paris, France